AN INVESTIGATION ON WET TRIBOLOGY OF DISPERSED SOLID LUBRICANTS IN THE PRESENCE OF SURFACTANT

A Thesis submitted in the fulfilment of the requirement for the degree of

DOCTOR OF PHILOSOPHY

IN

MECHANICAL ENGINEERING

Submitted by

HARPREET SINGH

Roll No. 901408003

Under the supervision of

Dr. Hiralal Bhowmick

Associate Professor,

MED, T.I.E.T, Patiala

Mechanical Engineering Department

Thapar Institute of Engineering & Technology, Patiala-147004, INDIA

(Deemed-to-be University)

March, 2021

CERTIFICATE

I, **Harpreet Singh**, Roll No. 901408003, hereby declare that the thesis entitled "***An Investigation on Wet Tribology of Dispersed Solid Lubricants in The Presence of Surfactant***" submitted to Mechanical Engineering Department at Thapar Institute of Engineering & Technology, Patiala, Punjab, India, for the award of the degree of "Doctor of Philosophy", is an authenticate record of my own research work carried out by me under the supervision of **Dr. Hiralal Bhowmick, Associate Professor, Thapar Institute of Engineering and Technology, Patiala**. The results presented in this thesis have not been submitted, in part or full, to any other University or Institute for the award of any degree or dilpoma.

Harpreet Singh

Harpreet Singh
Roll No. 901408003

Place: Thapar Institute of Engineering & Technology, Patiala

Date: 1/3/21

This is to certify that the above statement made by the candidate is correct to the best of my knowledge.

Verified by:

Dr. Hiralal Bhowmick
(Supervisor)
Associate Professor
Mechanical Engineering Department
Thapar Institute of Engineering & Technology
Patiala-147004 (Punjab), India

ACKNOWLEDGEMENT

First and foremost, I wish to thank my supervisor **Dr. Hiralal Bhowmick** for his valuable support, supervision, guidance and belief in me. I am thankful for the positive suggestions and meticulous guidance that helped me to improve my scientific writing and carry out the new research. I feel really motivated and honoured to work under his guidance throughout my entire Ph.D. work.

I wholeheartedly thank the doctoral committee members **Dr. T.P.Singh,** (Chairman, Doctoral Committee), **Dr. O.P. Pandey, Dr. A. K. Singh, Dr. Dheeraj Gupta** and **Dr. Hiralal Bhowmick** for the feedback and reviews that were given on my research proposal and progress monitoring presentations. Their guidance was beneficial for me to improve my research work. Sincere thanks to **Dr. S. K. Mohapatra (Sr. Professor)** for his support and positive feedback during the research work**.** I am also thankful to **Dr. Tarun Nanda** and **Dr. Gagandeep Bhardwaj,** our Ph.D. coordinators for their approachability and keeping me informed with all the relevant communication throughout E-mails.

A special thanks to the office of the Mechanical Engineering Department for providing all the facilities required for the research work. I am thankful to the office staffs of the ME department at Thapar Institute of Engineering & Technology for their help and cooperation throughout my study. I sincerely thank **Dr. SS Mallick**, Laboratory for Bulk Solids and Particulates, MED and the staffs of Chemical Engineering Department and School of Chemistry, TIET for their help and cooperation in providing the lab resources during my experimental works. I am also thankful and present deep regards for Mr. Lalit Kumar and Mr. Narinder Singh for their valuable feedback during research work in the Central Workshop premises.

Thanks to all my labmates and colleagues for their support and a very special and sincere thanks to Mr. Parampreet Singh, Mr. Sandeep Singh, Mr. Manpreet Singh, Mr. Sarbjeet Kaushal, Mr. Kamaljit Singh, Mr. Kulwinder Singh Chani, Mr. Jaswinder Singh, Mr. Jashanpreet Singh, Mrs Bandhana Sharma, and Mrs. Sehaspreet Kaur Toor, who had helped me a lot during my research work.

I am also thankful to Dr. Rafat siddique (DoRSP,TIET), Dr. S.S. Bhatia (DOAA,TIET) and Sophisticated analytical instrument(SAI) facility, TIET,Patiala, staff who

provided me the financial and academic assistance throughout my research work as well as for conference publications.

I would like to thank my parents Mr. Jagsir Singh and Mrs. Karmjeet Kaur for their valuable support and encouragement to complete my research work. A huge thanks goes to my brother, Mr. Gurpreet Singh and his wife Mrs. Amandeep Kaur, for their understanding and continuous support during my thesis work. I am very thankful to my nephew, Harjot Singh, for his love and smile which gave me encouragement and positivity during my work. I want to thank my elder brothers, Mr. Gurpinder Singh Dhindsa, Mr. Varinder Singh and Mr. Amandeep Singh for their help and encouragement during my study period.

I want to thank my elder sisters and relatives, Mrs. Gursharn Kaur, Mrs. Kamalpreet Kaur and Mrs. Manjeet Kaur and younger sister Jaspreet Kaur , for their sympathy and encouragement in the tough times. I want to thank my elder brothers and relatives, Mr.Pritpal Sidhu, Mr. Kuldeep Hans, Mr. Jagdev Hans,Mr. Parminder Kler, and Mr. Gurkamal Singh who advised me to keep patience and hard-working during publication process.

I would also like to thankful to my close friends Mr. Manjit Singh Virk, Mr. Ramandeep Singh Dhillon, Mr. Kamaldeep Singh, Mr. Harmilap Singh Mann, Mr. Deep Singh Sidhu, Mr. Jaskarn Singh and Mr. Varinder Singh who feel me always cheerful and with their positive vibes during the whole thesis work.

I want to dedicate this thesis to my loving parents, my PhD Supervisor and All the people in my life who touch my heart.

Finally, I bow and thank the Almighty, without whom I could have not completed this journey of completing my research work for the highest degree in the engineering discipline.

Harpreet Singh

ABSTRACT

The use of solid additives to enhance the properties of lubricating oil has been gaining immense interest in various automotive and metal working applications, owing to a preference towards the modernization of mechanical components and their compatibility with the environmental friendly additives. These factors help in reducing the friction as well as wear, which in turn, facilitate the enhanced life of the mating parts and improved energy efficiency of systems. Various particles such as MoS_2, WS_2, Cu, CuO, graphite, hexa-boron nitride (h-BN), soot, graphene, diamond-like carbon (DLC), etc are being tested as potential oil additives. Recently, tribologists have concentrated on tubular structured solid additives such as carbon nanotubes (CNTs) because of their high aspect ratio, flexibility, and unique chemical, optical and mechanical properties. It is worth to mention here that the major obstacle for the usage of micro/nanoparticles in the tribological arrangements is their poor solubility and speedy agglomerate formation, which results in excessive wear and depletion in tribo performance. This problem can be handled by functionalizing the nanoparticles or using the surfactants and dispersants.

In this context, it is worthwhile to mention that the target tribo-pair plays a prominent role in the selection and compatibility of particle additives for their potential utilization. To overcome some of the limitations associated with the use of Al-alloys in the tribological applications, the development of AMMCs are getting growing interest amongst the researchers. AMMCs are potential candidate materials for various applications due to their superior properties such as high specific strength and thermal conductivity, better corrosion and wear resistance, low cost, low coefficient of thermal expansion and high toughness. A few examples related to the commercial usage of AMMCs for the tribological application include: Al-SiCp composite material by Duralcan, Martin Marietta and Lanxide for making of pistons; Saffil reinforced AMMC diesel engine pistons by Toyota; AMMC cylinder liners by Honda; Nissan's Al–SiC connecting rods; and SiC-reinforced aluminium brake rotors.

Thus, composite tribocontact such AMMC/steel or AMMC/CI tribopair is an important domain of industrial research in-line with the demand of improved engine tribology, as well as other metal working applications. However, most of the reported studies are related to dry sliding conditions. In the applications where lubricated contact exists, such as between piston-cylinder and metal-working applications, it requires a great deal of research to gain

insight on the tribological behaviour of these developed composites. The situations in these cases can be effectively dealt, by tailoring the material properties to suit these applications along with the implementation of an improved lubrication with the help of nano/micro lubricants. It is seen that the antiwear properties of composites are significantly enhanced by the use of various reinforcements, however, antifriction properties of self-lubricating composites are still beyond the reach of the desired level to suit the specific applications, such as that required to overcome the friction loss in IC engine components and surface finish with a MQL lubricated condition in metal-working applications.

Studies using base mineral oil have their own importance because such studies set the preliminary insight for an additive to be used as anti-wear (AW), anti-friction (AF) or both. Moreover, the effectiveness of lubricant formulation using the solid particle additives is influenced by particle's dispersion capability and stability in the suspension. This is often enhanced by functionalizing the nanoparticles or using surfactant and dispersants. Moreover, application of surfactant functionalized solid additives in the development of liquid lubricants involves interesting and intricate features which should be taken care of while developing or formulating such type lubricants for the composite materials, such as AMMCs. However, such studies involving functionalized nanodispersions while improving the tribological behaviour of composite surfaces are also not available in the literature.

Thus, a comprehensive study is necessary to get the insight of the tribological behaviour of particle-laden lubricant and to compare with fully formulated commercial oils so that the findings can be suitably accommodated while developing the novel commercial oil package for any specific applications involving composite materials. Along-with the blending of base oil with various additives, great care should be taken in the detailed investigation of the microstructural, morphological and phase analysis on the lubricating contact surfaces.

Thus, the present research work will be directed towards the combinatorial approach of utilizing the benefit of composite materials and particle-based lubrication to attain the improved tribological properties. For the present research work, a systematic attempt is made to explore and address some of the fundamental issues related to the formulation and modification of a particle-based lubricant for the lightweight composite material, using the selected solid lubricant and surfactant.

Based on this proposed rationale, the authors carried out a comprehensive investigation on the influence of surfactant functionalized particle-based lubricants on the tribological characteristics of h-AMMC/Steel tribopair. For the preliminary screening, three grade-I base

oils, two SAE grade fully formulated industrial oils, and four types of particle additives are used for the tribological investigation. Based on the detailed pilot study, a suitable grade of base oil (SN500), a fully-formulated commercial oil (SAE 20W50), and a solid particle additive (MWCNT) are finalized for the comprehensive tribological investigation. Comparative tribological characteristics of both hAMMC/EN31 and hAMMC/CI tribopairs has been analyzed based on the worn-out fractography. This is followed by a detailed investigation on the tribological performances of MWCNT-in-oil and surfactant functionalized MWCNT-in-oil. For the better insight of the lubrication and friction-wear mechanism, thermophysical properties of prepared suspensions and characterization of the worn-out surfaces of h-AMMC are carried out using various techniques such as SEM, EDS, XRD, and Raman spectroscopy. To functionalize the MWCNT particles, Sorbitan mono-oleate (SPAN-80) is used in MWCNT-in-oil suspension. The study reveals some interesting insights on the tribological characteristics of MWCNT laden lubricants in the presence of surfactant, which might be connoted for the future development of the lubricants to be used in the industrial applications. An in-depth investigation of the underlying lubrication mechanism reveals that four primary sub mechanisms are responsible for the improved tribological characteristics of surfactant functionalized MWCNT-in-oil lubrication. Comparative performance analysis of prepared oil lubricants with commercially available formulated oils has been discussed in detail. Wear mechanisms map is also established in the case of functionalized lubricants based on the critical observations.

Finally, the conclusions and the findings from the present research work have been summarized and useful recommendations are made for the future scopes of work.

TABLE OF CONTENTS

LIST OF FIGURES

LIST OF TABLES

LIST OF ABBREVIATIONS

AMMCs	:	Aluminium Metal Matrix Composites
Al_2O_3	:	Aluminium Oxide
API	:	American Petroleum Institute
ATS	:	Aminopropyl Trimethoxy Silane
ANOVA	:	Analysis Of Variance
AF	:	Anti-Friction
AW		Anti-Wear
AFM	:	Atomic Force Microscopy
BAC	:	Benzalkonium Chloride
BZT	:	Benzethonium Chloride
B_4C	:	Boron Carbide
CB	:	Carbon Black
CNTs	:	Carbon Nano Tubes
CI	:	Castiron
CTAB	:	Cetyl Trimethylammonium Bromide
CTAC	:	Cetyl Trimethylammonium Chloride
CMC	:	Critical Micelle Concentration
CPP	:	Critical Packing Parameter
DOE	:	Design Of Experiments
DPS	:	Dual Particle Size
EHD	:	Elastohydrodynamic
EDS	:	Energy Dispersive Spectroscopy
EP	:	Extreme Pressure
$FeSi_2$	:	Ferdisilicite
FIB	:	Focused Ion Beam
FTIR	:	Fourier-Transform Infrared Spectroscopy
FWHM	:	Full Width At Half Maximum
Gr	:	Graphite
GNF	:	Graphite Nanofibers
h-BN	:	Hexa Boron Nitride

h-AMMC	:	Hybrid AMMC
HLB	:	Hydrophilic–Lypophilic Balance
IF	:	Inorganic Fullerenes
LP	:	Liquid Paraffin
MMLs	:	Mechanically Mixed Layer
MMC	:	Metal Matrix Composites
MoS_2	:	Molybdenum Disulpihde
MWCNTs	:	Multi-Walled Carbon Nanotubes
PRAMMCs	:	Particulate Reinforced Aluminum Metal Matrix Composites
PIBS	:	Poly-Isobutylene Succinimide
SEM	:	Scanning Electron Microscopy
SiC	:	Silicon Carbide
SWCNT	:	Singlewalled Carbon Nanotubes
SDS	:	Sodium Dodecyl Sulfate
SLS	:	Sodium Lauryl Sulfate
SPAN-80	:	Sorbitan Mono-Oleate
SWR	:	Specific Wear Rate
TiC	:	Titanium Carbide
WS_2	:	Tungstun Disulphide
UTS	:	Ultimate Tensile Strength
WR	:	Wear Rate
XRD	:	X-Ray Powder Diffraction

LIST OF SYMBOLS

m	:	Meter
h_{cen}	:	central film thickness
E'	:	reduced Young's modulus
a_h	:	area of head group
p_o	:	Hertzian pressure
µm	:	Micrometer
I_c	:	maximum chain length
La	:	mean inter-defect distance
min	:	Minutes
mm	:	Millimetre
nm	:	Nanometer
U_m	:	mean velocity
V	:	hydrocarbon chain volume
vol	:	Volume
wt	:	Weight
η	:	dynamic viscosity
λ	:	film thickness ratio
µ	:	frictional coefficient
R	:	Radius
W	:	normal load
α	:	pressure viscosity coefficient
k_s	:	Thermal conductivity of solid
c_{ps}	:	Specific heat capacity of bulk solid surface
τ_0	:	Characteristic Eyring shear stress
$\bar{p}$	:	Average contact pressure
k_{lub}	:	Lubricant's thermal conductivity
χ	:	Non-dimensional thermal parameter
w_v	:	Hydrodynamic load shared by the lubricant

CHAPTER 1
INTRODUCTION AND OVERVIEW

1.1 INTRODUCTION

In a recent study it was reported that approximately 23% of global energy consumption is associated to the tribological contacts [1]. Poor tribology elevates the friction and wear losses in an automobile engine, which, in turn, increase the oil consumption and reduces the service life [2]. The automobile consists of many tribological elements like bearings, pistons, transmissions, etc and it has been found that friction loss accounts to as much as 48% of total energy consumption within the engine [3]. Many models are proposed and modifications are given to save energy consumption due to severe friction and wear of contacting surfaces or poor lubrication contacts [4]. Energy losses in automobiles, machineries and other equipment caused by poor tribo-design can be substantially reduced (by 40% in the long term) with the help of the development of new surfaces or materials and designing suitable lubrication package [1]. Moreover, improved tribology also brings along the reduced emission of CO_2, which in turn, enormous cost savings annually. Accordingly, various approaches have been followed since decades to improve the tribological behavior of moving contacts. Figure 1.1 shows a schematic of the various approaches that are followed for such purposes.

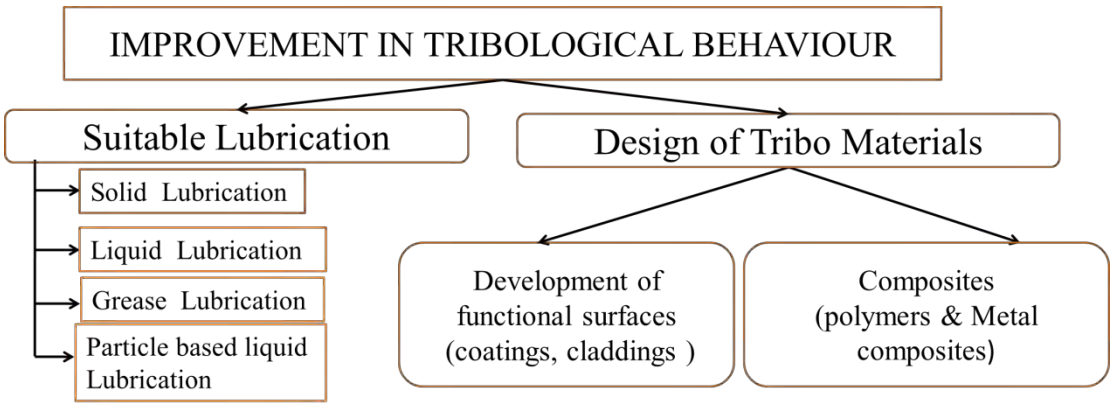

Figure 1.1: Methods of improvement in the tribological behaviour

1.2 SOLID AND LIQUID LUBRICATION

One of the most efficient means to control friction is to apply a lubricant in solid or liquid form. Some of the advantages of solid lubrication are their effectiveness at high loads and speeds, high resistance to deterioration in storage and high stability in extreme temperature, pressure and reactive environment. Liquid lubricants offer replenishment ease and minimal fluctuating coefficient of friction. They diminish friction by preventing the sliding interfaces from harsh or direct metal-to-metal contacts or by generating an easily shearing, but highly durable separating layer on the rubbing surfaces. However, they are prone to surface chemistry changes under high temperature, and provide oxidation provoking environments [5]. For example, engine oils or lubricants can proficiently detach the mating contacts of rings and liners, depending upon the variations in the values of sliding velocity and other operating conditions, thus preventing a severe friction and wear phenomena. The various additives present in the oil provide extra safety by creating lubricious boundary film in the circumstances of direct metal-metal contacts. Consequently, these liquid/solid lubricants make possible the safe, smooth, and long-lasting running of engine components and other mechanical systems [6].

Typically industrial lubricants contain more than 85% base oil and rest a variety of additives to impart the desirable characteristics. Base oils are utilized to prepare lubricating motor oil, greases, and metal working fluids. Different applications require certain compositions to contribute to specific properties of the oil. The lubricant viscosity at various temperatures or viscosity index (VI) is a critical factor for the selection of the lubricant. There are five distinct groups of base oils, as defined by the American Petroleum Institute (API). These groups are categorized based on their refining method and properties such as viscosity and the proportion of saturates and sulfur content [7]. Oils under group I-III are refined from petroleum crude oil, whereas group IV base oils are full synthetic oils, such as Poly Alpha Olefins (PAO). On the other hand, group V includes all other base oils not included in Groups I-IV. Group I & II base oils are the most common types used for the industrial oils, especially in automotive engine oil formulations, due to their availability, low price, as well as the desirable properties for intended applications. Group I base oil are also designated either by solvent neutral (SN) or bright stock (BS).

The main families of additives for commonly used industrial lubricant are listed in Figure 1.2 [8].

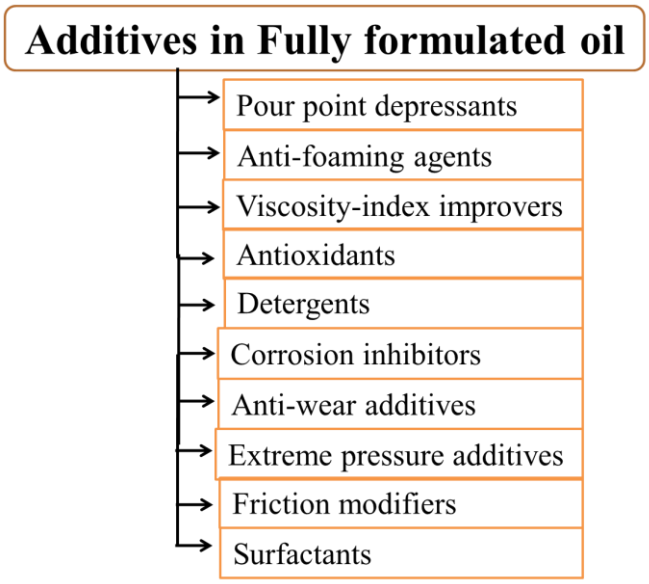

Figure 1.2: Various types of additives in fully formulated oil

However, it is quite a challenging task to develop an effective lubricant for the complex tribosystems such as in piston ring-cylinder liner or metal forming applications in which the aim is to achieve very low friction and wear without compromise of load bearing capacity. Now-a-days, to overcome some of limitations associate with the liquid lubricants and to enhance the lubricating oil properties, use of solid additives has been gaining immense interest in various automotive and metal working applications.

1.3 PARTICLE-BASED LUBRICATION

Tribologists develop a quest for improved lubrication characteristics of conventional lubricants because these lubricants cannot be tailored for specific rubbing contacts. Currently, particle-based lubricants, due to their inherent advantages, are trying to fill the gap in-between consumer needs and product development [9,10]. The nanofluid or nanosuspensions have a significant number of potential applications, such as in oil extraction [11], biomedical applications [12], drug delivery systems [13], and many more.

Particle-based lubricant typically consists of three elements; the primary solvent (base oil), the micro/nanoparticles and the surfactants or dispersants and other additives that occupies the interface region between the particles and the fluid [14]. Nano-sized particles are in demand as the potential oil additives for many reasons. The prime advantage of using nanoparticles is that they are small enough to penetrate between the minute surface gaps and thereby alter the tribology of the contacts. Also, due to their small size, there is little restriction for particles to pass through oil galleries. The major advantages of particle-based lubrication over the other conventional liquid lubrication includes are as follows.

- Combinations of liquid and solid lubrication have superior synergistic effect on friction and wear performance.
- Liquids with particle additives can support high pressure and can perform well from low to high load applications.
- Solid Lubricants with carrier fluids provides self-healing & better replenishment.
- Due to their small size, micro/nanoparticle (MP/NPs) can enter easily into contact asperities, so stable lubrication.
- Enhanced tribology due to the ball bearing effect, film effect, exfoliation effect, etc under the tribo-contacts.
- Exhibits better heat transfer, especially for nanoparticles.

Thus, one of the potential approaches to reduce the total energy consumption in a mechanical system is particle-based lubrication. This type of lubrication process can reduce friction as well as the wear of mating surfaces. Hence, the smooth, durable, and efficient running of mechanical systems is possible.

1.3.1 Particle additives

Solid lubricants such as MoS_2, WS_2, hexagonal boron nitride (h-BN), graphite, and boric acid can offer excellent lubricant characteristics [15–17] along with anti-frictional and wear performances [18,19]. Lamellar or layered crystal structure is reliable for exceptional friction performance by the most of the inorganic materials. Since the last few years, various tribologists had tested various particles such as MoS_2, WS_2, Cu, CuO, graphite, h-BN, soot, graphene,

polymers etc as potential oil additives [20–29] [30][31]. Recently, CNTs are emerging out as one of the prominent research interests amongst the tribologists due to their high aspect ratio, superior mechanical and many more desired properties [32–35].

A brief overview of the most widely used solid lubricants which can be potential candidates for the selection of particle additives in the lubricant are listed below.

Graphite: Structurally, carbon atoms in graphite are hexagonal in orientation (Figure 1.3), and the interplanar bonding between them is relatively weaker. In sliding contacts, these type of structures can contributes the excellent lubricious properties, because of weak inter-lamellar bonding that facilitates easy shearing along slipping planes [36,37]. In the air environment, graphite is the right choice for lubrication, however, graphite is not effective in vacuum [38]. Primarily, graphite was merely used as the solid lubricants in high-temperature applications, where organic lubricants are believed to be inappropriate [39].

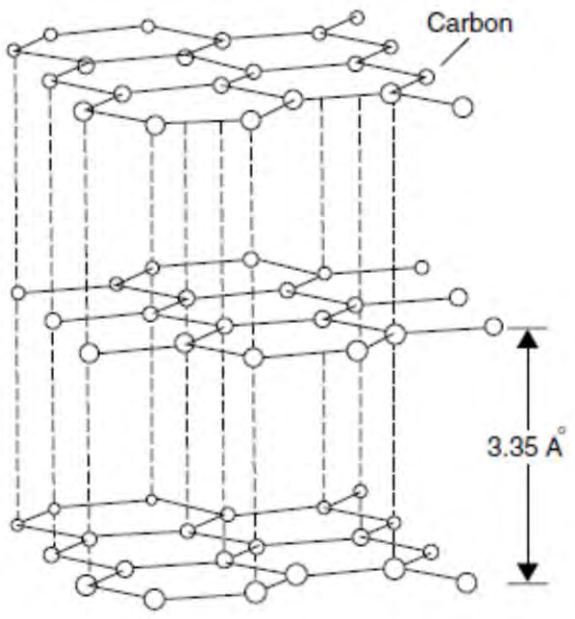

Figure 1.3: Layered crystal structures of graphite [5]

Metal dichalcogenides: Metal dichalcogenides exist in the form of MZ_2, where M is Mo or W, and notation Z belongs to S or Se. In the crystal structure of MZ_2, atoms in the same lamella are bonded strongly by covalent forces while adjacent lamellas are bounded by relatively weak van

der-Waals forces as shown in Figure 1.4. In a crystal lattice, the unit cell has hexagonal symmetry, and in 2-H configuration, two adjacent layers are considered [40].

MoS_2 and WS_2 are inherently synthesized in fullerene-like structures. These inorganic fullerenes (IF) in nanometric sizes exhibits numerous properties like seamless nature, elasticity quasi-spherical, and chemical stability that may induce profitable results in the field of tribology [41,42].

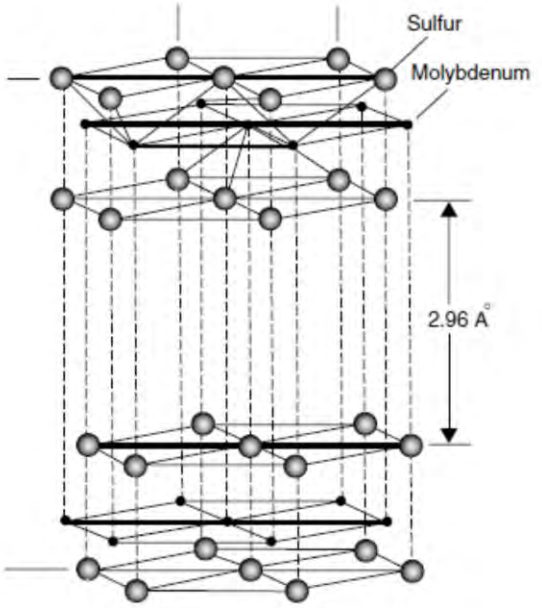

Figure 1.4: Schematic crystal structures of MoS_2 [5]

Boric acid (H_3BO_3): Boric acid is another potential solid lubricant due to its layered crystal structure (Figure 1.5). Boric acid is having relatively high load carrying capacity and low steady-state friction coefficient and shear strength and is abundance in nature [43,44].

Figure 1.5: Lamellar structure of boric acid [44]

Carbon nanotubes (CNTs): Discovery of CNTs [41,45] has gained the attention of scholars due to their excellent properties. In the family of CNTs, multi-walled carbon nanotubes (MWCNTs) are of particular interest for the industrial applications. MWCNTs consist of multiple layers of graphene superimposed and rolled in on themselves to form a tubular shape (Figure 1.6) [46,47]. Rich chemistry of carbon atoms makes itself possible for reactions and manipulations as per necessitate. Owing to this nature and unique physic-chemical properties, MWCNT can be modified and optimized to play a significant role in numerous technological applications, including the advancement of tribology [46,48], as shown in Figure 1.7.

Figure 1.6: MWCNT [47]

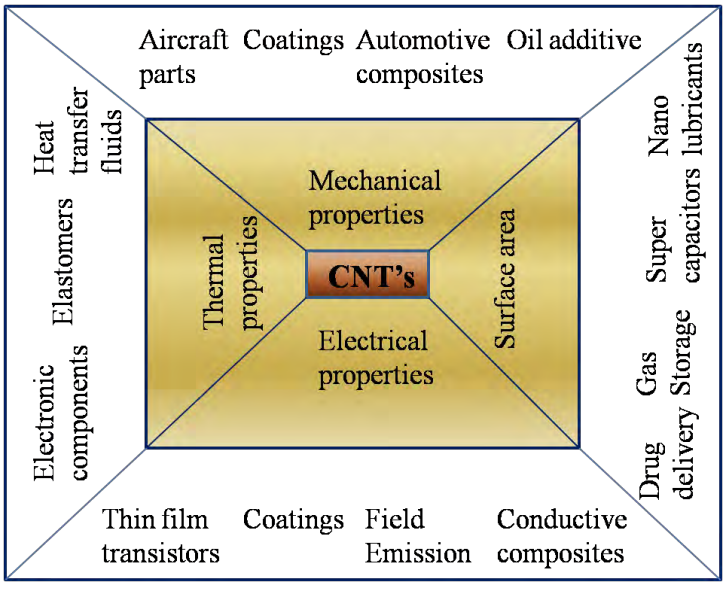

Figure 1.7: MWCNT properties for various potential applications [46]

Nanoclay: Nanoclays are made of layered mineral silicates which can form complex clay crystallites by stacking these layers [49], each layer unit being in the form of octahedral or tetrahedral sheet [50]. There are several forms of nanoclay, and Montmorillonite (MMT) is one of them which has been widely explored. Their organically modification makes them potentially applicable in many applications [51]. It is a known fact that some chemical processes may occur during friction [52,53]. Recently, a cheap nano-clay additive (Figure 1.8) has been tested as a lubricating enhancer [54].

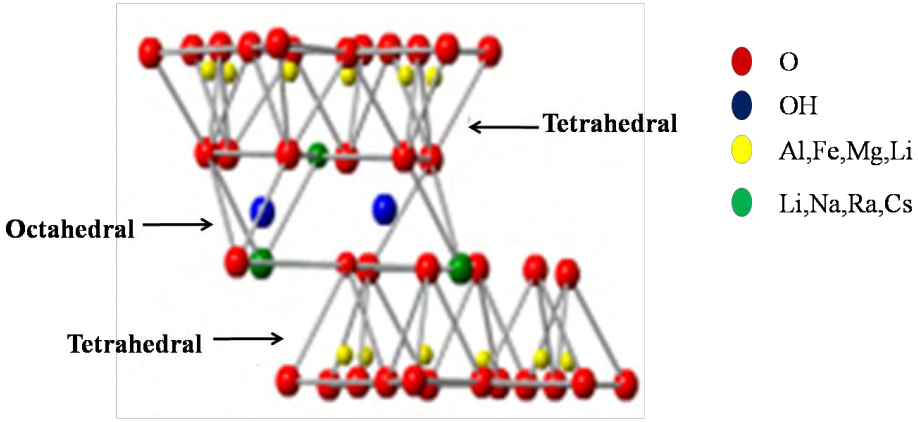

Figure 1.8: Crystal structures of clay minerals [55]

1.3.2 Challenges of micro/nanoparticle-based lubrication

Colloidal solutions comprising micro/nanoparticles have some stability issues. They agglomerate inside the lubricant, thereby precipitation occurs. Precipitated particles may not behave efficiently in rubbing contacts as individual particles act. Recently, Hong et al. [56] reported a critical review on the dispersion of nanoparticles in the lubricant oil. Some micro/nanoparticles have environmental impacts, and therefore usage in oil dispersions must be retrieved. Synthesis or mass production of the particles is still a point of conflict. The cost of these particles is a limiting factor. Even so, many authors claimed their improved performance in oils, but large scale market introduction is still needed promising effort.

Perhaps, the major challenge of using these particles is that their exact interaction mechanisms for the contacts tribology are still unknown or un-established. However, many authors had reported various mechanism studies to illustrate the action routes of particle additives under different conditions.

1.4 METAL MATRIX COMPOSITES (MMCs)

In this context, it is worthwhile to mention that the materials of target tribo-pair plays a prominent role in the selection and compatibility of particle additives for their potential utilization [57]. Material loss or wear loss mainly depends upon the nature of the interface, as well as the mutual compatibility between the contacting surfaces. Composite materials are derived or engineered from two or more naturally occurring materials, for the betterment of chemical, physical, and mechanical properties. There are various classifications for composites. Based on the nature of the matrix, it can be classified into three broad categories viz. MMCs, PMCs, and CMCs.

MMCs are in growing demand for various numbers of modern technologies such as automobiles, aerospace, marine, and sports. Apparently MMCs must be able to withstand high loads without rupture, deformation, or breaking while they are put in applications, as well as must be able to maintain their excellent tribological properties over long duration in the tribological applications. Particulate reinforced metal matrix composites (PRMMCs) have been proven to be better as compared to the conventional monolithic materials owing to their high stiffness and strength, low-density, low cost of manufacturing. MMCs based upon the light metals are gaining attention from many industries, including the automotive [58]. Among the light weight MMCs, aluminium based composites are more popular, and extensive research is going on in respect of their development and use for the manufacturing of the tribo-mechanical components. That is why, they are briefly discussed in the subsequent sections.

1.4.1 Aluminium metal matrix composites (AMMCs)

In today's era of ever growing demand of fuel-efficient and reduced energy consumption by the automotive vehicles, use of aluminium alloy and its composite is getting great attention for the automobiles components. The characteristic properties of aluminium, alongwith its cost and accessibility as compared to other materials make it the ideal candidate to replace heavier materials in the car. However, one of the major drawbacks of aluminium alloys includes its low wear resistance in tribological applications. To overcome some of the limitations associated with the Al-alloys, the development of AMMCs are getting growing interest amongst the researchers. The major improvements in the properties of AMMCs are manifested in the form of improved strength, stiffness and damping capacity, improved antiwear and high-temperature properties, and better control of thermal expansion coefficient.

From the last few decades, a great deal of works has been carried out internationally in the field of AMMC to explore its potential applications for automotive piston [59,60]. Since the present research proposal will be aimed at the development of particle-based lubrication for the selected AMMC-steel tribo-pair, so rather than critically reviewing the development and research on the composites, this section highlights the importance of AMMCs in the tribological application. Many authors have tribologically tested different reinforced composites for dry sliding conditions. For tribological applications, the majority of the researches have shown that there is a significant improvement in the wear resistance of these composites. Many of these studies used Al6061, 6063, 7075, A390, A356 as metal matrix, and SiC and Al_2O_3 as hard reinforcements [61–65]. To improve the anti-seizure and friction properties, soft reinforcements such as graphite are also being used [66,67].

A few examples related to the commercial usage of AMMCs for the tribological application include: Al-SiCp composite material by Duralcan, Martin Marietta and Lanxide for making of pistons; Saffil reinforced AMMC diesel engine pistons by Toyota; AMMC cylinder liners by Honda; Nissan's Al–SiC connecting rods; and SiC-reinforced aluminium brake rotors [68]. The machinability issues associated with the MMCs hinderd the widespread use of aluminium composite. However, these challenges are being addressed through various R&D activities worldwide and was spelt out in the AMMC Roadmap 2002 [69]. University of Wisconsin-Milwaukee developed Al-SiC-graphite, and Al-alumina-graphite composites with reduced silicon carbide for brake rotors, piston and cylinder liners to overcome the cost and machinability barriers [70,71].

Thus, composite tribocontact such Al-SiCp/steel tribopair is an important domain of industrial research in-line with the demand of improved engine tribology, as well as other metal working applications. However, most of the reported studies are related to dry sliding conditions. In the applications where lubricated contact exists, such as between piston-cylinder and metal-working applications, it requires a great deal of research to gain insight on the tribological behaviour of these developed composites. The situations in these cases can be effectively dealt, by tailoring the material properties to suit these applications along with the implementation of an improved lubrication with the help of nano/micro lubricants. It is seen that the antiwear properties of composites are significantly enhanced by the use of various reinforcements, however, antifriction properties of self-lubricating composites are still beyond the reach of the desired level to suit the

specific applications, such as that required to overcome the friction loss in IC engine components and surface finish with a MQL lubricated condition in metal-working applications.

1.5 SURFACTANT

It is worth to mention here that the major obstacle for the usage of micro/nanoparticles in the tribological arrangements is their poor solubility and speedy agglomerate formation, which results in excessive wear and depletion in tribo performance. The effectiveness of lubricant formulation using the solid particle additives is influenced by particle's dispersion stability in the suspension [72]. This problem can be handled by functionalizing the nanoparticles or using the surfactants and dispersants [13-16]. However, such studies involving the tribology of composite materials are not available in the literature.

Surfactants are surface-active substances which reduce surface tension of the fluid or fluid dispersions. They are composed of a polar hydrophilic head group and a polar long hydrocarbon tail chain, which can be linear, branch, or aromatic. Classification of surfactants based on their polar head group is as shown in Figure 1.9 and described below.

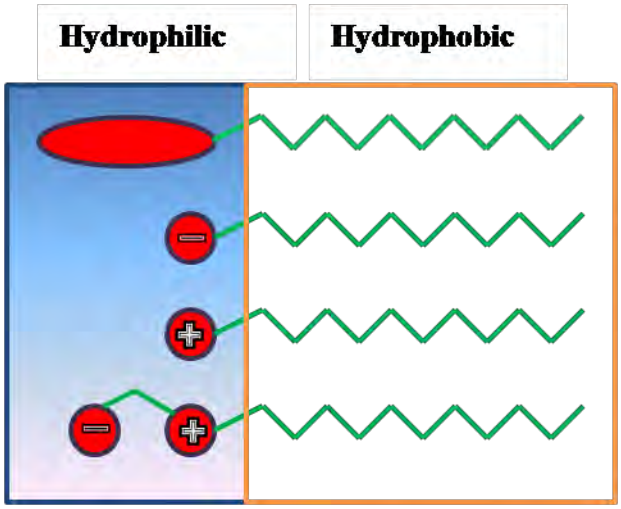

Figure 1.9: Surfactant classification (nonionic, anionic, cationic, amphoteric)

Nonionic Surfactant: The head group of these surfactants contains no charge groups. Many long-chain alcohols such as fatty alcohols, cetyl alcohol, oleyl alcohol, Spans and Tweens are the examples of nonionic surfactant.

Anionic surfactant: The head of an anionic surfactant carries a net negative charge. Ammonium lauryl sulfate, sodium lauryl sulfate, sodium dodecyl sulfate, etc are some of the commonly used anionic surfactants.

Cationic surfactant: The head group of this type of surfactant contains a net positive charge. Commonly used surfactants of this category are CTAB, CTAC, Benzalkonium chloride (BAC), Benzethonium chloride (BZT), etc.

Amphoteric surfactant: If both cationic and anionic groups are attached to the same molecule, then surfactant is known as zwitterionic or amphoteric. Amphillic nature permits them to self-assemble into a micelle to reach an energy balance. Once the hydrophobic end of the surfactants occupies the surface of micro/nanoparticles in the solvent, the tendency to cluster/aggregate formation is reduced considerably, as shown in Figure 1.10.

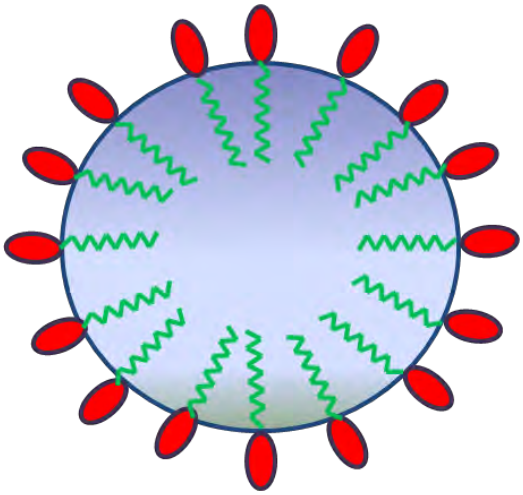

Figure 1.10: A schematic diagram of a micelle

1.6 REGIMES OF LIQUID LUBRICATION

The behaviour of lubricated tribological contacts depend upon the operating lubrication regime. Stribeck curve or Stribeck–Hersey curve (as shown in Figure 1.11) is a tool to define the lubrication regime between two mating surfaces. Stribeck curve plots the variation of friction as a function of a dimensionless parameter ZN/P, where Z is the dynamic viscosity, N is the speed and P is the load.

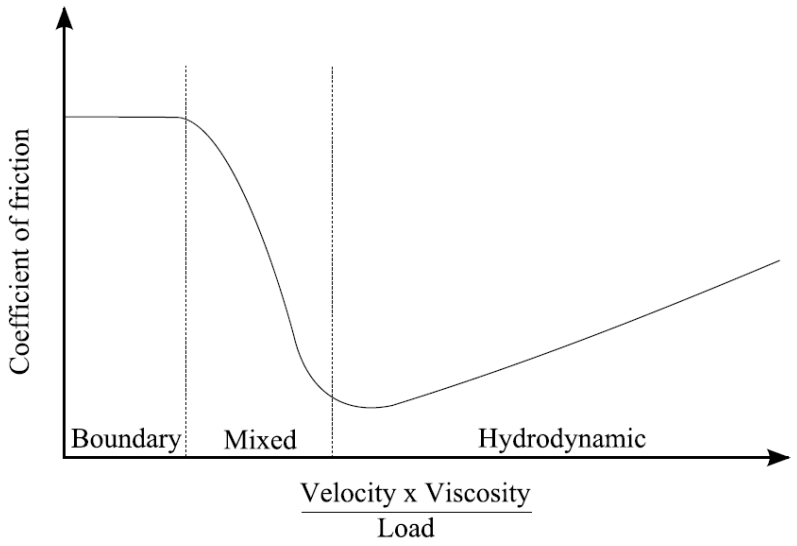

Figure 1.11: Stribeck curve for defining regimes of lubrication [73]

The characteristics of various regimes of lubrication are briefly explained below

1.6.1 Hydrodynamic or full film lubrication regime

Hydrodynamic lubrication is the condition when a relatively thick film of lubricant separates the load-carrying contacting surfaces. It is a stable lubrication regime, and direct metal-to-metal contact does not happen during the steady-state working of mechanical components. In this regime, the lubricant pressure is induced by the wedging action caused by the motion of the surfaces.

1.6.2 Elastohydrodynamic lubrication regime

In this regime of lubrication, the load is adequately high for the surfaces to be deformed elastically under the partial hydrodynamic action. Elastohydrodynamic lubrication is more prevalent between the rolling contact surfaces, for example, ball and rolling element bearings.

1.6.3 Partial or mixed lubrication regime

In this regime intermittent asperity contacts of the surfaces take place in the partial presence of thin layer of lubricant. Mixed lubrication regime can occur when the velocity is relatively low, but the load is high enough, or when the lubricant viscosity is significantly reduced.

1.6.4 Boundary lubrication regime

Boundary lubrication regime is the condition when the thickness of the fluid film is negligible, and there is substantial asperity contact. Component working in this regime is susceptible to the chemical and physical properties of thin surface films rather than the properties of the bulk lubricant. In an internal combustion engine, in a single stroke, the piston ring-cylinder liner interface may experience hydrodynamic, mixed, elastohydrodynamic and boundary lubrication [74,75].

1.7 MOTIVATION

The tribological response of aluminium and its alloys has long been proven to be the poorest. However, with the growing demand for light-weight materials in various components such as in cylinder-piston liner arrangement, the challenge and demand for improved lubricated tribological behavior of these materials has become an essential goal. Particulate reinforced AMMCs are being increasingly explored and are in growing demand for various numbers of modern technologies due to their improved properties, combined with momentous weight savings over conventional alloying materials.

The dry sliding behavior of AMMCs using a variety of reinforcements has been studied so far. Lubricated sliding of particulate reinforced composites is fascinating and but less explored arena. Now-a-days, to overcome some of limitations associate with the liquid lubricants and to enhance the lubricating oil properties, use of solid additives has been gaining immense interest in various automotive and metal working applications. The application of particle-based lubricants has been more manifested owing to a preference towards the modernization of mechanical components and their compatibility with environmentally friendly additives.

The utilization of micro/nano additive in fluids shows many attractive and exciting features that give them the potential to be used in various applications requiring effective heat transfer and lubricated tribology. However, till date micro/nanoparticle-based lubricants have been examined for their tribological performance and optimized for steel-steel contact pairs and aluminium-steel pairs. It is yet to be explored for hybrid composite/steel contacts. Moreover, the application of additive technology in liquid lubricants and characteristics of surfactant-based suspension might reveal some exciting features into the studies. The present research work will be directed towards the combinatorial approach of utilizing the benefit of composite materials and particle-based lubrication to attain the improved tribological properties.

1.8 THESIS OVERVIEW

The current thesis work has been organized into the following chapters:

Chapter 1: In this chapter, a brief overview of aluminium metal matrix materials, role of tribology in the global energy consumption, and particle-based liquid lubrication has been discussed. A brief introduction of tribology, various regimes of lubrication, and components of particles based lubrication are highlighted. The utilization of particle-based lubrication in various applications and challenges of using particle additives has been summarized in the present chapter. Finally, the motivation behind the present work has been outlined.

Chapter 2: A comprehensive literature review is presented related to the lubrication mechanism of micro/nanolubricants, tribological behaviour of various particle additives, surfactant-based particle dispersions, and development of AMMCs for the tribological applications. At the end of the section, research gaps are identified and highlighted.

Chapter 3: In this chapter, problem identification, research objectives, proposed plan of work, and methodology adopted for the present study have been discussed. A brief discussion on the various experimental procedures and analysis techniques for tribological study has been also provided. A detailed description of the raw materials used in the various stages of investigation for the current study is also provided.

Chapter 4: In this chapter, experimental investigations related to the selection of suitable tribopair, particle additive, base oil, and surfactant has been reported. Characterization of fabricated AMMC, selected oil, particle additives and surfactant has been performed and presented in this chapter.

Chapter 5: In this chapter, a detailed discussion on the tribological investigation on the particle-based lubricant without the presence of any surfactant and dispersion has been made. Comparative tribological characteristics of both hAMMC/EN31 and hAMMC/CI tribopairs has been analyzed based on the worn-out fractography.

Chapter 6: In this chapter, the underlying lubrication mechanism of non-functionalized and surfactant-functionalized MWCNT-in-oil has been presented. Selection of surfactant, prediction of operating lubrication regime using film thickness and film thickness ratios for different lubricant formulations, and subsequently identifying underlying friction-wear-lubrication mechanism has been explored and presented. An in-depth investigation of the underlying lubrication mechanism reveals that four primary sub mechanisms are responsible for the

improved tribological characteristics of surfactant functionalized MWCNT-in-oil lubrication. Comparative performance analysis of prepared oil lubricants with commercially available formulated oils has been discussed in detail. Wear mechanisms map is also established in the case of functionalized lubricants based on the critical observations.

Chapter 7: The conclusions and the findings from the present research work have been summarized in this chapter. Finally, some recommendations are made for the future scopes of work.

.

CHAPTER 2

LITERATURE REVIEW AND IDENTIFICATION OF RESEARCH GAPS

2.1 LITERATURE REVIEW

This chapter focuses on the review of the latest developments that have taken place in the field of composite material tribology, as well as in liquid tribology, mainly in the domain of additive based micro/nano lubricants for improved tribological applications. Significant research is going on in the field of oil formulation using different micro/nanoparticles as potential oil additives for the conventional tribopairs. The latest literature available in the domain of present research, as well as the tribological behaviour of ferrous/non-ferrous materials under dry/ lubricated contacts is reported in this section.

2.1.1 Lubrication Mechanisms for Micro/Nanolubricants

Various authors have proposed the mechanism of nanolubrication with the addition of various micro/nanoparticles in base oils. They reported a variety of mechanisms such as ball-bearing effect, protective film, colloidal effect, exfoliation [23,76–81]. A brief discussion on the proposed mechanisms mentioned above is made below.

2*.1.1.1 Ball bearing effect*

Rapoport et al. [76,77] had conducted a comparative study based on different morphological particle additives (Nano IF-WS_2, micro 2H-WS_2, and micro MoS_2 pallets) in oil. They suggested that the microscopic ball bearing mechanism is responsible for improved tribological properties of spherically shaped IF nano-additives on the contrary to micro-disulfide additives. They also reported that the elastically hollow structure of inorganic fullerene-like metal dichalcogenides nanoparticles acts as spacers and slide against the friction pairs and inhibits the direct contact between the moving surfaces. In an another study with C60 fullerenes slide against steel, Bhushan et al. [82] attributed the reason of remarkable reduction to the ball bearing effect of compact C60 transfer film on the surface of steel. However, further studies by Schwarz et al.

[83] into the subject of the ball bearing mechanism in C60 fullerenes lead to a few contradictions for profitable tribological properties.

Golan et al. [84] verified the possibility of a rolling effect mechanism in the case of WS_2 nanoparticles. They observed that WS_2 transfer film on the tribomates was responsible for a drastic reduction in the values of friction under specified conditions. Lahouij et al. [85] also conducted a similar type of mechanism study with the utilization of TEM-Atomic force microscopy under varying tangential and normal loading conditions. The authors claimed the unerringly spherical and crystalinity effects on the rolling friction mechanism in the case of IF-MoS_2 particles study.

Lee et al. [86] studied the effect of graphite nano-additives on the lubrication properties of commercial mineral base oils, using two different concentrations. Graphite as an additive showed the beneficial effect in terms of frictional properties due to ball-bearing action and morphological properties by smoothening the valleys. The effect of dispersant alkyl aryl sulfonate on tribological properties was also investigated by them. The addition of dispersant in nano-oil helped in the de-agglomeration of the clustered particles.

2.1.1.2 Film effect

Many authors [78,79,87,88] have tried to emphasize the mechanisms of transfer tribofilm of lamellar MoS_2 to some depth. The layered structure of MoS_2 makes it beneficial for effortless shearing and exfoliates them in the forms of sheets, transfers onto tribomates to constitute the anti-friction, as well as wear resistive shielding film. Thus, the tribology of additives in a base fluid is controlled by the process of film formation. However, the process of film formation on the substrates varies with particle to particle. Greenberg et al. [40] studied the tribological properties of IF-WS_2 nanoparticles dispersed in API grade-I base oils of three different viscosities under different regimes of lubrication; hydrodynamic, mixed, and boundary. The authors proposed that the transfer film formation mechanism decreased the friction to almost half of its original value in the case of mixed lubrication regime. Moreover, the authors reported that the formation and stability of transfer film was not much effective in boundary regime and hydrodynamic regime.

2.1.1.3 Colloidal effect:

Colloidal oil suspensions of nano-additives might access elastohydrodynamic (EHD) contacts and there, mechanical confinement may be possible for the growth of erratic layers and make the lubricants tribologically superior. The colloidal effect has been noticed under the conditions of low speed rolling contacts and boundary regime of lubrication [23,80]. The authors suggested that the formation of erratic or patchy layers of boundary film is not feasible in high-speed situations.

2.1.1.4 Third-body material transfer/ exfoliation

Third-body model were crafted for a clear understanding of the IF-MoS_2 and IF-WS_2 mechanisms under extreme contact zones by Rapoport et al. [81]**.** As per their model, 3rd body is nothing but the base fluid containing wear trashes and delaminated nanosheets of nano fullerenes. Analogous studies on the exfoliation process of IF-MoS_2 and IF-WS_2 also had been discussed by other researchers [89,90]. Nano-compression tests were performed under varying states of shear loading by Lahouij et al. [91]. The performance of IF-WS_2 was investigated, and it was found that it was quite similar in action and mechanism of IF-MoS_2. The ease of deformation of IF was investigated using high-resolution SEM, which bestows the inference of the compressive strength of nano-additives of different sizes [92].

2.1.2 Developments in particle-based lubrication using inorganic solid lubricants

Till date several micro/nanoparticle-based lubricants have been examined for their tribological performance and optimized for steel-steel contact pairs and aluminium-steel pairs [93–96].

2.1.2.1 Boric Acid (H_3BO_3) and Boron Nitride (BN)

Lubrication properties of H_3BO_3 and BN have been explored over the past several decades to for their use as an industrial lubricant [97–106]. Düzcüko˘glu and Acaro˘glu [43] had investigated the antiwear performances of commercial mineral oil, vegetable oil and a combination of vegetable oil and boric acid. The found that boric acid-containing oil reduces the surface damage by physically covering the surfaces with a firm film of hard boron crystals. Lovell et al. [44] prepared an environment-friendly lubricant by homogeneously mixing boric acid powder additives with canola oil. Based on their friction-wear experiments, they found that the lubricant containing nanosized boric acid additive performed better than all the other

lubricants, in terms of antifriction and antiwear performance. However, it was observed that there are difficulties associated with the use of these particles alone as a lubricant in the extended duration contacts since boric acid powder dehydrates or is forced out of the contact zone during sliding contact [107].

Charoo and Wani [28] investigated the friction and wear behaviour of SAE 20W50 engine oil with different concentrations of h-BN nanoparticles. They observed that the lubricant with h-BN exhibits superior tribological characteristics. Based on their investigation of wear scars they found that h-BN nanoparticles form a boron-rich boundary film on the surface, which reduces the friction and wear. Subsequently, Charoo and Hanief [108] investigated the tribological characteristics of h-BN, WS_2 and graphite additives in SAE 20W50. They again found that the nanolubricant with h-BN is better than that of WS_2 and graphite, in reducing COF and wear.

2.1.2.2 Nanoclay

MMT clay is a naturally occurring layered phyllosilicate material and is widely used as a reinforcement for polymer composite materials [109–112]. The suggested tribological mechanism associated with this particles is exfoliation and tribofilm formation on the surface [113,114]. However, their use as a lubricant additive for the improved tribology is yet to be explored [115–117].

Pena-Paras et al. [118] carried out a case study on the application of MMT nanoclay based lubricants for lowering the tool wear. They tested with the various concentrations of MMT nanolubricants and observed an increase in the wear resistance of the wire-bending part of the tool by 30%, as compared to the unfilled base lubricant. Recently, in an another study carried out by Rebis et al. [54], a cheap nano-clay was added to mineral oil to enhance the lubricating properties. The authors found no straightforward correlation between R_a and wear scar diameter (WSD), film thickness, and friction coefficient.

Another variant of nanoclay, hallosite nanotubes (HNTs) have a high modulus, suitable to be used as EP additive. Fernández et al. [119] used HNTs as green additives for improving the tribological properties of lubricants. Their results showed that the addition of 0.05 wt% HNTs can delay scuffing initiation and increased the load-carrying capacity by 72%. In their study they could attain a reduction of COF by 70%. After a detailed investigation of the wear track they found a a tribofilm on the track, which they believed was formed by the exfoliation of HNT´s

outer sheets caused by the high pressure. However, it was also found that a higher particle concentration (0.10 wt%) diminishes the enhancing effect of HNTs due to agglomeration [120].

2.2.2.3 MoS_2 and WS_2

Many authors reported the use of commercially layered MoS_2 powders, usually configured as solid lubricants, to prepare dispersions in various oils and demonstrated the beneficial effects of friction and wear reduction [40,81,121–131]. Hu et al. [121] evaluated the tribological performance of liquid paraffin (LP) containing vafrious morphologies of MoS_2 as additives. Their results revealed that all types of MoS_2 additives improve the tribological properties of LP, however, nanosized MoS_2 particles are more effective as compared to microsized MoS_2.

An et al. [122] performed the tribological tests using nano-lamellar WS_2 and MoS_2 s as oil additives. It was also found that the oil dispersions with nano-lamellar disulfide particles exhibit the better antiwear properties as compared to commercial powder. Ilie and Tita [123] had investigated the tribological performance of 30 nm-sized MoS_2 nanoparticles, under two friction conditions such as a block-on-ring tribometer and a four-ball tribometer. It was observed that the load-bearing capacity of the lubricant is increased due to the formation of protective film of MoS_3 as a result of piling of nano-sized particles on friction pairs. The authors also revealed that the nano-sized MoS_2 particles showed a smaller COF and higher wear resistance than that of the common MoS_2 particles.

Rosentsveig et al. [129] performed tribological testing using nanoparticles in two synthetic PAO oils, and results were compared to bulk MoS_2 and IF-WS_2. Tests were carried out under the conditions of high pressure and low humidity. The IF-MoS_2 exhibited a very low coefficient of friction, and the lowest rate of wear was recorded among the measured systems. Tribological performance study had revealed that the IF nanoparticles strongly depends on their crystalline order and size.

Praveena et al. [130] investigated the effect of friction using MoS_2 suspended in hexadecane oil at 150°C under steel-steel contacts. The friction data were compared with the introduction of nominally dry MoS_2 particles under similar material contacts (steel-steel). Following their study, the authors observed that in dry experiments, the friction coefficient was directly proportional to temperature change, while the reverse was right in the case of wet experiments.

Rabaso et al. [131] studied the tribological effect of the size and morphology of inorganic fullerene- particle additives in the oil, using four different types of IF-MoS_2 under the pure-sliding and severe boundary conditions. The authors reported high wear reduction using the particle additives, and it was confirmed by optical profilometry. However, it was observed that under the fixed conditions, the size and morphology of the IF particles do not influence the tribological performance.

In the series of mechanism investigations of nanoparticles, another study was carried out by Kalin et al. [132] using MoS_2 multi-wall nanotubes (MWNTs) under a boundary lubricated regime. The authors evaluated that MoS_2 (MWNTs) in base oil can reduce friction more than 2 times, and wear loss by 5-9 times approximately. The authors proposed a film effect mechanism for this improved tribological properties. The authors also have suggested the exfoliation action routes, which were believed to be more reliable and possible mechanisms of friction reduction than the rolling action of nanotubes.

2.1.3 Developments in particle-based lubrication using carbon-based solid lubricants

Most widely used carbon-based solid lubricants include graphite, carbon black, graphene and MWCNT. While graphite has been explored as solid lubricant since decades, graphenes and CNTs are being highly explored for various other applications. Recently, MWCNTs are being explored as oil additive due to their inherent properties. Some noteworthy literature reports are available on the use of MWCNT under dry and lubricated steel-steel tribo-contacts [10,133–139]. Hwang et al. [10] studied the tribological effect of the size and morphology of various carbon-based particles such as graphite, graphite nanofibers (GNF), carbon black (CB), and CNT in commercial mineral oil, using a disc-on-disc tribometer. They claimed that nanosized particles at 0.1% by volume concentration as an additive in oil showed noteworthy improvement in lubrication characteristics. Nanosized particles act as a spacer in the oil, thereby minimizing the direct contact of asperities and hence reduce friction coefficients. The authors also concluded that spherically shaped nanoparticles are much effective in reducing friction coefficients of friction as compared to fibrous nanoparticles due to their less agglomeration in solvents.

Su et al. [136] investigated the tribological properties of MWCNT-in-vegetable oil, with different particle sizes and volume fractions. They observed an improved tribological characteristic in the presence of MWCNT which they attributed to the fact that MWCNTs could

penetrate the valleys of surface asperities provide a ‘‘roller bearing’’ effect. However, in the case of thick and long MWCNTs as additive, the agglomeration and interlocking of MWCNTs increase the resistance for relative motion between sliding surfaces, causing an increased friction coefficient. They also observed the reduced abrasive wear and adhesive wear, with the addition of MWCNTs in vegetable oil. Singh and Suresh [140] examined the friction-wear properties of MWCNT as oil additive (0.5 wt. %) to evaluate the particle's performance as an extreme pressure agent. As per their observation, it was indicated that the MWCNTs can effectively enhance the EP behavior of oil.

Salah et al. [141] tested the carbon-rich fly ash and commercial CNT as the lubricant additive in the 150 SN base oil. The obtained results showed that fly ash shows superior frictional characteristics over the commercial CNTs. In an another study carried out by the authors [142] CNTs of fly-ash were tested as lubricant additives in 100SN, 500SN, and 150BS base oils and compared with that of other commercial graphene, SWCNTs and MWCNTs. A superior frictional performance was observed with CNTs of fly ash and claimed that CNTs of fly ash may be a good alternative and low-cost lubricant additive.

Nunn et al. [143] carried out tribological investigation of various nanocarbon additives in PAO oil. A comparative analysis of friction coefficient was carried out using nanodiamond, SWCNT/MWCNT, onion-like carbon (OLC), or nanographene platelets (NGPs). They found that the presence of sp_2 nanocarbon in oil reduces the friction coefficient of PAO by 8–12 times approximately, whereas nanodiamond additive is more effective in the wear reduction.

2.1.4 Developments in surfactant functionalized particle-based lubricants

The selection of suitable surfactant depends upon the lubricant properties as well as the properties of the tribopair materials. The selection of surfactant depends on the nature of formulated lubricant desired for any specific application. Kailas et al. [144] in their work highlighted the key considerations associated with the selection of surfactants in metal cutting fluids formation. Demas et al. [26] studied the tribological properties of poly-alpha-olefin (PAO10) base oil containing nanosized BN and MoS_2. They had used benzethonium chloride surfactant for Al/CI contacts, operating at 20, 40, and 100°C temperatures. It was noticed that at their selected operating parameters, BN did not offer suitable anti-friction property, while MoS_2

nanoparticles are efficient in friction as well as wear reduction. The cationic surfactant used in their study showed a positive influence not only in creating stable dispersion but also in noticeable reduction in friction and wear. Based on the spectroscopic analysis they revealed that the a tribo-chemical film generated on the substrate contributed to the improvement of the lubrication performance in the case of MoS_2 nanolubricant, while BN nanolubricants showed negligible traces of tribofilm.

Bhowmick et al. [145] investigated the tribology of carbonaceous nanoparticles suspension in hexadecane under steel-steel contacts. They also compared the tribological performance of suspensions containing carbon black and diesel soot particles. A Poly-isobutylene succinimide (PIBS) surfactant was used to prepare stable dispersions in hexadecane for all these tests. Based on their investigation they claimed that the lubricity and the tribological performance of these particles are greatly influenced by the physical structure and chemistry of particles. The authors also claimed that the grafting of the surfactant on the nanoparticles has a profound effect on the particle dispersion. Srinivas et al. [146] studied the extreme-pressure property of 600 N base oil dispersed with two concentrations of 0.05 and 1.0 wt. % of nanosized MoS_2 particles and with 1 vol. % of PIBS as the dispersant. Extreme pressure behavior testing was performed on a four-ball wear tester and obtained an improvement in the seizure load and load-wear index in the case of nanosuspensions as compared to base oil.

Aralihalli and Biswas [147] evaluated the friction coefficients of nanometric MoS_2–oil formulations dispersed with two dispersants under steel-steel sliding contacts. Two dispersants-ATS and SPAN 80 were used to graft on the particle surface and charge the particle negatively, which eventually reduced the agglomerate size substantially. The coefficient of friction was found in the range of ~0.03 approximately. The authors suggested that the friction mechanism is influenced by the chemistry of the surfactant molecule. Sonali et al. [148] conducted a stability study of SDS modified nano MoS_2 additive dispersed in engine oil, using the DLS technique. The optimum concentration of the surfactant was checked by the bubble pressure method.

Muzakkir et al. [149,150] also explored the tribological importance of the MWCNTs as lubricant additives, in the presence of surfactant. To reduce the agglomeration of nanoparticles they used a suitable amount of TX-100 surfactant. They observed that the lubricant containing functionalized MWCNTs with surfactant is able to reduce the coefficient of friction more remarkably. Based on

these experiments, the authors determined the optimum quantity of MWCNT for the minimum wear of the friction pairs.

Rabaso et al. [151] investigated the usage of succinimide-based dispersants for the nanosized inorganic fullerenes (IF) in fully formulated lubricants. They reported that the usage of the selected dispersants play a predominant role in controlling the tribochemistry of the contact, either by the excessive adsorption on the surfaces or by encapsulating the released molybdenum disulfide platelets, which prevent the tribofilm adhesion. However, they could find a balance between nanoparticle concentration and friction reduction, by adopting a very low dispersant concentration and after a running-in period.

Chebattina et al. [152] investigated the effect of the size of MWCNTs additives in gear oil tribology. To enhance the dispersion stability and to shorten the length, MWCNTs were mildly processed in a ball mill and stabilized with a SPAN80 surfactant before dispersing in the lubricant. The size and structure of the milled particles were assessed using electron microscopy and Raman spectroscopy, whereas the stability of the dispersed MWCNT was evaluated using light scattering techniques. It is found that the stability of the lubricant is increased by the ball milling and subsequently, the lubrication performance has improved significantly. However, it was also observed that ball milling for the extended period results in the adverse effect on the MWCNT as oil additives.

Lijesh et al. [153] analyzed the tribological performance of nanolubricant using MWCNT. They observed that the tribological properties of the mineral base oils are enhanced significantly with the addition of MWCNT, particularly under extreme contact pressure conditions. However, agglomeration of MWCNTs significantly deteriorated the performance. Therefore they recommended that a suitable surfactant or dispersant is essential to maintain the MWCNTs in the de-agglomerated state.

2.1.5 Developments in the dry tribology of hybrid AMMCs

Kumar et al. [154] reported the wear properties of Al6063 reinforced with graphite (Gr) and aluminium oxide (Al_2O_3) composite using a pin-on-disc wear monitor. Two compositions: Al-6%Al_2O_3, Al-6%Al_2O_3-1%Gr were fabricated via stir casting method. From the observed result it was concluded that the binary composite offers more wear resistance as compared to mono-

reinforced composite. The authors also remarked that the multi-axially forged specimens exhibited more strength than as-casted samples owing to the existence of pores in as-casted state. Pai et al. [66] synthesized liquid stir cast Al6061–Gr–granite dust hybrid composites and tribological properties of these composites had been investigated. Precipitation hardening treatment was done for improvement in hardness values before sliding wear tests. The fractography study of worn-out specimens using SEM for different combinations of load, speed, and composition, has been investigated. They found that the hybrid combinations of granite dust with a certain composition yields in higher mechanical properties and improved wear resistance. In the year 2016, a critical review on the tribological behaviour of Al/SiC/Gr hybrid AMMCs was carried out by Singh [155]**.** The study revealed that an increase in the Gr content in AMMC beyond a limiting value can deteriorate the tribological properties. In a recent study carried out by Miloradovi´c et al. [156] it was revealed that the stability and the thickness of mechanical mixed layer (MML) plays a critical role in defining the wear performance of the composite. They also observed that hybrid AMMC performs better than the single particle-reinforced AMMC. In a similar tribological study by Mosleh-Shirazi et al. [157] it was observed that Al/SiC/2%Gr hybrid nanocomposites performed better than the Al/SiC nano-composites.

Lokesh and Mallik [158] investigated the dry sliding wear behaviour of heat treated Al6061/3wt % graphite/(3-9wt %)SiCp hybrid composites, using a pin-on-disc machine. Their experimental results showed that an increased content of SiC particles, in the presence of graphite greatly stimulate the development of antiwear layer between the pin and counterface.

2.1.6 Developments in the lubricated tribology of AMMCs

Babić et al. [159] studied the lubricated tribological properties of compocast A356/SiC/Gr hybrid composite using a hydraulic lubricant. The analysis has shown the presence of MML on the surface of composite block. Wear rate of composite was found to be 3 to 8 times lesser than that of the base metal. Walker et al. [160] reported the wear characteristics of AMMCs reinforced with 15.% of Cr_3Si, $MoSi_2$, Ni_3Al, and SiC particles, sliding against a M2 steel in the presence of a commercial synthetic oil. The contact pressure between the sliding pair was estimated to the range of ~750–890MPa. They found that the $MoSi_2$ and Cr_3Si reinforced alloys exhibited the lowest wear rate.

Akhlaghi and Zare-Bidaki [161] investigated the influence of graphite on the dry and oil-impregnated sliding wear characteristics of sintered Al2024/graphite composite. They found that an increase in graphite content upto a 5 wt% reduces the coefficient of friction and wear rate for both dry and wet sliding, however, further addition of graphite did a complete reversal in the wear behavior.

Panwar et al. [162] investigated the tribology of Al6061/red mud composite for conducting the tribological experimentation. It has been found that an increased content of red mud, along with the reduced size of particles lead to improved tensile strength and impact energy. A SAE 20W-40 lubricant was used for lubricated tribological experiments from which they were able to attain a very low specific wear rate under the lubricated condition. Their study highlighted that instead of the disposal of red mud and it can be used as an economical reinforcement for AMMC.

In a recent study carried out by Pradhan et al. [163] it was seen that the coefficient of friction remains low in the alkaline environment as compared to the other environments. Shrivastava et al. [164] investigated the tribological properties of 10%SiC-Al7075 composite with various sliding speeds and loads under dry, lubricated, and inert gas environment. The lubricated experiments were conducted with a SAE20 oil, using a pin-on-disk tribometer. They observed th maximum COF for inert condition and minimum for lubricated condition. Following a detailed investigation of the worn-out surfaces, they proposed that the shearing and re-organization of a thin lubricating film of particles between the contacts is responsible for the reduced coefficient of friction and wear.

Poria et al. [165] studied the lubricated sliding tribological behavior of stir-cast Al-TiB_2-nano Gr hybrid composites with varying loads, speeds, and wt% of reinforcements. The lubricated sliding wear test was carried out using a commercial lubricant (SAE20W40). Their study revealed that without any change of solid lubricant or TiB_2 in the matrix if the contact is lubricated, tribological characteristic of Al-5.5TiB_2-4Gr composites enhanced significantly. They remarked that in the lubricated condition, wear depends on the stability and interaction of lubricant film with the contact surfaces.

Srivyas and Charoo [166] investigated the sliding wear behaviour of graphene reinforced hybrid AMMC under boundary lubricated sliding conditions. They had used variable concentration of graphene nanoplatelets (GNP) to the Al-6 wt% Al_2O_3 composite for the lubricated sliding. They observed a very low and stable COF and wear. It was proposed that the exceptional lubricating

effect of the GNP particles alongwith the layer of lubricating oil was responsible for the low friction and wear. They reasoned that the 2D GNP particles form a protective layer at the sliding interface, which easily shears because of the weak Vander wall force.

2.1.7 Developments in the particle-based lubricant/nanolubricant for AMMC tribology

Dixit and Khan [167] investigated the role of graphite size on the lubricated sliding wear behaviour of Al-10 wt% SiC composites. The wear tests were conducted in different lubricated environment such as oil, oil+ 5wt % graphite (7-10 μm), and oil+ 5wt.% graphite (100 μm). Results showed that the oil-in-graphite lubricated conditions led to the less wear rate of samples than that in oil alone. The addition of smaller sized graphite particles to the oil lubricant led to the minimum wear rate. They attributed it to the possibility of the more stable lubricating film formation caused by the smaller graphitic particles in the oil. Recently, Charoo and Wani [168] investigated the friction and wear properties of Si_3N_4/SiC nanocomposite using a diamond nanolubricant wherein they observed a very low friction and wear coefficient when sliding under a normal load of 600 N.

2.2 RESEARCH GAPS

The comprehensive literature review presented above mainly involved with dry and the lubricated tribology of composites or hybrid composite, as well as the developments in the implementation of the nanolubricant for the more conventional tribopairs. It has been observed that the antifriction and antiwear properties of the composites can be enhanced either by hybridization of composites or lubricating the contacts, but to a certain extent. AMMCs are one of the preferred materials and are in growing demand for the applications requiring light-weight energy saving system components. The superior tribological characteristics of these developed AMMCs (such as ultra-low friction and wear, accompanied by a high load carrying capability) can be achieved by implementing a suitable nanolubricant, which is certainly beyond the reach of self-lubricating composites or composites sliding under liquid lubrication.

However, based on the latest developments on the dry and liquid tribology of composite materials, it is observed that there is still a huge potential left in the study of the micro/nanolubricant formulation for the alloys and composite contacts. Based on the comprehensive literature review presented in this chapter following gaps are identified.

- Lubricated tribology of hybrid composite contacts is a less discovered arena. There is still a huge scope of work exist, especially for the applications requiring a ultra-low friction-wear and high load carrying capacity.
- A very limited work has been carried out on the particle based lubrication of composite contacts to explore the detailed interaction mechanisms of dispersed solid lubricants, with or with the presence of surfactant/dispersant.
- Particle-based lubrication using MWCNT or surfactant-functionalized MWCNT is yet to be explored for the composite tribology. Majority of the studies involving the MWCNTs, with or without the functionalization is available for the aqueous lubrication
- There is no comprehensive work reported in the literature on the comparison of tribological performance of surfactant-functionalized nanoparticle additive-based fully formulated commercial oil and base oils.
- The role of thermophysical properties of oil and surface textures of composites in defining the tribological behavior of AMMCs is yet to be understood.
- Rarely, any work is available in the literature detailing the selection of any specific nanoparticle additive which will best suit the tribological characteristics of the target composite
- The multiphysics and multi-scale modeling of the tribological characteristics of the lubricated AMMC sliding contact is yet to be explored.

CHAPTER 3
RESEARCH OBJECTIVES, MATERIALS AND METHODOLOGY

3.1 INTRODUCTION

Based on the literature survey discussed in the previous chapter, this chapter presents the problem statement and research objectives, proposed plan of work, raw material information and the methodology adopted for the present study. It also encompasses the information on the various experimental procedures and analysis techniques used to carry out the proposed research work.

3.2 PROBLEM FORMULATION

Many proposed models and modifications are suggested to save energy consumption due to severe friction and wear of contacting surfaces or poor lubrication contacts. Lubricant formulation is one of them. Owing to the potential benefits of micro/nanolubricant, there is a growing usage of particle-based liquid lubricant. Metal metal matrix composites have proven to be better as compared to the conventional monolithic materials and a few instances of the commercial usage of AMMC for tribological applications have been already mentioned in the chapter 1.

For an engineering application involving the composite materials it is an essential requirement that the novel lubricant formulation or the modification of the existing lubricant to be made. However, the development of the nanolubricants for the composite is still an unexplored area. The innovation in this area of lubrication can help in reducing the cost involved in the development of costly composite materials. However, while developing the novel lubricant for the composite tribocontacts, we need to address some of the fundamental issues, such as stability of the suspension, thermophysical properties of the prepared lubricant, particle-oil-surfactant interactions under the composite tribo-contact and the underlying lubrication mechanism.

Studies using base mineral oil have their own importance because such studies set the preliminary insight for an additive to be used as anti-wear (AW), anti-friction (AF) or both and

the fully formulated oils are prepared by the blending of these base mineral oils with various additives. As mentioned earlier, agglomeration of particle additives is one of the main challenges in the formulation of nano/micro lubricant, so the selection of surfactant or de-agglomerating agent plays a critical role in a novel lubricant formulation. Moreover, application of surfactant functionalized solid additives in the development of liquid lubricants involves interesting and intricate features which should be taken care of while developing or formulating such type lubricants for the composite materials, such as AMMCs. Thus, a comprehensive study is necessary to get the insight of the tribological behavior of particle-laden lubricant and to compare with fully formulated commercial oils so that the findings can be suitably accommodated while developing the new industrial oil package for any specific applications involving composite materials.

The present research work will be directed towards the combinatorial approach of utilizing the benefit of composite materials and particle-based lubrication to attain the improved tribological properties. Therefore, for the present research work, a systematic investigation will be made to explore and address some of the fundamental issues related to the formulation and modification of a particle-based lubricant for the lightweight composite material, using the selected solid lubricant and surfactant.

3.3 RESEARCH OBJECTIVES

Based on the gaps identified from the literature review, following research objectives are proposed through the present research proposal ***"An Investigation on Wet Tribology of Dispersed Solid Lubricants in the Presence of Surfactant***".

a) Characterization of base oils, solid lubricants, and materials for tribocontacts.
b) Investigation and selection of suitable base oil for tribological applications.
c) Tribological investigation on the selected solid lubricant dispersed to the selected base oil.
d) Formulation of micro/nano lubricant using a suitable surfactant.
e) Tribological investigation and mechanism study of formulated lubricant.
f) To compare the performance of prepared oil lubricant with commercially available formulated oil.

3.4 PLAN OF WORK

A systematic approach has been adopted to carry out the present works to meet the proposed research objectives. The plan of work, which is followed for the present research, is shown in Figure 3.1.

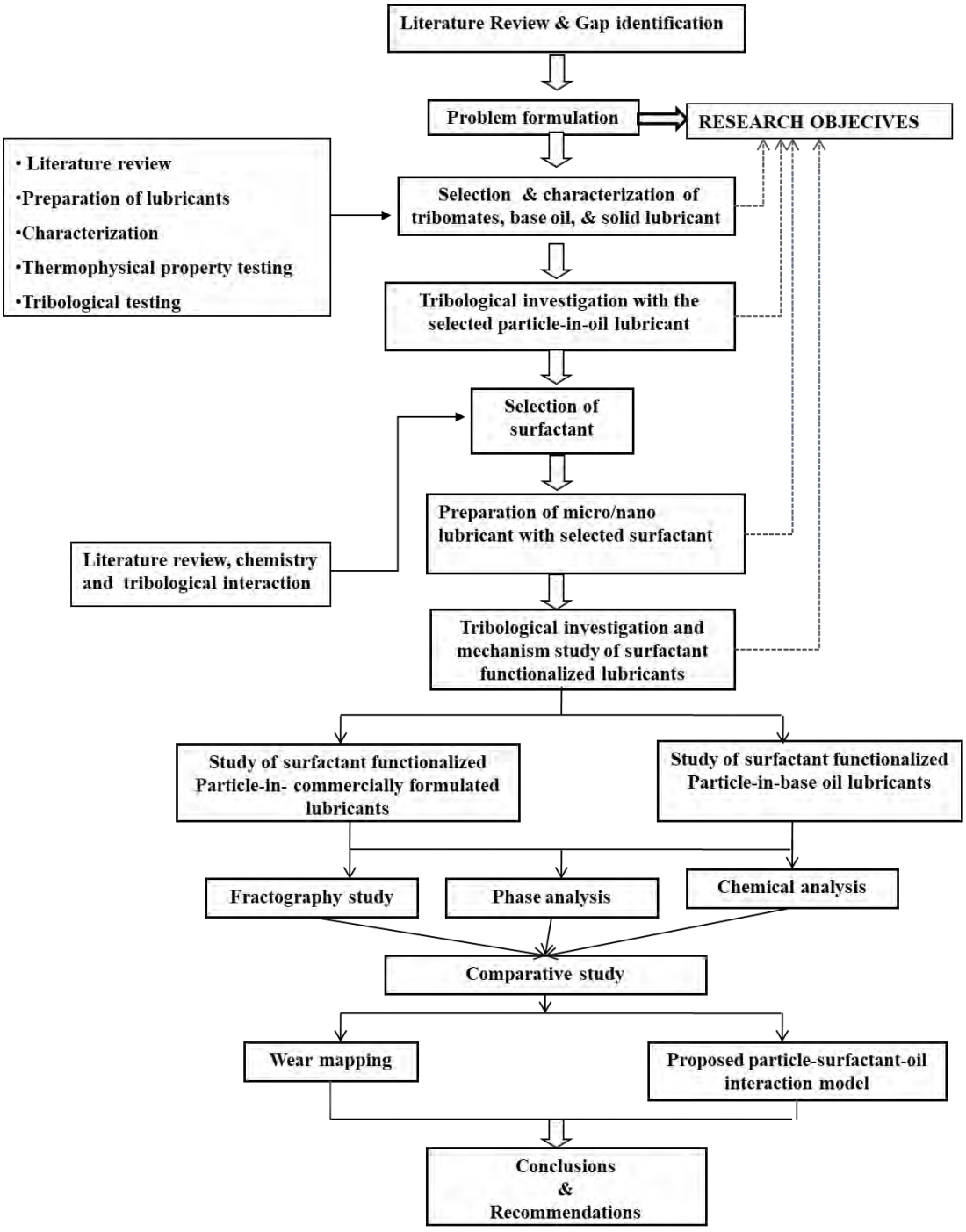

Figure 3.1: Methodology for the proposed work

At the very outset, a comprehensive literature survey is carried out to identify the potential research gaps and to formulate the research proposal. The major objectives of the proposed research are then defined. This was followed by the preliminary selection of the various raw materials, such as base oils and solid lubricants, including the tribomates. Selected base stocks were blended with solid lubricants using an ultrasonicator probe. Thermophysical and stability studies were performed for the prepared nanodispersions. Based on the pilot studies a final selection of all the components of the tribosystem is made. In-depth surfactant chemistry, along with a comprehensive literature survey, facilitates the selection of surfactant in nano/micro oil dispersions.

Afterward, tribological investigation was carried out with the selected particle-in-oil lubricant, where the composition of lubricants is controlled by varying the type of solid lubricants in the selected base stock, with and without surfactant. After the tribological tests, the wear patterns on the pins were investigated in the subsequent stages. Microstructural characterizations helped in understanding the fundamental mechanism of interaction between tribomates and particles via lubricated as well as in dry contacts. Relevant techniques were used to study the microstructures and phase analysis, including SEM, EDS, XRD, Raman, etc.

This was followed by a detailed investigation on the lubrication mechanism and surfactant-particle-oil interaction mechanism. For this purpose, in addition to the characterization of friction and wear behavior of tribomates, the thermophysical properties, surfactant chemistry, dispersion stability etc will be explored for different compositions of nanolubricants. A comparative tribological investigation then followed to compare the performance of surfactant-assisted oil dispersions and commercially available formulated oil. Finally, a statistical tool will also be used to study the effect of operating parameters on the performance of the tribopair and to develop a wear map.

3.5 DETAILS OF RAW MATERIALS

3.5.1 Preliminary screening of materials for tribopairs

Aluminium alloy and its composites find their potential applications in the automobile components such as in pistons, cylinders, as well as in metal-working industries. Material selection criteria involved the requirement of high strength to weight ratio, hardness and wear-resistance AMMC. To meet the ever-demanding light-weight and high-performance materials for various tribological applications and equally to overcome the challenge involved with the use of

aluminium alloys in this research development and functional performance of a hybrid AMMC has been investigated.

Al6061 alloy is much explored because of their technological importance and found to be highly corrosion and oxidation resistant, and exhibits moderate strength. For these reasons the matrix material for the present research has been taken as Al6061-T6. Type of reinforcement plays a critical role in defining the properties of the developed composites. Different reinforcement gives different properties in composite materials. The selection of reinforcement for making composite should depend upon the desired properties like thermal stability, low density, increase strengthening in metal matrix, as well as how these reinforcements interact and form interfacial bonding with metal matrix. In hybrid composite two or dual reinforcements are used i.e., one hard reinforcement and another soft or functional reinforcement. In this study, SiC (average size = 50 μm, polydisperse) used is as the hard reinforcement and graphite (average size = 30 μm, polydisperse) as soft reinforcement. Prior to the selection, detailed comparisons of the properties for a few alternative hard reinforcing agents were made as shown in Table 3.1.

Table 3.1 Selection of hard reinforcement

S.No	Reinforcing agent	Density (g/cm^3)	Thermal Expansion ($10^{-6}/K$)
1.	Boron nitride	3.45	1.2
2.	Boron Carbide	2.52	9.4
3.	Aluminium oxide	3.98	8.1
4.	Titanium carbide	4.93	7.0
5.	Titanium diboride	4.52	8.0
6.	Zirconium dioxide	5.68	12.2
7.	Aluminium nitride	3.26	4.5
8.	Silicon Carbide	3.21	11.0

The excellent mechanical and physical properties, alongwith the reasonably good thermal properties of SiC helps in improving the properties of metal matrix when it is added to the matrix. Some of the thermo-mechanical properties of SiC is listed in Table 3.2. There are numerous works available reflecting the benefits of SiC in AMMCs. Due to the improved mechanical and the thermal properties as compared to the other ceramics, SiC enhances the wear-resisting behaviour of the Al-SiC metal matrix composite.

Table 3.2 Thermo-mechanical properties of SiC

Vickers Micro-hardness (HV_{50})	2000-2500
Elastic modulus	410 GPa
Melting Temperature	2730^0C
Thermal Conductivity	120W/m^{0}K
Fracture Toughness K_{IC} (MPa $m^{1/2}$)	4.0

On the other hand, steel and CI are obvious choice for the counter surfaces as many potential applications, such as automotive piston-cyliner liners of some of the modern engine technology rely on these. Though, ductile CI traditionally used for the liner, however, it is metallurgically heterogeneous, prone to weak adhesion to the coating. The ductility and the strength of steel, alongwith the coefficient of thermal expansion can be the potential pair with a suitably developed composite piston materials. For the present investigation, initially AMMC/Steel and AMMC/CI tribopairs are chosen for the pilot tribological investigation under the dry and liquid lubrication. Al-SiC or Al-SiC-graphite composites have been suitably fabricated and used as the pin material for the present study. EN31 (Composition: 0.95-1.12 C%, 0.40-0.6 Mn%, 0.25-0.35 Si%, <0.005 S%, <0.008 P%, 1.0-1.56 Cr%, <0.05 Ni%, and 0.059 Mo%) and grey CI (Composition: 90-92 Fe%, 3.2-3.6 C%, 0.3-0.6 Mn%,2.1-2.5 Si%, 1.0-1.55 Ni% and 0.02-0.025 S%) is used as the disc material on the pin-on-disc tribometer The density of the various powdered and bulk materials are listed in Table 3.3.

Table 3.3: Density of the other powders/materials used for tribomates

Material	**Purpose**	**Density (g/cm^3)**
Al6061-T6	Matrix phase	2.7
Graphite(C)	Reinforcement	2.2
Steel(EN31)	Disc specimen	7.8
Cast iron(CI)	Disc specimen	6.99

3.5.2 Preliminary screening of particle additives to be used for the particle-based lubrication

The particle additives for the particle-based lubrication of the present work are selected from some of the proven solid lubricants. Besides, Nanoclay and MWCNT remained unexplored for the particle-based lubrication of composites. The lubricant additives chosen for the present study include MoS_2, MWCNT, Boric acid (H_3BO_3) and Nanoclay. Besides, prior to shortlisting for

further study using these particle additives they are assessed for their thermal stability to suit the high temperature applications.

Table 3.4: The allowable temperature range for the thermal stability of various solid lubricant materials.

Particle additive	**Thermal stability**
MoS_2	less than 450 ^{0}C [122]
MWCNTs	420-1300* [169]
Graphite	upto 500 ^{0}C [170]
Boric Acid	Less than 180^{0}C [171]
Nanoclay	Less than 200^{0}C [172]
Note:*results were reported for argon-rich environment	

The reinforcing powders were procured from central drug house, Delhi, India. The particle additives for lubricant were purchased from Nanoshell, Inc.,India. The details of CNT used for this work is shown in Table 3.5.

Table 3.5 Detail of Soft Reinforcement (CNT)

Diameter of CNT	10-20 nm
Length of CNT	3-8μm
Density	1.5 g/cm^3

3.5.3 Preliminary screening of base oils and commercial oils

The base oils can be categorized into two generic classes (mineral oil and synthetic oil), as shown in Figure 3.2. In most of the cases synthetic oils are generally superior to mineral oil. Mineral motor oil, on the other hand, is developed directly from crude oil. For high temperature applications these are superior in terms of lubricity and stability over long periods of time. As per the API classification group IV oils are primarily referred to PAO synthetic oil. Some of the strengths of these oils over the mineral oil include higher VI and oxidation stability, superiority in low and high-temperature performance, and lower volatility. However, these synthetic

lubricants are not recommended when additive solubility, lubricity, and film strength are of prime importance. They are also are more costlier than the mineral oils (Table 3.6).

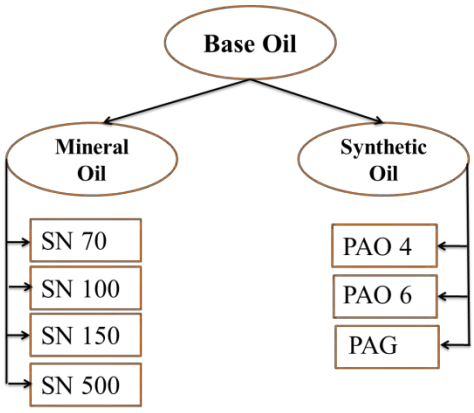

Figure 3.2: Schematic diagram of generic classification of base oil

For the application requiring superior corrosion resistance and medium range VI and operating temperature, often mineral oil base oils are as good as synthetic oils [173]. For these reasons, mineral oils are commonly used in the majority of applications. Besides, they are cheaper (usually, 4 times less than PAO), and have reasonable service capabilities. That is why, mineral based oils are shortlisted for the present investigation.

Table 3.6:Comparison of essential properties for mineral oils and PAOs [173]

Criteria	Mineral oil	PAOs
Cost	L	M
Seal compatibility	AA	AA
Corrosion stability	E	E
Oxidation stability	BA	AA
Viscosity range	AA	A
Flash point	M	AA
Pour point	A	L
Temperature ranage	BA	AA

Note: E, AA, A, BA, L, M stands for Exceptional, above average, average, below average, low and medium respectively.

Generally, higher VI oils are preferred for lubricant formulations and accordingly, VI-improvers are being extensively used to formulate the multigrade oils. However, it has been observed that under the high-stress/shear conditions, the VI-improved fluids loose their efficiency and do not contribute to the film thickness and traction to the predicted levels [174]. In this regard Group I

base oils along with the particle additive might be a preferred option. Grade-I olis are solvent-refined and the cheapest base oils on the market. Commonly available base oils of grade-I include SN70, SN150, SN500, etc, whereas the most widely used formulated oil includes SAE30, SAE10W30, SAE15W30, SAE15W40, SAE20W50. For the preliminary screening, three grade-I base oils (SN70, SN150, and SN500) and two SAE grade fully formulated industrial oils (SAE 15W40 and SAE 20W50) were shortlisted for the tribological testing. The selection of the base and industrial oils was based on various factors such as low cost, ease in availability, and similarity in the base stocks in both base and commercial oils. Samsoil, Pvt., India supplied these oils.

3.6 CHARACTERIZATION METHODS

A brief overview of the techniques and equipment used for the various experimental investigations in the present study is given below.

3.6.1 Microstructures and morphology of composites and raw materials

3.6.1.1 Scanning Electron Microscopy (SEM) and Optical microscopy

The microstructural and elemental composition analysis of fabricated composites and various raw materials was carried out in a SEM (Make: JEOL JSM-6510LV, Oxford Instruments). The SEM used for the present work is shown in Figure 3.3. An Energy Dispersive X-Ray Analyzer (EDX or EDS), attached to the SEM helped in the the compositional information of the sample surface. A metallurgical optical microscope was also used to investigate the morphology and microstructure at the low magnification.

Figure 3.3: Scanning Electron Microscope (Courtesy: SAI Lab, TIET)

Figure 3.4: Optical Microscope (Courtesy: Advance Measurement Lab, TIET)

3.6.2 Microhardness Characterizations

The microardness characterizations of composites and alloys were carried out in terms of Vicker's micro-hardness. Microhardness of the samples were measured using a Vicker's micro-hardness tester (Maker: Leitz, Germany). The Vicker's micro-hardness indentations were taken at 300 g load and 20 s of dwell time.

Figure 3.5: Vickers Micro-hardness Tester (Courtesy: A.M. Lab, TIET)

3.6.3 Phase and Chemical analysis

3.6.3.1 X-Ray Diffraction (XRD)

The XRD study was carried out in an XPert PRO PANanalytical diffractometer using Cu *K*α radiations. For this purpose, X-rays were produced with high-speed electrons from a hot tungsten (W) filament. The XRD measurements were carried out at room temperature, and the scan rate and scan range were maintained at 1^{o} min^{-1} and 10^{o} to 90^{o}, respectively. Using XRD, the various phases present on the worn-out tracks were identified.

Figure 3.6: X-Ray Diffractometer (Courtesy: SAI Lab, TIET)

3.6.3.2 Fourier-transform infrared spectroscopy (FTIR)

Before the detailed tribological investigation, SN500 and SAE20W50 base oils were characterized using a FTIR, to extract the information on the major functional groups present. A FTIR with a resolution of 1 cm^{-1} (Perkin Elmer, Spectrum RX-I, India) was used for the present study to identify the functional groups present in the oils and film on the wear tracks.

3.6.3.3 Raman spectroscopy

Raman spectroscopy has been proven to be a powerful nondestructive technique for the characterization of carbon-based materials, and has become an indispensable tool for understanding many fundamental aspects of all sp^2 carbons, including MWCNT. Presence of disorder, graphitization and carbon-carbon interaction [175–178] are well assessed using this technique. In this technique, the excitation of the atomic structures is typically done with a

monochromatic light source (laser) of specific known energy (wavelength). However, this is a volume-sensitive technique, so absolute intensities must not be used for a quantitative comparison. Instead, intensity ratios, such as the I_D/I_G or the I_{2D}/I_D ratio, are widely accepted, with the first one known as the defect index and the latter one as purity index. While using the integral peak intensity, the full width at half maximum (FWHM) of the peaks can be related to the crystallinity of the analyzed graphitic carbon structure [179]. All the experiments carried out in the present work used a laser excitation wavelength of 514.5 nm and beam intensity of 12.5 mW.

3.6.3.4 UV-Vis-spectroscopy

This tool can be used for the identification of chemicals, and carry out the quantitative determination of different organic and inorganic compounds in solution. The underlying principle of this spectroscopy is related to the interaction of light with matter. When the ultraviolet radiation interacts with the sample, it is absorbed and increases the energy content of the atoms or molecules or excites the electrons from the ground state towards a higher energy state. As a result, a distinct spectrum is produced, the peaks at specific wavelength being associated to the particular chemical compound. For the present work, UV-Vis spectroscopy was used to monitor the stability of nanofluids by observing the maximum absorbance and the corresponding wavelength, their decrement with the extended time after the preparation of the nanofluids.

3.6.4 Dispersion and thermophysical characterization of particle-oil suspensions

The fluid dispersions for the present work were processed with a ultrasonication (Make-Oscar Ultrasonics, Mumbai, India). A Brookfield-DVII +Pro characterized the rheological properties of the prepared dispersions. A thermal bath was attached to the viscometer so that the effect of temperature on various lubricant concentrations to be studied. A Pt-100 type sensor is used for the measurement temperature of fluid dispersion. Moreover, steady-state measurements were taken under varying shear rate (3.40 s^{-1} to 34.00 s^{-1}) conditions using SC4-31 as a spindle for particular lubricant formulations. Thermal conductivity measurements were done with transient state method KD2-pro apparatus (Decagon Devices, Inc.). KS-1 needle or probe (heater as well as a temperature sensor) having diameter 1.3 mm and length of 60mm was used to carry out measurements, which is absolutely immersed in the dispersion. Prior to record the data, the probe was calibrated using glycerol. All the experiments involving the rheological and thermal studies were conducted in the temperatures range of 30°C-60°C.

3.6.5 Functional Characterizations-Unlubricated and Lubricated Sliding Wear Tests

Tribological tests have been carried out using a pin-on-disk tribometer. The equipment is established in the Department of Mechanical Engineering of TIET, through the in-house research grant and is shown in Figure 3.7.

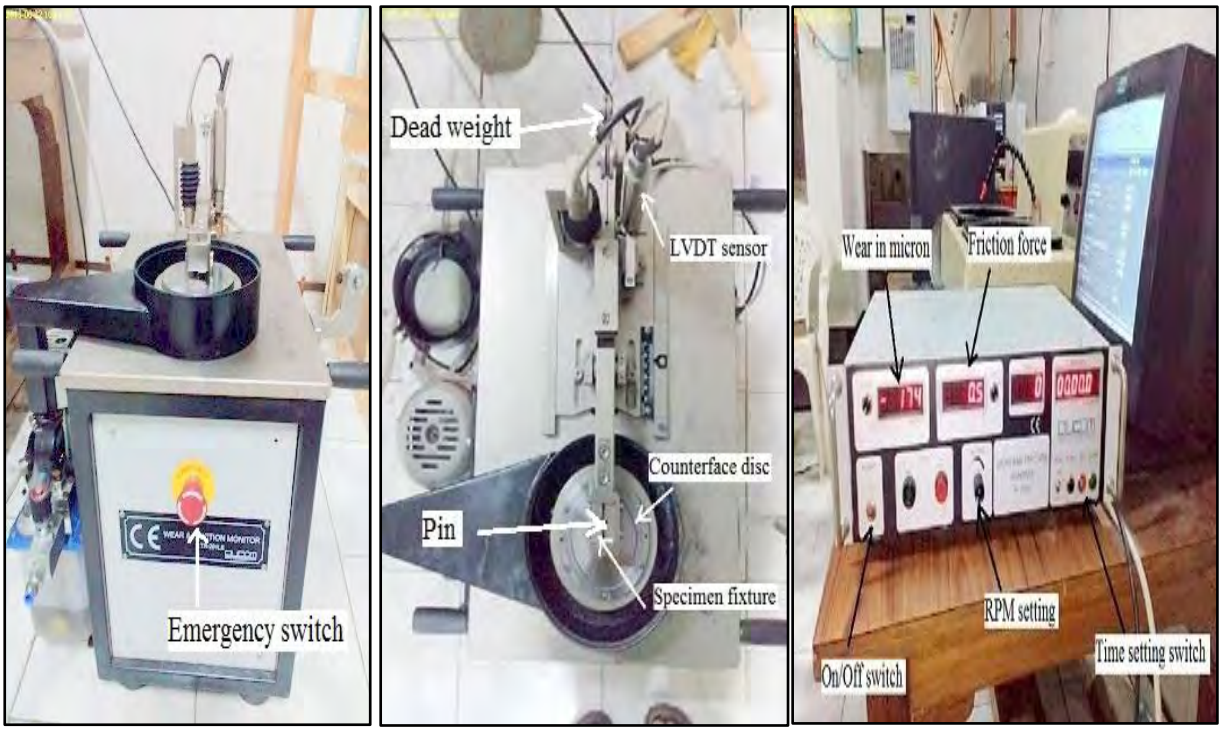

Figure 3.7: Tribometer - pin-on-disk

Before each test run, pin and disc samples were cleaned with acetone or benzene. An automatic digital indicator provides the frictional forces encountered during the sliding contact. Wear rates were estimated based on the weight loss by weighing samples before and after each experiment with the help of a digital weighing balance (Greifensee, Switzerland).

After the sliding wear tests, the samples were gently rinsed with acetone in an ultrasound bath for 10 seconds in order to remove the majority of the excess oil while preserving most of the adhered particles and layers on the worn surfaces. It is important to mention that the time period of ultrasonication for rinsing is taken low so that it insignificantly affects the adhered third bodies, ensuring only removing the loosely attached particles. On the other hand, use of acetone

cannot be neglected for preparing and rinsing samples to separate out loose debris and contaminations prior to characterization techniques.

Various operating parameters and the materials associated with the tribological investigation at the various sages are listed in Table 3.7.

Table 3.7: Material specifications and operating parameters for friction-wear testing

Parameters	**Description**
Test configuration	Pin-on-disc (Model: TR-201LE, Ducom).
Pin material specifications	Material: Al6061, AMMC (Al6061/SiC) & hybrid-AMMC (Al6061-SiC-Gr)
	Geometry & Size: hemispherical; ϕ 6 ×35 mm
	Initial roughness, R_a: 0.12-0.17 μm
Disc material specifications	Material: Hard bearing steel EN31 and CI (for preliminary stage)
	Size: ϕ 100 × 8 mm
	Initial roughness, R_a: 0.19-0.25 μm
Applied load	9.8, 29.5 & 49 N
Sliding speed	0.1-2.5m/s
Time of test	1800 sec
Sliding distance	180-2250 m
Lubrication	Fresh oil lubrication, dry solid lubricants, particle-based liquid lubrication, and surfactant-assisted particle-based liquid lubrication
Lubricant flow rate	1.5ml/100sec
Temperature conditions	30±2°C,

The testing parameters shown in Table 3.7 are chosen carefully to suit the application demand. In the metal forming applications the contact pressure may go upto a few hundreds MPa, whereas in IC engine contact pressure at the piston ring-cylinder wall interface is function of combustion gas pressure. However, the contact is mostly subjected to the boundary to mixed film lubrication. For the present study, the combination of the high load, the moderate speed, and the small

amount of lubricant flow allowed the system is designed to operate near the boundary lubrication regime.

The contact pressure induced in the dry contact by the selected operating load in the present study is estimated and listed in Table 3.8. The present study emphasizes that whenever application demands high load and speed between sliding contacts, such situations can be well managed by introducing an appropriate lubricating oil to reduce temperature rise and friction, and consequently wear rate. In the metal forming process, the study can be beneficial in terms of the development of forming fluids for aluminium alloy composites. This present investigation can be extended to the study of novel material pairs for piston-cylinder arrangement with few additional testing parameters such as temperature and extreme pressure conditions.

Table 3.8: Information about contact pressure.

Load	**Contact pressure(MPa)**
9.81	774.23
29.43	1116.65
49	1323.94

All the sliding tests were repeated more than four times to make sure for the reproducibility of the results; the mean values from these trials were reported. After the test runs, the specimens were gently rinsed using the cleaning solvent in an ultrasonic bath to wipe out excessive oil content. This also helped in preserving the majority of the adhering elements and films on the worn-out specimens.

CHAPTER 4

EXPERIMENTAL INVESTIGATIONS: CHARACTERIZATION AND SELECTION OF THE COMPONENTS OF THE TRIBOSYSTEM

4.1 INTRODUCTION

The wet sliding of AMMCs is itself a complicated job. The influence of particle additives and addition of surfactant makes the phenomenon intricate. A well-planned methodology and systematic experimental trials are necessary for proving the scientific findings. The following sections briefly explain the various characterization and experimental results related to the selection of tribopair, particle additive, and surfactant. For a better insight into the lubrication mechanism, the thermophysical properties of fluid properties have also been investigated.

4.2 MORPHOLOGICAL CHARACTERIZATION OF POWDERED MATERIALS FOR AMMC

SEM images of as-received materials such as silicon carbide and graphite are shown in Figure 4.1 .The average size of the SiC particles is observed as 50 μm and graphite's average size is in the range of 30 μm, with the presence of a few large sized particles.

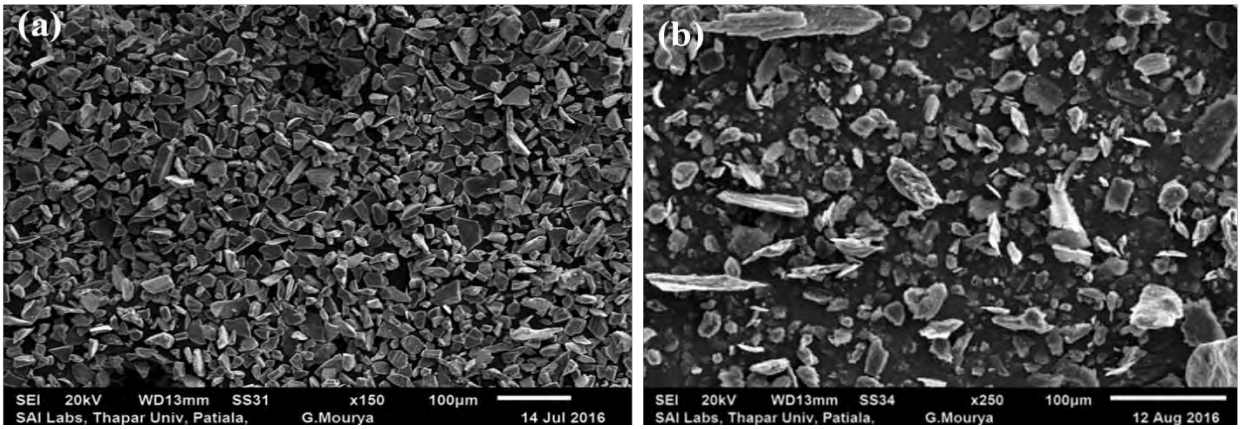

Figure 4.1: SEM micrographs of as-received: (a) Silicon carbide (SiC) and (b) Graphite (Gr) powders

4.3 MICROSTRUCTURAL AND HARDNESS CHARACTERIZATION OF AMMC

A stir casting approach was used to fabricate the aluminium metal matrix composite. From the earlier works on AMMC it was observed that reinforcement of SiC in the range of 10-20% may be more effective in terms of the ductility, hardness and strength which are desired for the intended purpose, whereas graphite can be added from 2 to 5 wt% to enhance its lubricating property. It is a well-known fact that the wear properties of a material depend primarily on its hardness [180].

Table 4.1: Hardness (HV) measurement for alloy and alloy composite specimens

Sample	Test1	Test2	Test3	Test4	Test5	Mean	St. deviation
Al6061	72	77	73	76	74	74.4	2.074
Al6016-5%SiC-2%Gr	78	79	80	81	90	81.6	4.827
Al6016-5%SiC-3%Gr	79	80	85	87	88	83.8	4.087
Al6016-5%SiC-4%Gr	77	82	84	77	73	78.6	4.393
Al6016-10%SiC-2%Gr	98	90	100	99	103	98	4.848
Al6016-10%SiC-3%Gr	100	108	96	103	105	102.4	4.615
Al6016-10%SiC-4%Gr	104	98	97	99	90	97.6	5.029
Al6016-15%SiC-2%Gr	112	114	122	104	101	110.6	8.355
Al6016-15%SiC-3%Gr	113	116	112	110	128	115.8	7.155
Al6016-15%SiC-4%Gr	106	105	119	116	121	113.4	7.440

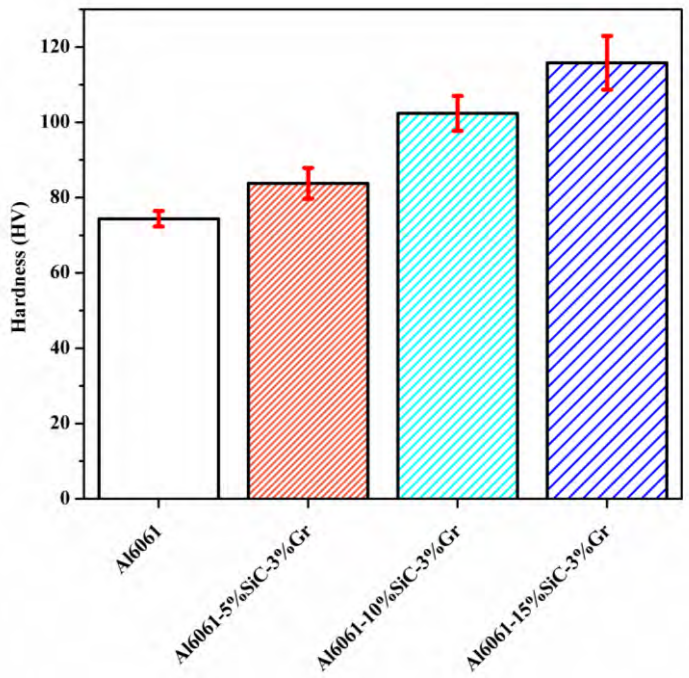

Figure 4.2 Hardness measurements for various samples viz. alloy and h-AMMCs

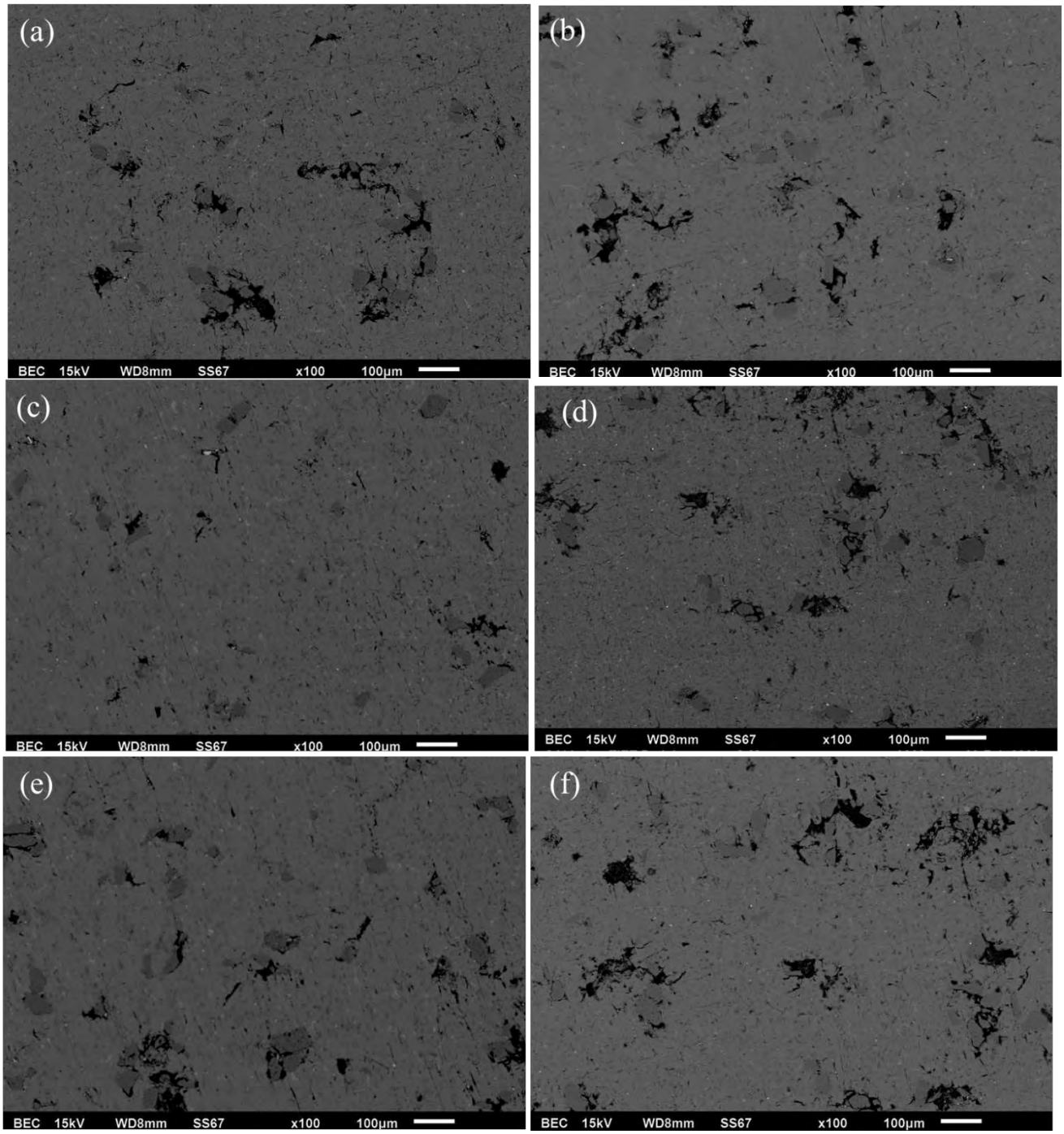

Figure 4.3 SEM micrographs for (a) Al6061-5%SiC-3%Gr, (b) Al6061-5%SiC-4%Gr, (c) Al6061-10%SiC-3%Gr, (d) Al6061-10%SiC-4%Gr (e) Al6061-15%SiC-3%Gr, (f) Al6061-15%SiC-4%Gr

To optimize the property, in the present work a pilot study on the hardness estimation has been carried out to select the suitable composition of the reinforcements. Vicker's microhardness test (Mitutoyo with Model: MVH-I) was carried out on the cast polished samples before analyzing

the sliding wear tests. The average hardness of the pin was estimated from the measured values at five different locations on the samples. Table 4.1 shows the evaluated hardness of the fabricated composites with various concentrations of the reinforcements. From the Table 4.1 it is observed that, although with the further addition of SiC and graphite after 10% and 3%, respectively, there is an increase in hardness but in a desired rate. Besides, the deviation associated with the measured values increases (Table 4.1 and Figure 4.2).

Following the preliminary investigation of the SEM micrographs (Figure 4.3) it was observed that at the higher percentage the inadequate dispersions of the reinforcements lead to the particle agglomeration. Besides, some of the earlier investigations reported that higher the SiC content, higher is the brittleness induced in the AMMC. Hence, for the subsequent study in the present work composite with a fixed weight percentage of silicon carbide (10%) and graphite (3%) is used. The average value of micro-hardness for the alloy and composite was found to be 74.4 HV and 102.4 HV, respectively.

On further investigation with the EDS, it is confirmed that the agglomerates around the SiC particles are graphite indeed (Figure 4.4-4.8).

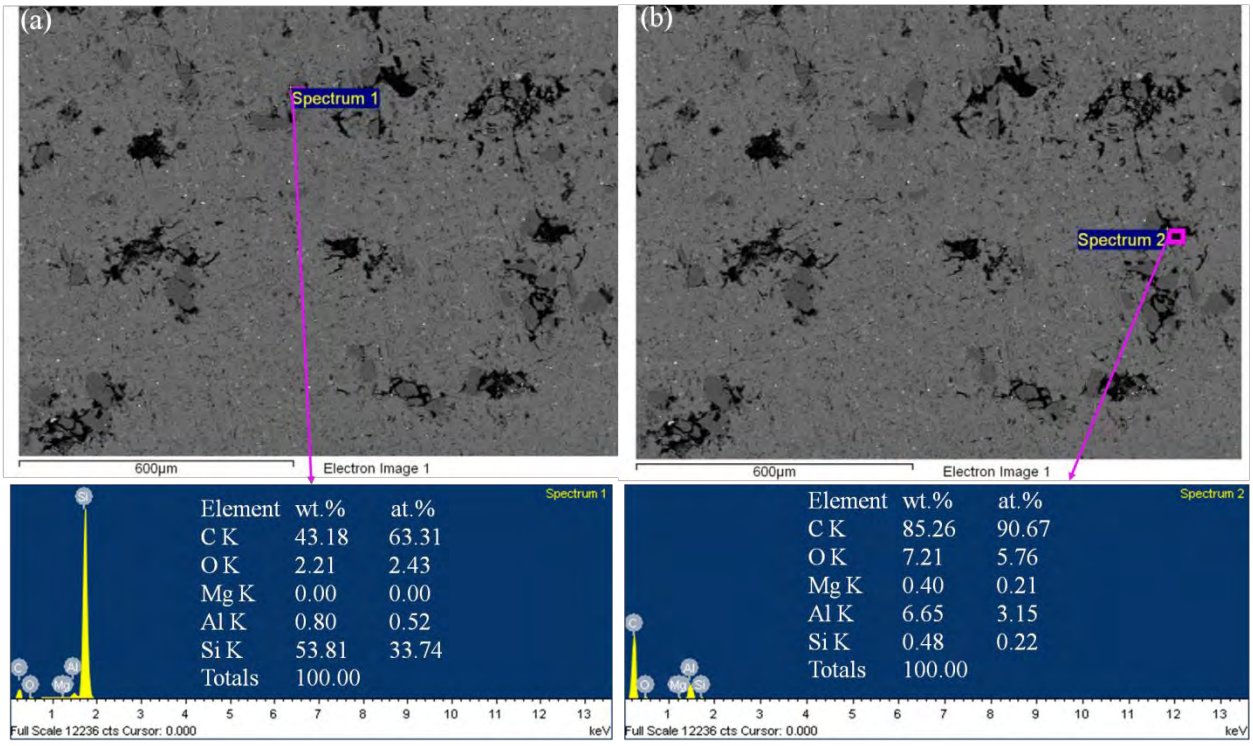

Figure 4.4: EDS on the reinforcements of h-AMMC

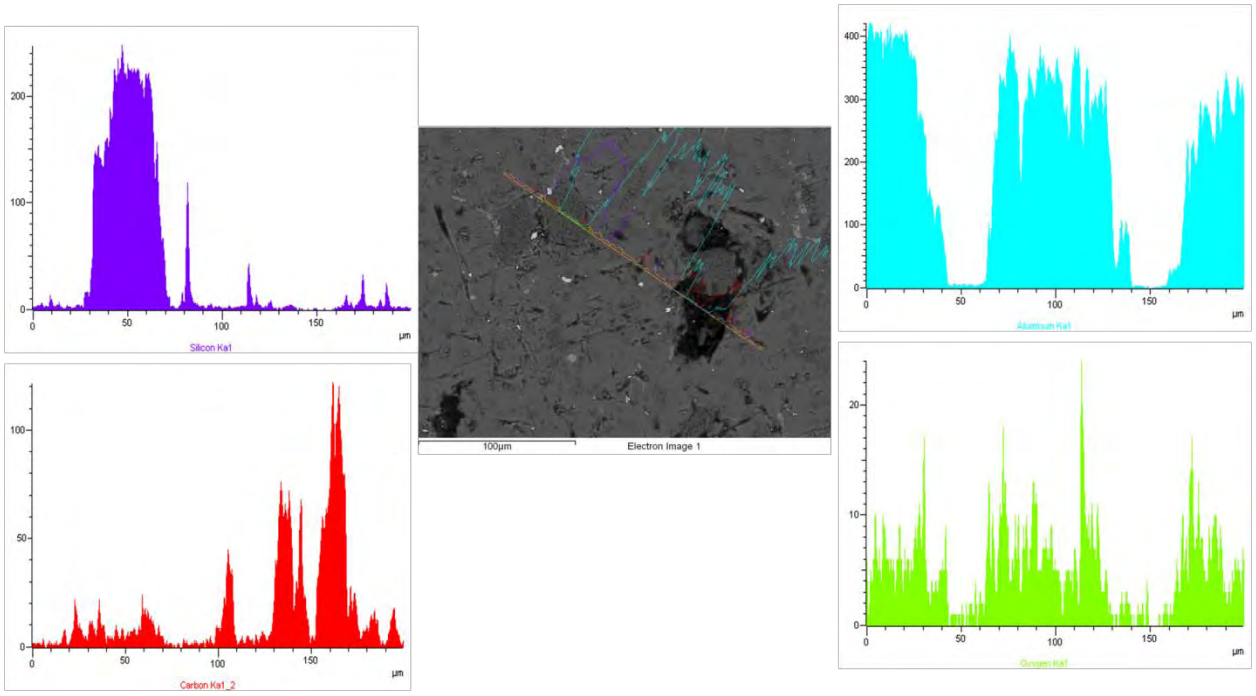

Figure 4.5: EDS line mapping on the surface of a fabricated h-AMMC.

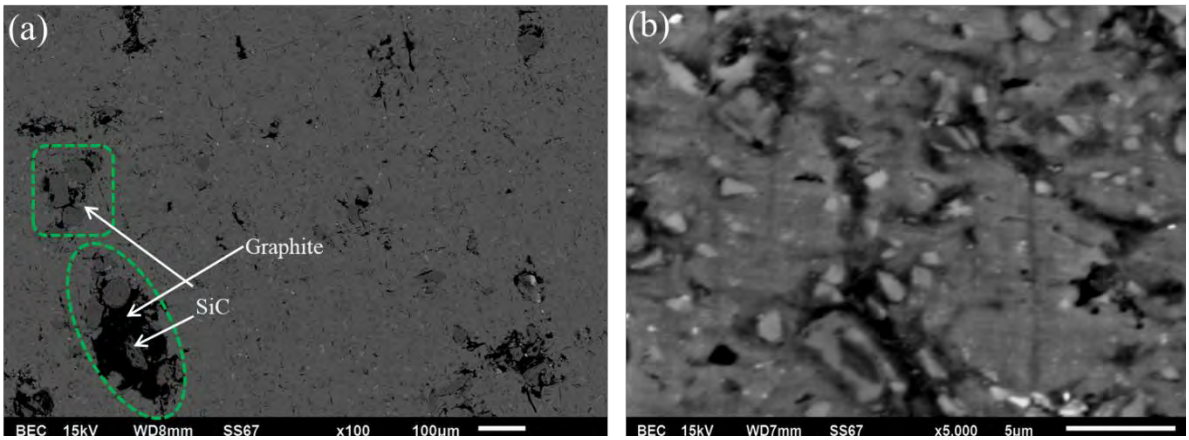

Figure 4.6:.(a)Agglomeration of reinforced particles are depicted by dotted circle(s), (b) Higher magnification SEM images of reinforced zone

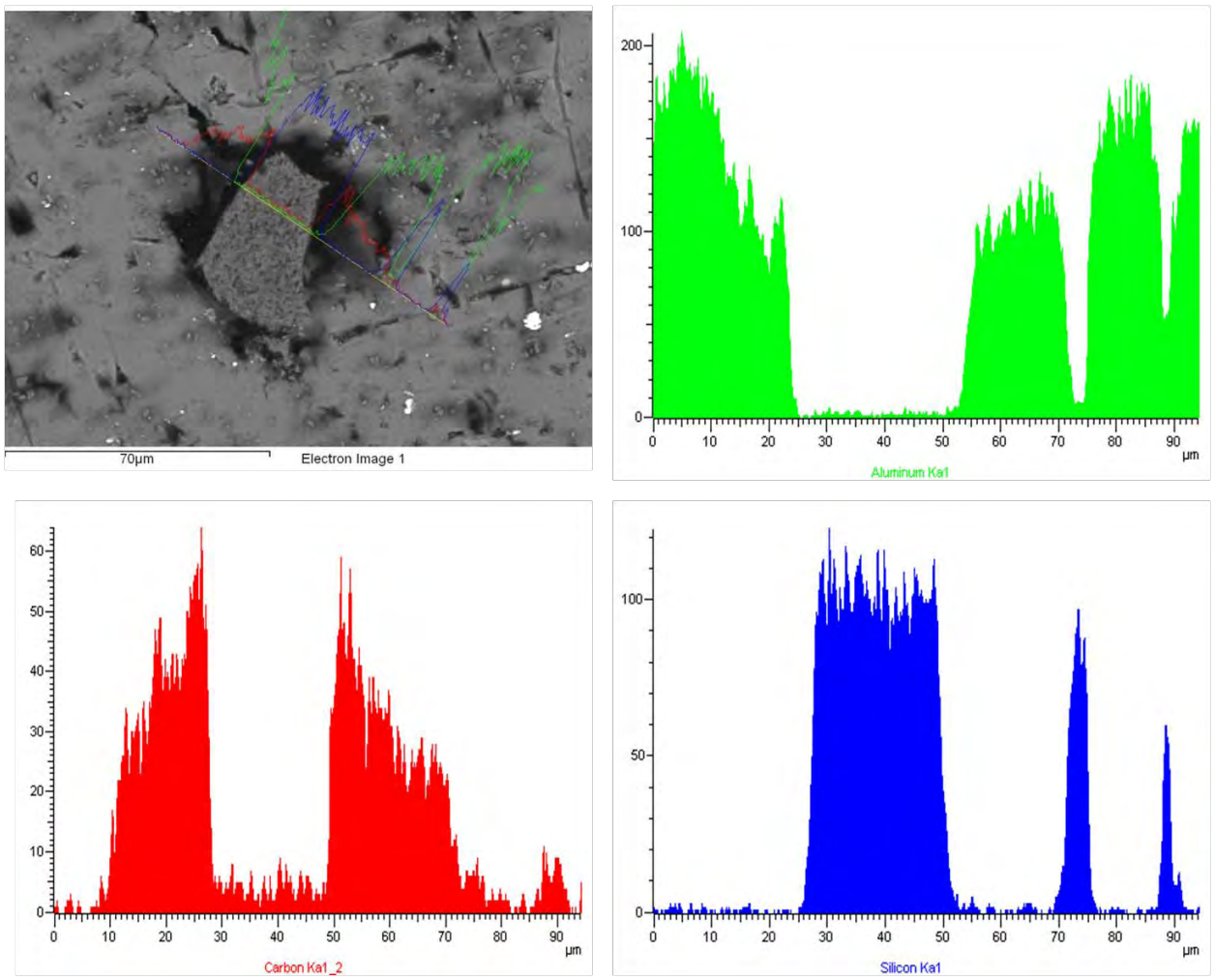

Figure 4.7: EDS micrograph showing presence of graphite at the interface of aluminium matrix and ceramic.

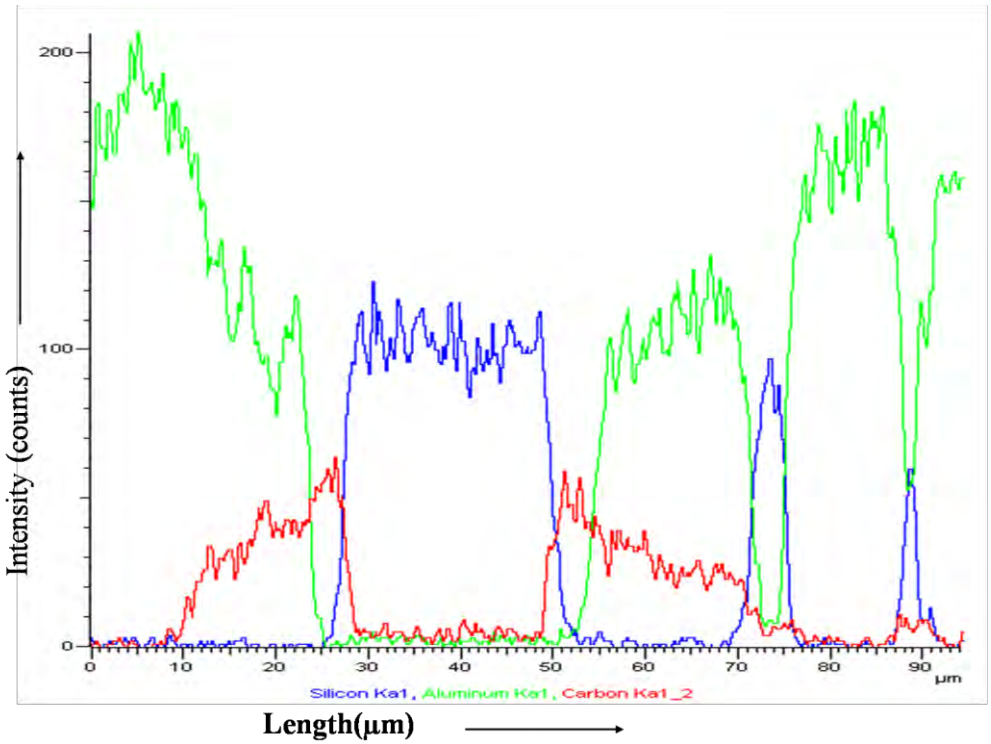

Figure 4.8: Comprehensive EDS plot (intensity versus length) showing presence of graphite at the interface of aluminium matrix and ceramic.

To assess the matrix property, EDS point mapping is also done on the matrix of the composite (Figure 4.9). From the figure it is clear that matrix remained as un-oxidized aluminium. The reinforcements are seen well distributed in the matrix. The SEM and optical micrographs, along with the EDS on various locations of the polished samples, confirm the presence of well-distributed hard reinforcements in the soft matrix phase of the composites. To further assess the phases on the surface of the h-AMMC, EDS is performed on the particle, particle-matrix interface and the matrix (Figure 4.10).

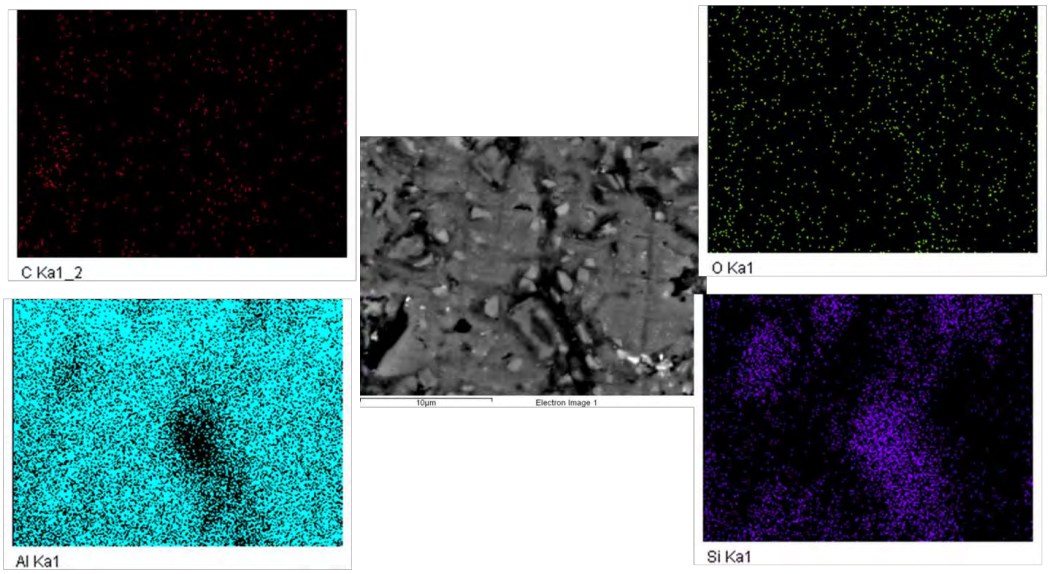

Figure 4.9: Point mapping the matrix of h-AMMC

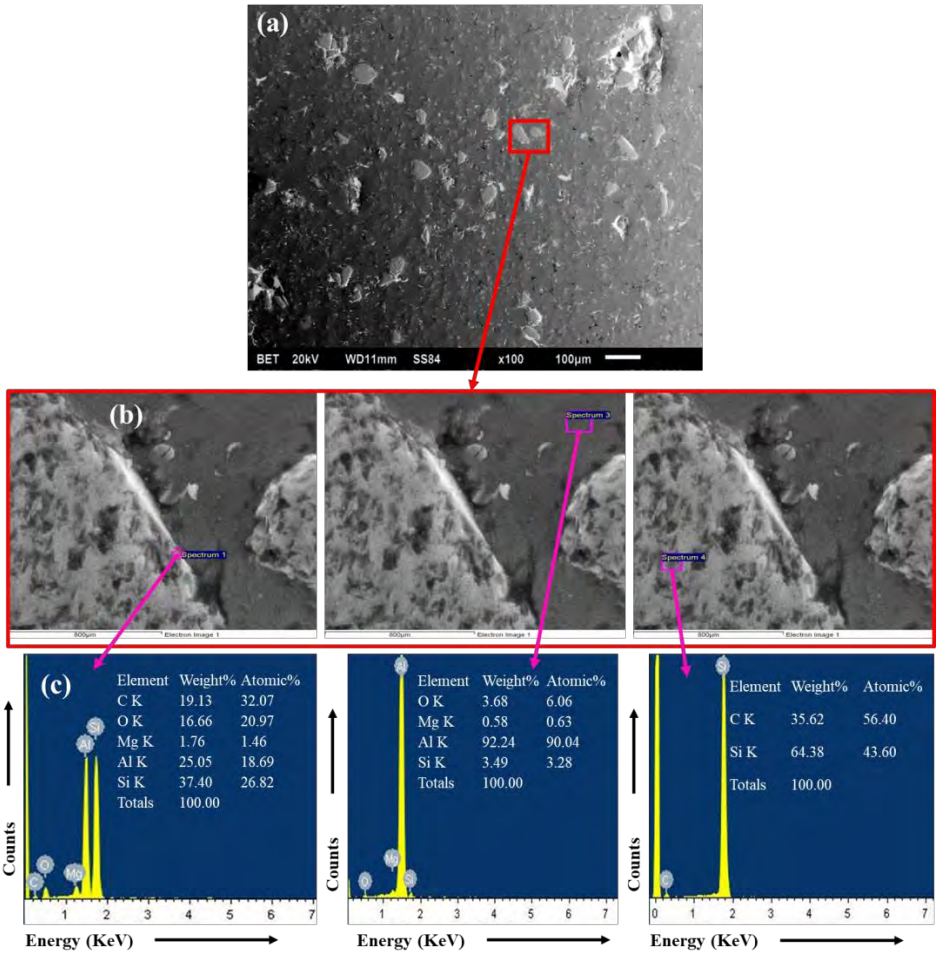

Figure 4.10: (a) SEM micrographs and EDS spectra at the interface, matrix and ceramic particle surface, (b) Optical image (Lieca 200X) of a stir-cast hybrid AMMC.

4.4 CHARACTERIZATION OF SHORTLISTED BASE OIL/LUBRICANT

As mentioned earlier, some of the key base oil properties required for lubricant formulation include the viscosity, VI, pour point, density, oxidation and thermal stability. Some of these properties are assessed for the shortlisted oils. The physical and chemical properties of the shortlisted oils, as mentioned in the previous chapter are listed in Table 4.2.

Table 4.2: Typical physical and chemical properties of base oils and fully formulated lubricants

Properties of Lubricant	SN 70	SN150	SN500	SAE 15W40	SAE 20W50
Kinematic viscosity at 40^0C, cSt	12.19	30.1	84	111	120
Kinematic viscosity at 100^0C, cSt	2.97	5.2	14	15	15.2
Viscosity index	>94	>94	>94	140	145
Density at 15^0C, g/cm^3	0.850-0.858	0.830-0.860	0.820-0.885	0.870-0.876	0.885-0.892
Pour point, ^{0}C	-18	-9	<(-25)	<(-30)	-30

The Table 4.2 reflects that SN500 and SAE20W50 can be the obvious choice for the present work to assess the fundamental insights of the particle-based lubrication of the composite contact. SN 500 base oil is most commonly used for the development of the traditional automotive lubricants. SAE20W50 is a fully formulated oil which one of the most commercial oils used as automotive lubricant. These two oils are then characterized with the FTIR to identify the functional groups present in them. Figure 4.11 shows the major absorption FTIR peaks around wave numbers 2924.20 cm^{-1}, 2854.35 cm^{-1}, 1461.20 cm^{-1}, 1376.99 cm^{-1} and 722.89 cm^{-1}. The stretching vibrations of CH_2 groups are encountered at 2924.20 cm^{-1} and 2854.35 cm^{-1}, and the bending of vibrations of CH_2 groups are occurred at 1376.99 cm^{-1}. The stretching of saturated alkyl group around the wave number 2924.20 cm^{-1} causes a significant loss in the transmittance of IR, causing an abrupt dip in the % transmittance as shown in Fig. 4.11[181] . The absorption peaks around at 1461.20 cm^{-1} and 722.89 cm^{-1} corresponds to aliphatic chain of C-C bond and the rocking vibration of long-chain alkanes, respectively. It is important to mention that the absorption peak observed at 960-965 cm^{-1} for commercial oil corresponds to the presence of zinc-based antiwear additive [182,183].

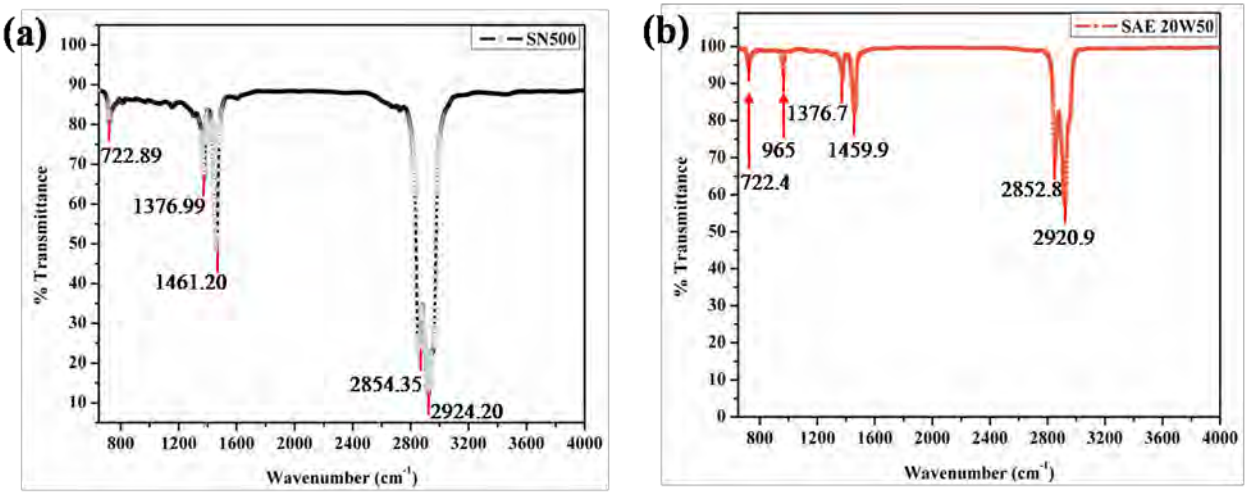

Figure 4.11: FTIR Spectra of (a) base oil (SN500), (b) Fully formulated oil (SAE 20W50)

4.5 FINALIZATION OF OIL AND TRIBOMATES BASED ON THE TRIBOLOGY

As mentioned earlier, Steel and CI was shortlisted initially for the disc material. To finalize the disc material a pilot tribological study was carried out. The friction response of the pair and wear rate of the h-AMMC pin were recorded, and is shown in Figure 4.12 and Table 4.3.

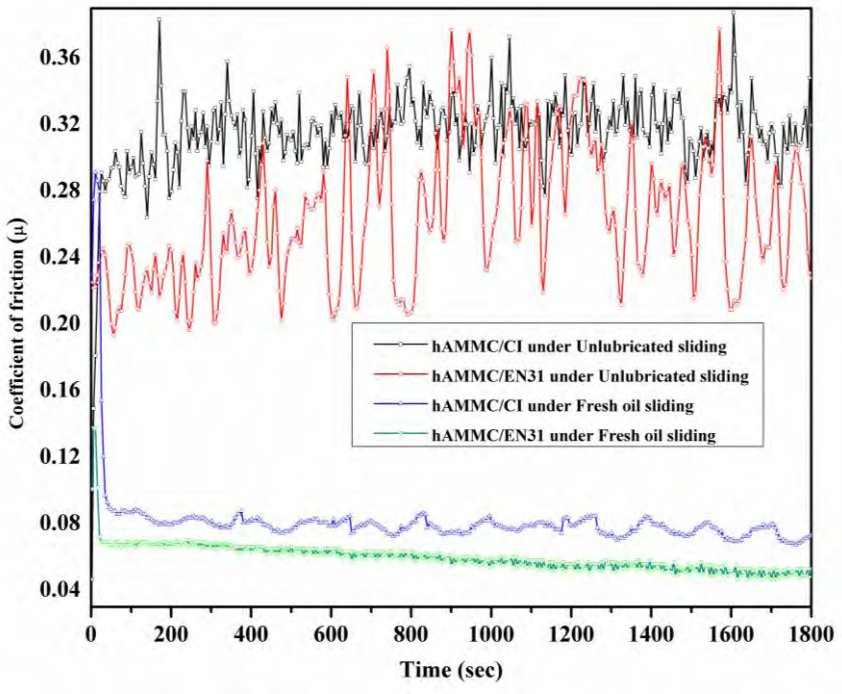

Figure 4.12: Friction response for the pilot study with h-AMMC/CI and h-AMMC/steel tribopair (applied load=9.81 N, speed=0.5 m/sec)

It is noticed from the friction plot (see Figure 4.12) that the AMMC-steel pair controls the friction coefficient more effectively as compared to the AMMC-CI pair. From the Figure 4.12 it is also observed that there are steep fluctuations in the value of COF for different combination of AMMCs, especially in case of unlubricated contact. There may be various factors that might attribute to this stiff fluctuation in the COF that may include the composite surface roughness of the contacting surfaces, material heterogeneity, metallic adhesion and intermittent third-body effect caused by the released hard and soft constituents of tribomates, etc. The underlying mechanism of this complex phenomenon is further explored for the selected pair of tribomates, in the next chapters of the thesis. In the case of unlubricated sliding of AMMC against steel, the COF value reaches 0.27, whereas it is 0.315 against CI. It is also observed that only a few friction data points are crossing the AMMC-CI friction response curve. When the tribo-contacts sliding condition changed from dry to fresh oil lubricated, the COF is further reduced to less than 0.09, which may be attributed to the formation of a thin lubricating film enriched with doped graphite particles. From the friction curves of wet sliding, it is evident that friction response for AMMC-EN31 is smooth, as no sharp peaks and valleys are observed. The wear analysis is then carried out, and the wear rate is computed by the weight loss method. In this method, the wear rate is calculated as the wear volume loss per unit sliding distance.

$$\text{Wear Rate, WR} = \frac{loss\ of\ wear\ volume}{sliding\ distance} \quad (4.1)$$

Where, wear rate is in mm^3/m, wear volume loss is mm^3 and sliding distance is in *m*.

The comparison of wear rates for both contacts is presented in Table 4.3. The wear rate of the hybrid AMMC is also better against steel, as supported by the data. Under lubricated and unlubricated conditions, the wear rates of composites siding against steel are found to be lower than those of cast iron surfaces. Thus, based on this pilot study, steel (EN31) will be used as the disc for the further tribological investigation.

Table 4.3: Wear rate comparison with h-AMMC/CI and h-AMMC/steel tribopair (applied load=9.81 N, speed=0.5 m/sec)

Lubrication condition	**h-AMMC-CI WR(mm^3/m) $\times 10^{-4}$**	**h-AMMC-EN31 WR (mm^3/m) $\times 10^{-4}$**
Dry	18.79±0.048	15.34±0.056
Fresh oil	6.32±0.014	0.04±0.008

A preliminary investigation on the tribological characteristics at various sliding speeds is then carried out with all the shortlisted oils. From the preliminary studies (Figure 4.13), it was noticed that SN500 and SAE 20W50 oils exhibit better frictional performance in contrast to the other mineral oils and fully formulated oil, respectively. Thus, these two oils, SN500 & SAE20W50 (one base oil and one fully formulated oil) are selected for the subsequent detailed investigation. It is also worth mentioning here that both SAE20W50 and SAE15W40 belong to same API service classification and has the semisynthetic base. Although at low speed condition where the boundary or boundary-mixed lubrication prevail they exhibit a noticeable difference in their friction performance, however, at the higher speed beyond a certain limit (in the present investigation it is nearly 1.2 m/s) when the operating regime shift towards mixed or unified mixed-EHL regime, they starts to preform identical due their comparable shear stability at the prevailed operating condition.

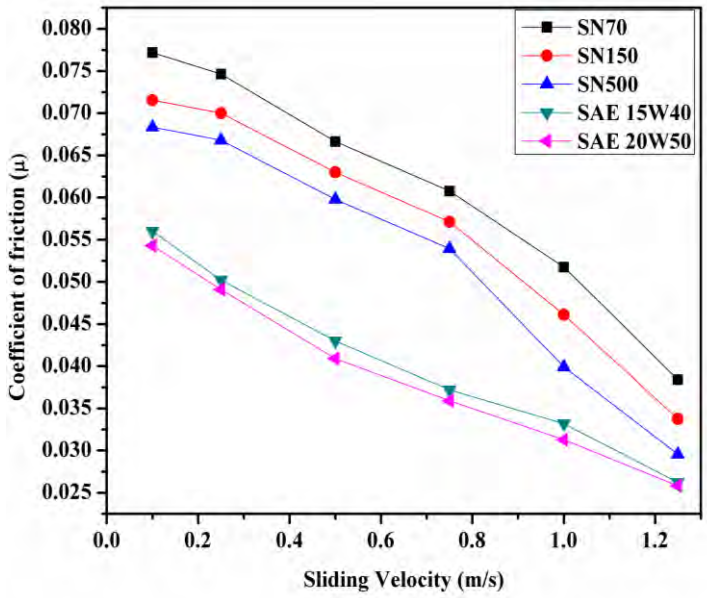

Figure 4.13: Stribeck curves for various oils (applied load=9.81 N)

To validate the enhancement of tribology due to hybridization, the AMMCs are then subjected to tribological tests with the selected disc. The selection of suitable pin is performed by judging against the friction performance of characterized hybrid composite (Al6061/SiC/Gr) with Aluminium-SiC composite (Al6061/SiC) pins. The average COFs for the AMMC/EN31 and h-AMMC/EN31pairs in dry and lubricated condition is shown in Figure 4.14. It is evident from the

figure that hybridization induces the lubricity under the contact and performs better than aluminium-SiC composite. In the case of hAMMC, the addition of graphite content increases the heat dissipation rate. Besides, their occurrence in the layered form (lubricious film) onto the sliding face acts as a solid lubricant, which in turn, lowers the frictional coefficients by minimizing the direct contact. Besides, the reinforced SiC particle in the hybrid composite act as load-bearing components and decreases the contact area between the tribo-contacts, and this leads to a somewhat decrease in the frictional coefficient [184–186]. Thus, hAMMC is finalized as the pin material.

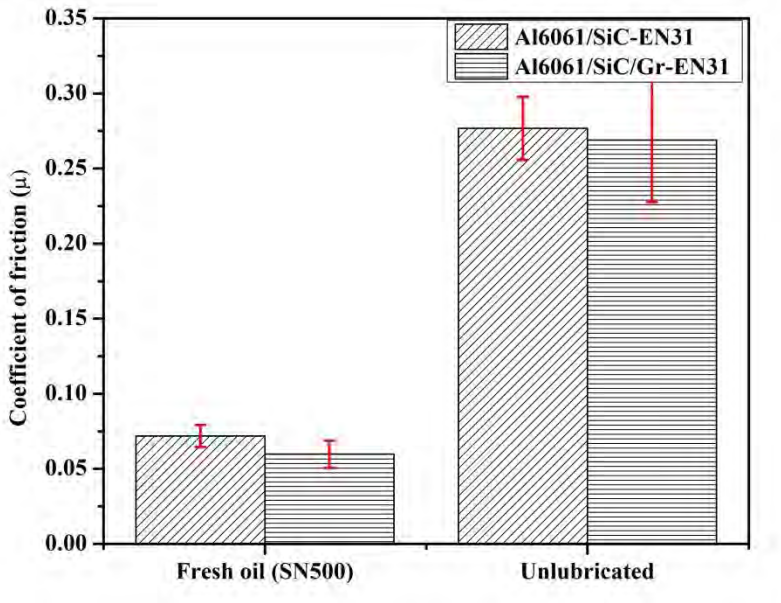

Figure 4.14: Coefficient of friction for AMMC-EN31 and hAMMC- EN31 contacts (applied load=9.81 N, speed=0.5 m/sec)

4.6 SELECTION AND CHARACTERIZATION OF THE PARTICLE ADDITIVES FOR THE NANOLUBRICANT

Oil dispersions are formed by suspending solid powders such as MoS_2, H_3BO_3, Nanoclay, and MWCNT in one of the selected oils. Their friction performance is then recorded (Figure 4.15). It is seen from figure that MWCNT shows the best frictional performance under AMMC-steel contacts, as compared to the other particle additives. This might be due to various phenomenons and features such as easy penetration into asperities owing to nanometric-size, better mechanical properties, thermal properties, and effortless sliding into graphene sheets. This motivates the

author to proceed for the detailed tribological investigation using MWCNT as the lubricant additive.

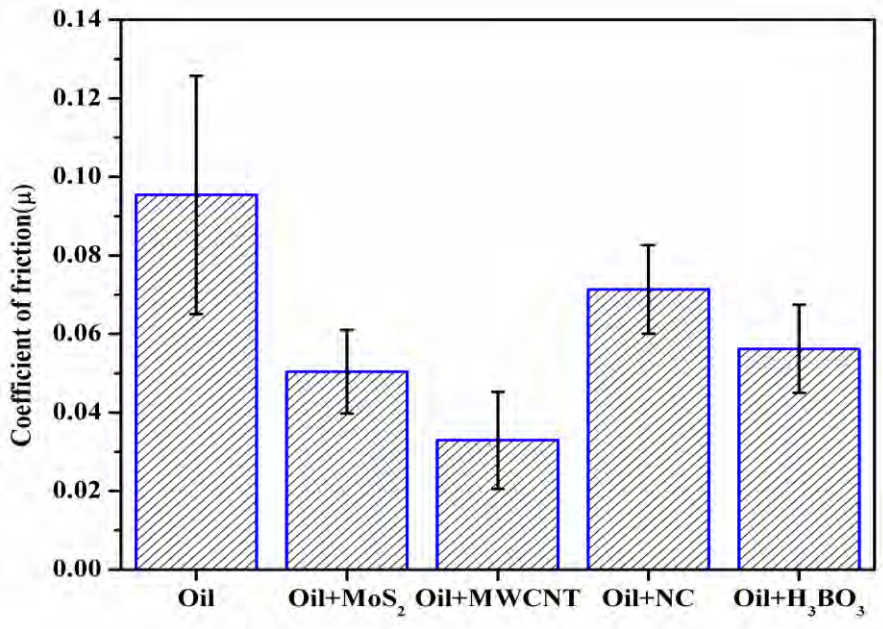

Figure 4.15: Coefficient of friction lubricated hAMMC-steel sliding conditions with various particle additives

The SEM micrograph of the MWCNT used for the present study is shown in Figure 4.16.

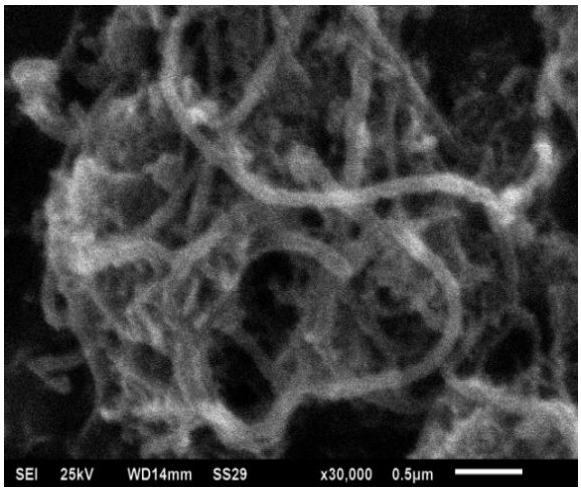

Figure 4.16: SEM micrograph of MWCNT

4.7 SUMMARY

The systematic selection procedure of tribopair, lubricating oil, and particle additive has been presented in this chapter. Lubrication mechanisms of particle-based liquid lubrication under hybrid composite employed for tribometric characterization have been explained with suitable illustrations. The summary of the final selection is listed in the following table (Table 4.4).

Table 4.4: Details of the selected tribopair, base oil, fully formulated oil and particle additive for the detailed tribological investigation

Components of the Tribosystem	**Materials**
Tribo-pin material	h-AMMC (Al-SiC-Gr)
Disc material	EN31
Base oil & Fully formulated oil	SN500 & SAE20W50
Particle additive for Lubricant	MWCNTs

CHAPTER 5

RESULTS AND DISCUSSION: TRIBOLOGICAL CHARACTERISTICS OF MWCNT-IN-OIL LUBRICANT UNDER hAMMC-EN31 AND hAMMC-CI TRIBOPAIRS

5.1 INTRODUCTION

It is a renowned fact that the piston-cylinder arrangement is primarily lubricated [187,188], but there are certain situations where the liquid lubrication system may fall shorts. Hence, it is essential to improve the performance of the selected pair in dry circumstances in the first instance. Based on a series of the preliminary investigation on the rheological and tribological characteristics, the concentration of MWCNT in the base stock is finalized as 0.1 vol.%. In the absence of any surfactant or dispersant, it was observed that a high fraction of the MWCNTs turned into clustered lumps. Comparative analysis of sliding friction behavior of hAMMC/steel and hAMMC/CI tribocontacts are investigated under various sliding conditions (unlubricated, oil(SN500)-lubricated and MWCNT-in-oil-lubricated) and is shown in Figure 5.1.

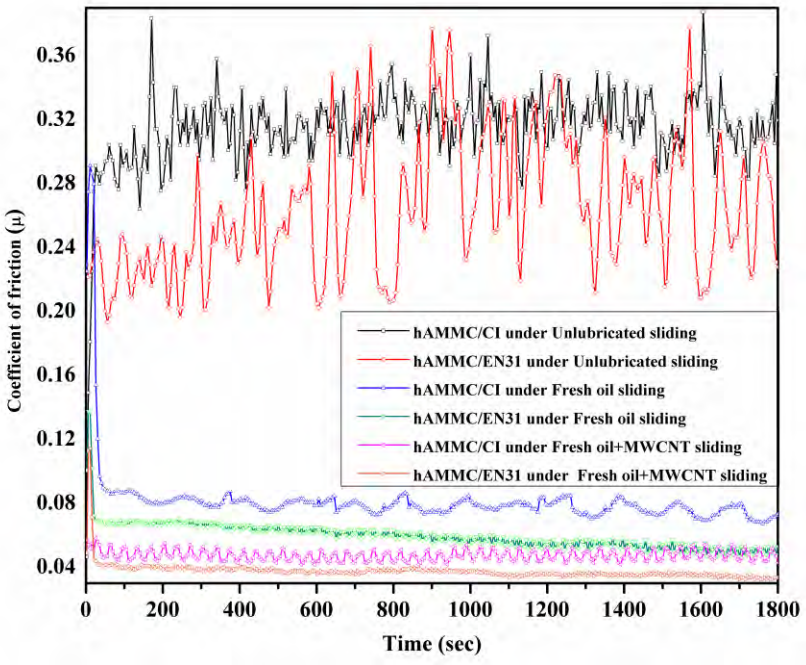

Figure 5.1: Friction responses with sliding time for both AMMC-CI and AMMC-EN31 contacts under various sliding conditions (unlubricated, oil-lubricated and MWCNT-in-oil-lubricated).

Table 5.1: Average cofs and their standard deviations for different contacts

Contact conditions	Average cof	Standard deviation
hAMMC-CI (Unlubricated)	0.32	0.026
hAMMC-EN31 (Unlubricated)	0.27	0.041
hAMMC-CI (Fresh oil lubricated)	0.08	0.024
hAMMC-EN31 (Fresh oil lubricated)	0.06	0.009
hAMMC-CI (oil+MWCNT lubricated)	0.05	0.003
hAMMC-EN31 (oil+MWCNT lubricated)	0.04	0.006

Figure 5.1 and Table 5.1 shows that for both AMMC-CI and AMMC-EN31 contacts, MWCNT-dispersed oils perform better than fresh oil samples. The friction curves are drawn for 1800 seconds so that the abrupt transition from lubrication regimes during sliding could be traced.

The average value coefficient of friction is 0.32 for hAMMC/CI and 0.27 for hAMMC /steel under dry contacts. A trend of reduced values of friction is observed for AMMC-EN31 under fresh oil, and fresh oil doped with MWCNT lubricated sliding. MWCNT-oil suspensions reduce the coefficient of friction from 0.059 (Fresh oil sliding) to 0.037 in case of hAMMC/steel and 0.048 in case of hAMMC/CI contact.

Moreover, it is evident that there is a stable friction coefficient response under the additive based lubricated contacts, in contrast to dry sliding tests. It can be explained by the fact that at a given volume concentration, additives form a continuous and stable protective film on the tribo-mates, and this film reduces the level of shear stress. Hence, no vivid fluctuation in friction and low standard deviations were observed. However, the detailed investigation on the friction-wear mechanism will be followed in the later sections.

On the other hand, the antifriction capability of the additives alone is not sufficient for particle additives to be regarded as potential commercial oil additives. Their antiwear performance must also be satisfactory under similar parametric conditions. When wear rate is calculated (Table 5.2), it is observed that under the hAMMC/steel contact MWCNT is approximately 80% more effective in controlling the wear performance than fresh oil, which is a significant improvement as compared to that of Al-B_4C/EN31 contact under similar condition for fresh oil, as well as MWCNT additized fresh oil, as reported in [189].

Table 5.2: Wear rate for hAMMC-CI and hAMMC-EN31 pins under different sliding conditions

Lubrication condition	**hAMMC-CI** **WR (mm^3/m) $x10^{-4}$**	**hAMMC-EN31** **WR (mm^3/m) $x10^{-4}$**
Dry (unlubricated)	18.79±0.048	15.34±0.056
Fresh oil	6.32±0.014	0.04±0.008
Fresh oil +MWCNT	1.09±0.008	0.008±0.001

5.2 FRICTIONS-WEAR MECHANISM UNDER DRY, OIL, AND MWCNT-IN-OIL LUBRICATION

5.2.1 Worn surface analysis of AMMC pins sliding against CI and EN31 discs under unlubricated sliding

Figure 5.2(a) and Figure 5.2(b) shows the wear tracks on composite pins sliding against CI and EN31 under unlubricated condition. The corresponding locations in the wear tracks marked by inset rectangles are selected for EDS analysis and tabulated in Table 5.3.

In the case of composite pins sliding against cast iron (see Figure 5.2(a)), the material is detached layer by layer, in the direction of sliding. Adhesive wear is detected as the prominent mode of wear in this case of sliding. Amount of iron present (40<Fe%<52 by wt.) in the EDS confirms this fact. Evidences of delamination and plastic deformation due to the influence of applied stresses can be seen easily on worn out surfaces. As one can see, the shiny (bare aluminium surfaces provides luster) edges on delaminated patches throughout the surface, no mechanically mixed layers are found in this context. Material transfer takes place from the counter surface to pin during sliding. These phenomena may increase the amount of wear and friction that occurred during the sliding of tribomates. It is interesting to mention that there are some smooth plateaus inside the worn track. Iron oxide films cover these smooth plateaus. In the EDS investigation (Spectra 2 in Figure 5.2(a)), Fe and O elements are detected in abundance (surpassing the wt% of Al, Si, and C elements), which confirms the above fact. In a nutshell, AMMC-CI dry sliding is encountered by adhesion, material transfer, oxidation and formation of discontinuous oxide layers.

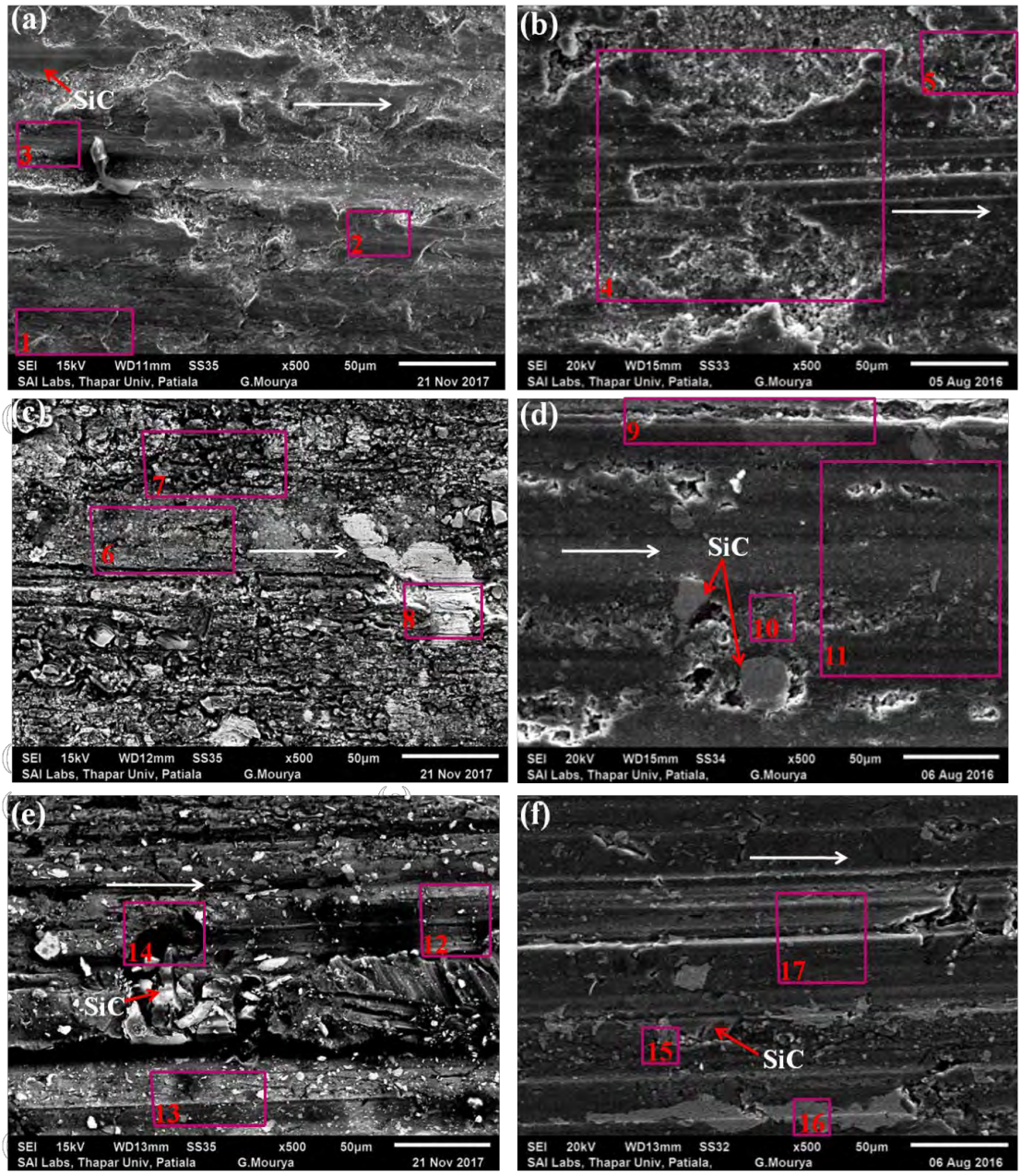

Figure 5.2: SEM micrographs of wear track of pins sliding under (a & b) dry sliding, (c & d) fresh oil sliding, (e & f) MWCNT additized oil. (a, c & e) AMMC-CI, (b, d & f) AMMC-EN31.

On the other hand, unlubricated dry sliding of composite surfaces against EN31 develops the mechanically mixed layers upon gradual pilling of interacting materials. This developed layer prevents the surfaces from severe damage. This MML is formed by the incidental mixing of tribo-pair materials that are present at the contact zones under normal loading conditions. This lowers the magnitude of both adhesion and abrasion between the contacting surfaces.

Table 5.3: Elemental analysis (wt.%) on the worn-out track of AMMC pin sliding (unlubricated) against CI and EN31 discs

Tribopair (Dry Sliding)	EDS spectrum	C K	O K	Mg K	Al K	Si K	Mn K	Cr K	Fe K	Ni K
hAMMC-CI	1	5.83	27.90	0.29	24.66	1.33	-	-	39.99	-
hAMMC-CI	2	3.84	37.36	0.19	4.14	1.87	-	0.27	51.95	0.38
hAMMC-CI	3	9.34	29.78	0.19	16.08	3.96	-	-	40.65	-
hAMMC-EN31	4	7.85	38.21	0.45	30.63	1.91	0.36	-	20.58	-
hAMMC-EN31	5	4.36	42.02	0.19	42.32	0.67	0.28	0.20	9.95	-

The carbide and solid lubricant graphite embedded in the matrix limits the deformation of the matrix and lowers the wear rate. Some carbide particles pulled out from the matrix act as a barrier for severe wear and changed the wear mechanism from adhesive to abrasive wear. Abrasion, mechanical mixing, oxidation, and plastic deformation through delamination are the observed wear mechanisms in this case, as observed from SEM micrographs (Fig. 5.2(b)).

The hypothesis of mechanical mixing is confirmed by the amount of iron (up to 21% by wt.) and chromium present in the EDS compositions (see Table 5.3). These layers cover most of the area in the wear pattern. This is a clear indication of the development of continuous mixed layers. The presence of mechanically mixed layers (MMLs) changed the wear mode from a 2-body to 3-body wear and decreasing the frictional coefficient of tribo-pairs as the formed layers act as a solid lubricant [190,191].

Moreover, the high percentage of oxygen also gives some indication of material oxidation in the wear zone. Besides the other trace elements (Mg, Si or Mn), a significant percentage of carbon is also observed (up to 8% by wt.) from the EDS. This can be attributed to the reduction of friction by acting as a solid lubricant, which also lowers the temperature of the junction by effective heat dissipation. It is believed that the thermal conductivity of graphite and silicon carbide particles controls the heat dissipation, thereby providing resistance to thermal softening. This, in turn, controls the seizure effect, unlike that of bare aluminium contacts.

5.2.2 Worn surface analysis of AMMC pins sliding against CI and EN31 discs under fresh oil lubrication

Figure 5.2(c) and Figure 5.2(d) shows the SEM micrographs of worn-out pins surfaces under fresh oil lubrication for both hAMMC/steel and hAMMC/CI sliding contacts. Table 5.4 shows

the EDS compositions for the respective spectra obtained from the selected zones, as shown in the micrographs.

Table 5.4: Elemental analysis (wt.%) on the worn-out track of AMMC pin sliding (fresh oil lubricated) against CI and EN31 discs

Tribopair (Fresh oil-SN500 Sliding)	EDS spectrum	C K	O K	Mg K	Al K	Si K	Mn K	Cr K	Fe K	Ni K
hAMMC-CI	6	12.74	13.27	0.30	55.59	7.62	-	-	10.30	0.19
hAMMC-CI	7	28.72	13.94	0.03	19.35	2.67	-	0.06	35.23	-
hAMMC-CI	8	9.43	1.88	-	3.30	2.31	-	0.17	82.91	-
hAMMC-EN31	9	18.10	31.80	0.24	44.26	0.64	-	-	4.97	-
hAMMC-EN31	10	11.98	20.87	0.36	35.48	7.51	-	-	23.79	-
hAMMC-EN31	11	12.38	9.04	-	72.76	2.44	-	-	3.39	-

From Table 5.2, it is observed that wear rates are lower in case of fresh oil contacts as compared to dry sliding conditions for both the tribopairs. From Figure 5.2(c), it can be seen that for the case of fresh oil lubrication under AMMC-CI contact, some minute adhesive wear scars and cracks are found on the wear tracks, caused by mild adhesion. The presence of oil transforms the severe wear regime into a mild wear regime. The presence of oil under the contact reduces heat generation, which in turn reduces the temperature increase at the interface, thereby reducing the formation of micro-weldments.

From the EDS inspection (Table 5.4), it is seen that the amount of oxygen present is lower than that of the dry run conditions. Oxidation wear is also reduced due to the formation of a lubricating film on the surface. Wear track is differentiated by three regions. The first one is the intensely dark zone (Spectra 7, Figure 5.2(c)), which accounts for oxidized pin-disc material interactions enriched by graphite accumulation. The second one is relatively smooth (Spectra 6, Figure 5.2(c)), which accounts for the adhesion of materials, and the third one is Fe rich grey zone(Spectra 8, Figure 5.2(c)) where a lump of material transferred during sliding. In contrast to dry sliding, there are some areas with smooth plateaus; however, a distinct continuation of cracks can be seen in this case. Moreover, layer by layer destruction is somewhat hampered by oil films, and the compaction of materials surfaces under loading can be seen in the lubricated sliding of AMMC-CI contacts.

In the case of fresh oil lubrication condition, some thin discontinuous grooves and pit formations are also observed in the SEM micrographs (Figure 5.2(d)). Mild adhesion wear between the surfaces may have been caused by the contact of carbides and steel surfaces. Besides, the existence of the smeared layer of graphite at the sliding surface acts as a solid lubricant which prevents the direct contact or adhesion of mating parts. Consequently, a relatively smooth worn-out pin surface can be seen, as shown in Figure 5.2(d). However, there are some zones present in Figure 5.2(d), where adhesive wear (in the spectra 10, in that notable amount of Fe and O elements are present) can be seen due to the interaction of mating parts. It is also evident that the percentage of oxygen in the EDS inspection (Spectra 11, Figure 5.2(d)) is notably lower than the previous dry sliding conditions. This is due to the reduced oxidizing wear in the presence of a protective oil layer. However, there are some regions (Spectra 9, Figure 5.2(d)) where cracks are encountered. It is worthwhile to mention that the presence of oxide layer, characterized by a significant amount of Fe and O with a different their morphology as compared to the film present in the rest of the track prevents further damage.

5.2.3 Worn surface analysis of AMMC pins sliding against CI and EN31 discs under MWCNT-in--oil lubrication

Figure 5.2(e) represents the wear tracks of the AMMC pin sliding under the MWCNT-oil-lubricated condition, against the cast iron material. Smoother and much leaner wear traces were found in this case. In this case a synergistic effect of doped graphite in matrix and MWCNT additive in oil can be observed which justifies the selection of MWCNT additive in the oil. This might be due to the better dispersion characteristics of MWCNT in SN500 oil, as well as the exceptional mechanical, thermal, and rheological properties of MWCNTs [11]. It is believed that the structural benefits, nanometric dimension, and subsequent formation of a stable and uniform tribo-film between the contact surfaces are causing the MWCNT-in-oil lubrication superior. The improved rheology in the presence of MWCNT is also reported by other researchers [192,193]. This, in turn, increases the ability of MWCNT-dispersed oil to stay between mating surfaces (Spectra 12 and 13 in Figure 5.2(e)), thereby decreasing the direct contact between them. Some scattered dark spots of carbon accumulation can also be observed (spectra 14, Figure 5.2(e)). Thus, there is a definite existence of the formed adherent carbonaceous tribolayer during sliding of graphite doped composite against graphitic cast iron in the presence of MWCNT as oil additives. This rationale will be investigated further in the subsequent chapter.

It is also observed that material transfer and oxidative wear is significantly reduced when MWCNT is used as an oil additive. Amount of Fe (less than 5% by wt.) and oxygen (too low) present in the EDS spectra in Table 5.5 supports this fact. Despite the reduced presence of Fe, still, there are possibilities for the formation of iron carbide apart from oxides of iron and aluminium. Thus, most of the wear is believed to be caused by mild adhesion.

Table 5.5: Elemental analysis (wt.%) on the worn-out track of AMMC pin sliding (MWCNT-in-oil lubrication) against CI and EN31 discs

Tribopair (Fresh oil+ MWCNT sliding)	EDS spectrum	C K	O K	Mg K	Al K	Si K	Mn K	Cr K	Fe K	Ni K
hAMMC-CI	12	37.79	6.95	0.50	44.85	5.05	-	0.05	4.82	-
hAMMC-CI	13	36.22	6.84	0.48	42.71	8.96	-	-	4.79	-
hAMMC-CI	14	86.97	-	0.12	11.31	-	-	0.03	1.03	-
hAMMC-EN31	15	25.05	-	0.13	0.89	-	-	0.92	73.01	-
hAMMC-EN31	16	9.77	5.88	-	1.97	0.70	-	1.07	80.61	-
hAMMC-EN31	17	13.70	4.60	0.18	80.85	0.58	-	-	0.69	-

On the other hand, in case of AMMC-EN31 contact under MWCNT-oil lubrication, a relatively smooth wear track with less damaged surface can be observed in this case. The synergistic effect caused by the coupling of solid lubricant from the matrix and CNT from liquid lubricant provides the adequate wear resistance for contacting surfaces. The presence of iron in Table 5.5 (spectra 15 and 16) supports the mild adhesive wear by the material transfer under loading. In some cases, ceramic particles may have led to cracking, which breaks the particles into finer fractions, which mixed with soft reinforcements [137]. During sliding, tangential displacements of individual graphene sheets of carbon nanotubes take place, which is regarded as the premium antifriction agents [48,191,194]. Some scattered abrasive wear scars on the surface of composite pin can also be noticed in the SEM micrographs, as shown in Figure 5.2(f). Thin exfoliated sheets of MWCNT cover the surface and prevent them from being damaged. These sheets might have settled at the ceramic-alloy interface. Even at the end of the friction sliding test, embedded MWCNT particles in SEM micrographs validated this.

The Raman spectrum depicts presence of the observed peaks corresponding to carbon nanostructures such as MWCNT and graphene sheets. The various bands such as G, D and 2D of graphitic structures in the spectrum were obtained on usual Raman shifts at 1575, 1340 and 2680

cm^{-1}. The presence of this thin carbonaceous layer, the roughness of pin is greatly reduced when sliding against steel, as compared to the CI (Figure 5.4).

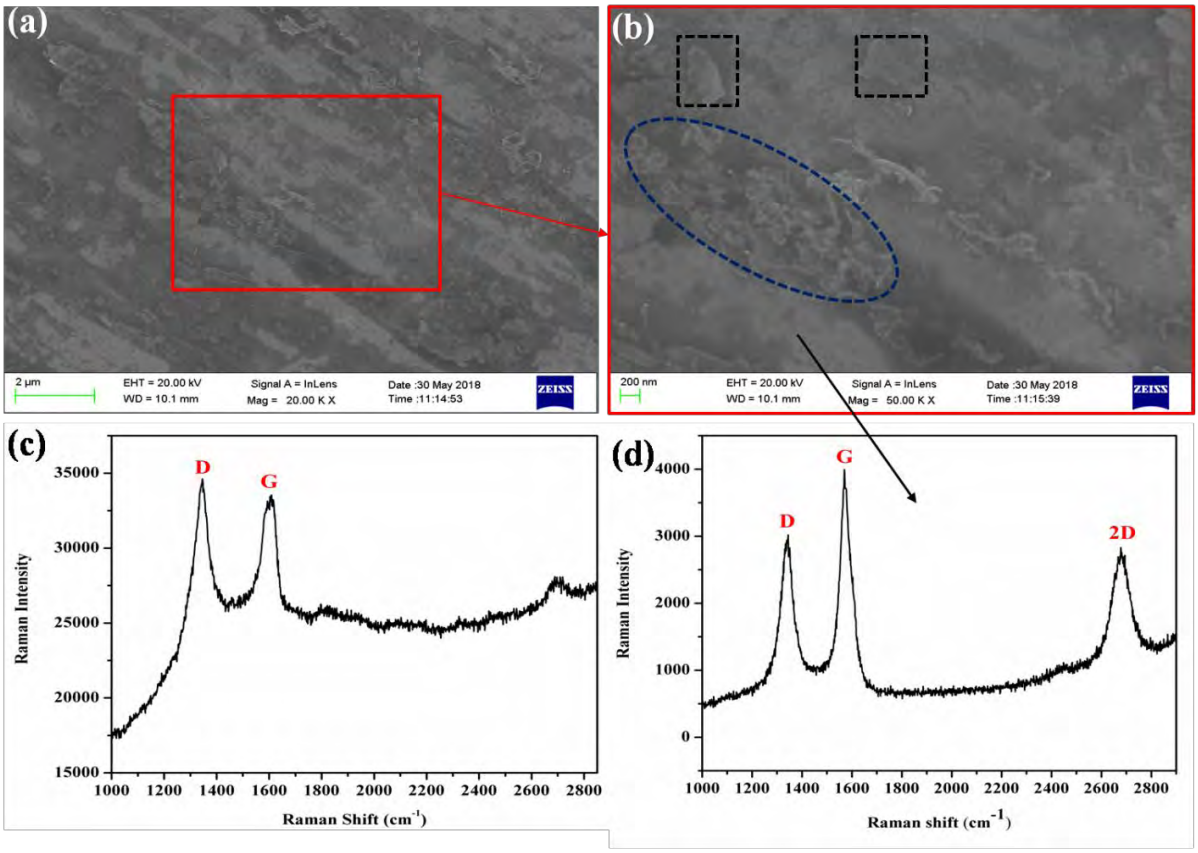

Figure 5.3: MWCNT-in-oil lubrication for hAMMC/EN31 contact (a) SEM image of the worn-out AMMC pin, (b) Enlarged view of the marked zone (distorted MWCNT represented by dotted ellipse), (c) Raman spectra of MWCNT, and (d) Raman spectra on the compressed and exfoliated MWCNT layers.

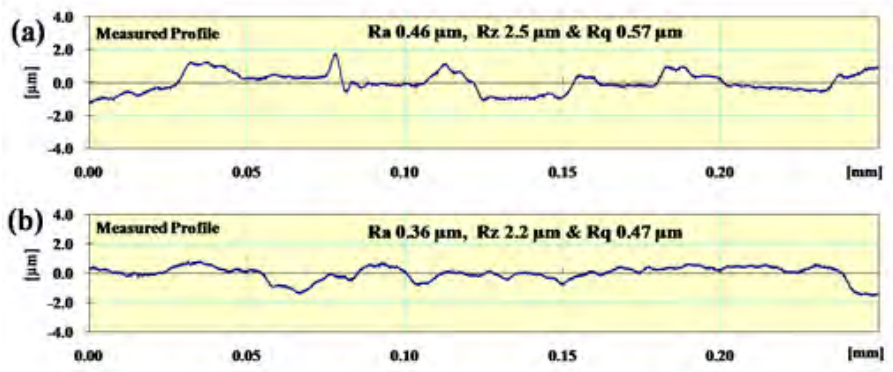

Figure 5.4: Surface roughness's of worn out AMMC pins sliding against (a) CI, (b) EN31, under the MWCNT-in-oil lubrication.

5.3 XRD ANALYSIS OF THE WEAR TRACKS

For further understanding of the wear mechanism under MWCNT-laden lubricated contact, XRD analysis is carried out. Figure 5.5(a) and Figure 5.6 shows the XRD patterns for wear tracks of worn-out AMMC pins surfaces sliding against CI subsurface. In this case, a significant amount of hexagonal structured magnesium silicate ($MgSiO_3$), iron oxide, and carbides are detected in the wear track. These silicates, oxides, as well as carbides of iron, are formed by the tribo-chemical reactions of AMMC surfaces with the debris from the cast iron (significant presence of Fe, along with a considerable amount of C and Si elements), under the CNT-doped mineral oil. Magnesium silicate is formed by the following reaction [195].

$$MgO+SiO_2 \longrightarrow MgO.SiO_2 \quad (5.1)$$

Some authors also discussed the polymorphism of magnesium silicate, which dealt with the formation of iron oxide and magnesium silicate from olivine, and illustrated by the reaction below [196].

$$3(Fe_2SiO_4+Mg_2SiO_4) +O_2 = 6MgSiO_3 +2Fe_3O_4 \quad (5.2)$$

Magnesium silicate products help to reduce friction due to hexagonal structure features. Some authors reported on the friction reduction capabilities of hydroxy-magnesium silicate with the feature of self-repairing properties under sliding contacts. Apart from this, a significant amount of amorphous aluminum hydroxide is also present on surface of the worn track. It is formed due to the interaction of aluminum debris and hydrocarbons (generally present in oil) with moisture from the surrounding atmosphere. The reduction of friction might have caused by this tribo-chemical reaction film [197]. However, the abundance of this amorphous tribo-chemical compound reduced the hardness of contacts [198,199]. However, the formation of iron carbide improves the hardness of the acting surface. Formed carbides reduce the direct asperity content, thereby minimizing the amount of adhesion. Because of this, the heat generated due to the thermal junction formed by tribo-pairs is minimized. Moreover, the presence of amorphous carbon and traces of carbides induces a lubricous layer which is resistant to wear [200].

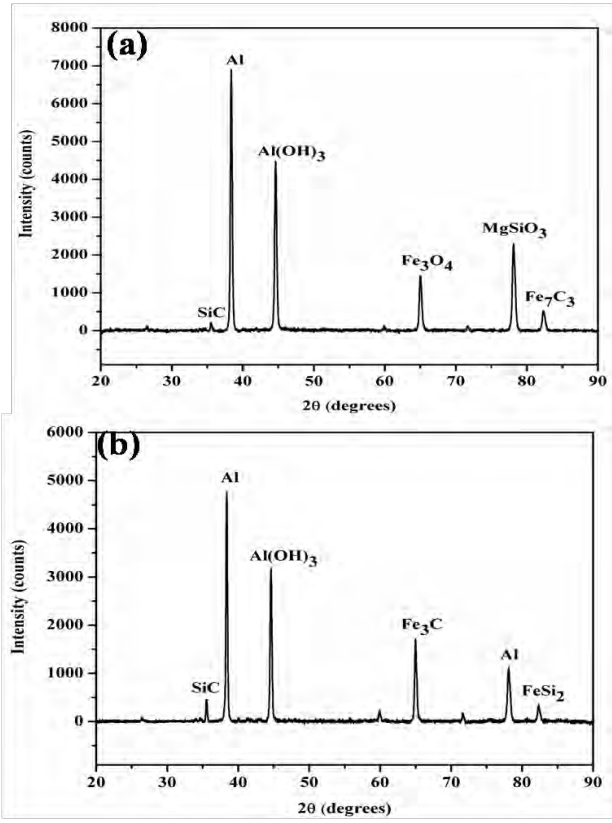

Figure 5.5: XRD analysis of worn-out AMMC pin surfaces sliding against (a) CI and (b) EN31 (under MWCNT laded lubricated condition)

However, it is sensible to mention here that no magnesium silicate compound was detected by the XPERT high score plus database on the AMMC pin sliding against EN31. In the case of AMMC-steel contacts, sliding under the MWCNT-oil lubrication, a small amount of ferdisilicite ($FeSi_2$) was also detected, apart from the iron carbide (Figure 5.5(b)). It is believed that the graphite present inside the aluminium matrix may have suppressed the formation of carbides [201]. Ferdisilicite minerals make the surfaces brittle. The brittleness of a film can affect the friction between the sliding surfaces. If the film substrate-interface is weak, the surface will be delaminated, thereby exposing the substrate under the traction [202]. The presence of secondary-phase silicon carbides protected the matrix alloy from a severe contact with the hard bearing steel surface and provided the beneficial effect in terms of friction. Moreover, this silicon carbide phase can bear intense amount of sliding, thereby reducing the contact area between lubricating sliding pairs.

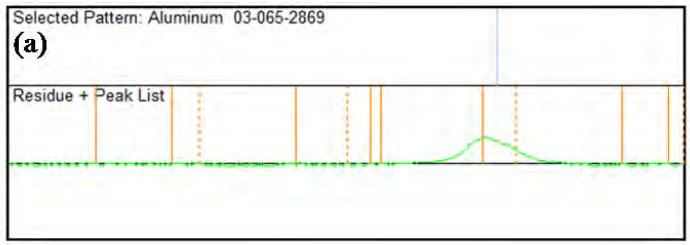

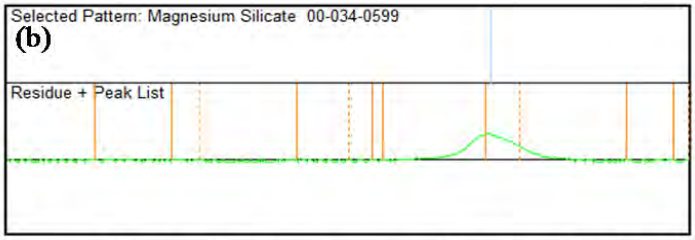

Compound/ Element	h	k	l	2 Theta(°)	I %
$MgSiO_3$	3	0	5	78.153	45%
Al	3	1	1	78.227	26.8%

Figure 5.6: XRD analysis for selected patterns of aluminium and magnesium silicate in the worn-out surface of AMMC pin

5.4 SUMMARY

An in-depth insight of the tribological characteristics of AMMC-CI and AMMC-EN31 pairs are evaluated in this chapter, in the presence of MWCNT-in-oil lubrication. It is observed that hAMMC-CI sliding contacts under fresh oil condition show the sign of oxidation, material transfer (Fe) onto AMMC, and adhesive wear. The resulting surface is relatively rougher. However, hAMMC-CI contacts under the MWCNT-in-oil lubrication exhibits less material transfer and formation carbonaceous layer leads to a smooth roughness profiles. In a nutshell, a complex lubrication mechanism may be prevailed under the MWCNT-in-oil lubrication and hence a detailed investigation on the lubrication mechanism of the MWCNT based lubrication is much needed. This will be the primary focus in the subsequent chapter, along with a comparative performance evaluation with the surfactant-functionalized MWCNT-in-oil lubricant.

CHAPTER 6

RESULTS AND DISCUSSION: UNDERLYING LUBRICATION MECHANISM OF NON-FUNCTIONALIZED AND SURFACTANT-FUNCTIONALIZED MWCNT-IN-OIL LUBRICANT

6.1 INTRODUCTION

A comprehensive tribological analysis of the hybrid AMMC sliding under fresh oil, MWCNT-based, and surfactant-functionalized MWCNT-based liquid lubrication is presented in this chapter. The friction wear tests were carried out using a pin-on-disk type tribometer at various parameters, as discussed in the previous chapters. The selection methodology of a suitable surfactant has been outlined. The finding of various experimental results, alongwith the tribological results are analyzed carefully and an underlying lubrication mechanism is presented in this chapter. Film thickness and film thickness ratio calculations have been done for better insight into the lubrication regime. Finally, based on the statistical analysis and experimental observations a comprehensive wear mechanism is mapped.

6.2 SELECTION OF SURFACTANT

The nature of head group and chain length of surfactant plays a vital role for the effective lubrication [203]. Nanodispersions of MWCNT are prepared by suspending them in oil in the presence of a non-ionic amphiphilic surfactant. As mentioned earlier, the non-ionic surfactant has hydrophilic and lipophilic groups permitting the steric interaction of additive particles and oil molecules, by assembling themselves at the interfaces between oil and the molecules. This self-interaction assemblies formed at the interface lowers the interfacial tension, resulting in better suspension characteristics.

The solubility of an amphiphilic type surfactant molecule in dispersions is designated hydrophilic–lipophilic-balance (HLB). The HLB value can be estimated using the following equation.

$$HLB = 20\left(1 - \frac{S}{A}\right) \tag{6.1}$$

Where S and A denotes for saponification number and acid number of the recovered acid for esters, respectively.

It is a well-known fact that the high value of HLB is soluble in water (polar agent), while lower HLB ones have a good affinity towards oil (non-polar) molecules. The selection of suitable surfactants are based on ease in availability, length of hydrophobic chain, hydrophilic–lipophilic-balance (HLB), and solubility characteristics. The selection of surfactants was made based on these facts. Amongst the nonionic surfactants ATS, SPAN, TWEEN, PEG, PIBS are explored and proven surfactant/dispersant in case oils [145–147,150,152,204]. The HLB values of some of the popular nonionic surfactant is listed in Table 6.1

Table 6.1 The list of HLB values for different surfactants

Surfactant	**HLB**
Span 20	8.6
Span 40	6.7
Span60	4.7
Span 80	4.3
Tween 20	16.7
Tween 40	15.6
Tween 60	14.9
Tween 80	15.0
PEG 460	11.0
PEG 860	16.0

From table 6.1 containing the HLB values for various listed surfactants, the HLB value of SPAN80 is least (i.e., HLB order follows: Span 80<PEG 460< PEG 860 < all TWEENS) and should have adequate solubility with mineral oil. Thus, Sorbitan esters, Span 80 (Sorbitan monooleate) were chosen from the class of non-ionic surfactants. The structure of the surfactant is presented in figure 6.1. The oxygen-based polymeric acid type surfactant SPAN80 encloses three hydroxyl (–OH) groups and one furan ring (See figure 6.1).

In the case of non-ionic surfactant-assisted dispersions, the stability is attained by steric repulsion between the micelles as the surface-active agent is non-ionic. For a stable environment condition, these steric repulsive forces are good enough to act against the attractive van der Waals forces that act between solid molecules and thus obstruct them from accumulation of particles and

flocculation of them. To prevent de-agglomeration, MWCNT was functionalized using a non-ionic surfactant Sorbitan monooleate (Span-80).

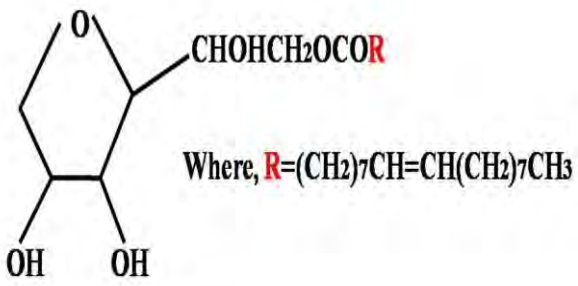

Figure 6.1 Structure of sorbital monooleate (SPAN 80)

Thus, various elements of the final tribosystem investigated in the present chapter is listed in Table 6.2 and the possible interaction of surfactant with the particle and oil molecule is represented by the schematic diagram, as shown in Figure 6.2

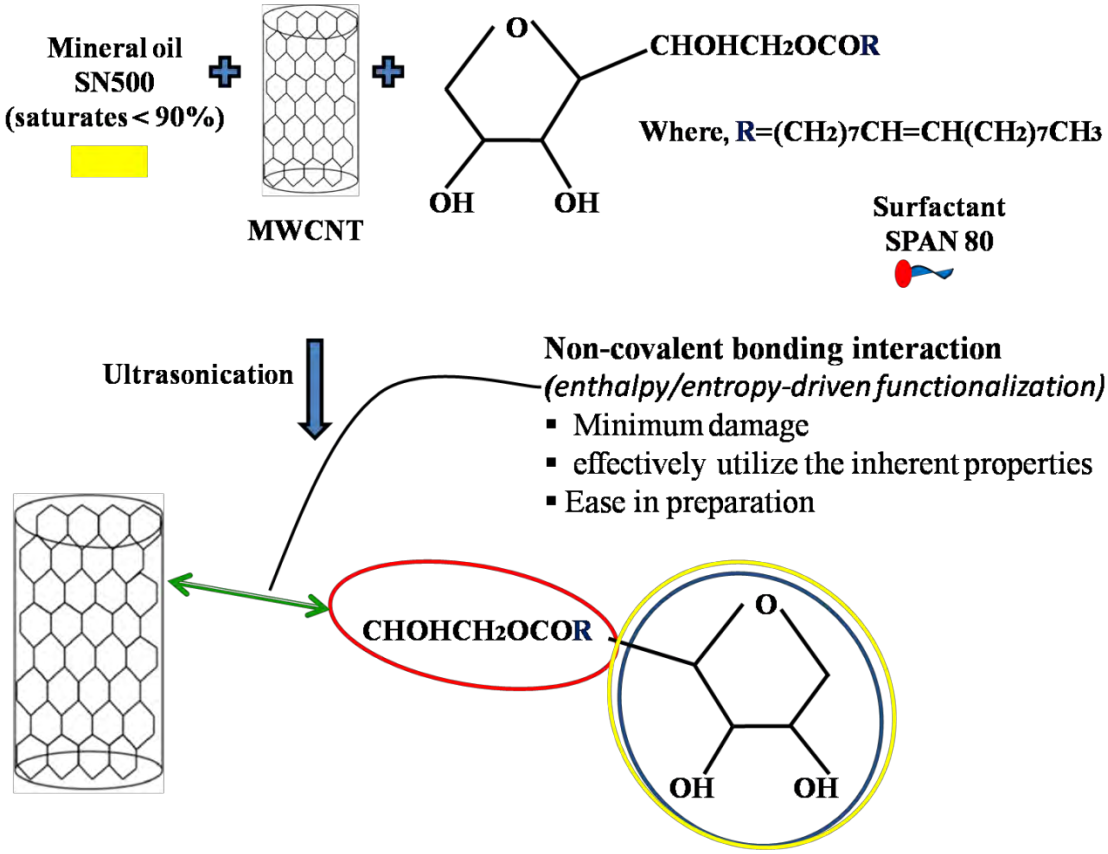

Figure 6.2 Schematic of the functionalization of MWCNT with a nonionic surfactant

Table 6.2 Elements of the final tribosystem

Elements	Materials
Tribo-pin material	h-AMMC(Al-SiC-Gr)
Disc material	EN31
Base oil/Fully formulated oil	SN500/SAE20W50
Particle additive	MWCNTs
Surfactant	SPAN80

The optimum concentration of the surfactant was estimated from a series of electrical conductivity experiments. The electrical conductivities were measured for the estimation of Critical Micelle Concentration (CMC) of the surfactant in SN500 in the presence of MWCNT. As per this method, CMC of the solution is predicted [205] from the inflection point of the electrical conductivity and concentration plot (see Fig.6.3). Figure 6.3 indicates that a surfactant concentration of approximately 0.04% is recommended to use to utilize the potential benefit of MWCNT laden oil, for further tribological investigation. Interestingly, at this CMC of the surfactant, the viscosity of the nanlubricant is remarkably enhanced (Figure 6.4).

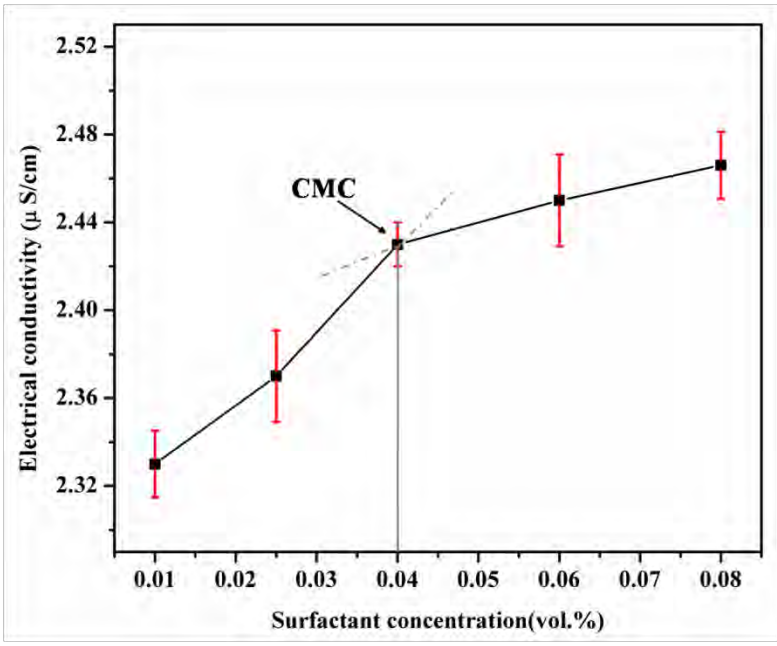

Figure 6.3 The variation of electrical conductivity of nanodispersions with surfactant concentration

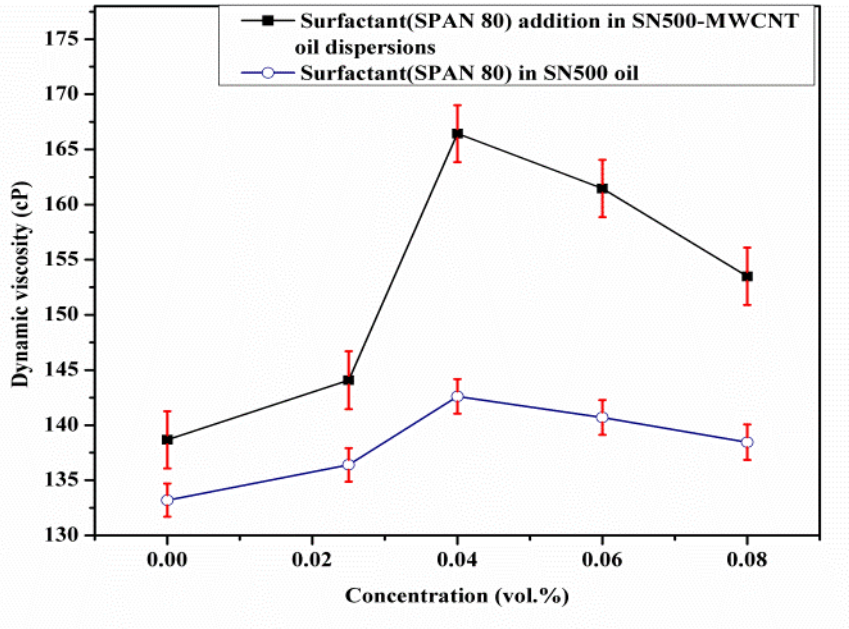

Fig. 6.4: Influence of surfactant concentration on the dynamic viscosities of fresh mineral oil and MWCNT-laden oil

To check the feasibility of using this optimum concentration of surfactant in the lubricant to be used, again a pilot experimentation on the tribological characteristics of the lubricant, with various concentration is evaluated. It is clear from the Figure 6.5 that at a specific concentration (0.04 vol.%) of surfactant, the COF is reduced to ~0.026. This significant reduction, as compared to fresh oil and MWCNT dispersed oil without any surfactant, depicts the importance and usage of surfactant modified-MWCNT in oils for low friction applications. Thus, the formulation of MWCNT-oil with a surfactant concentration of near CMC value is quite helpful for the low frictional response. It is worthwhile to mention that the viscosity of Non-Newtonian surfactant solutions is increased with the surfactant concentrations (Figure 6.4) due to the heterogeneity and randomness induced by the suspended particles in the solution. On the other hand, non-ionic surfactant, such as SPAN80 has a drag reduction property, which depends upon the length and molecular weight of alkyl chain [206]. For a surfactant to reduce the friction by viscous drag, the surfactant solutions need to contain aggregates of the surfactant molecules. Once this condition is achieved at CMC, the synergistic effect of micelle and the well-dispersed particle additive starts to play a predominant role in enhancing the lubricity of the contact (Figure 6.5). However, at the higher concentration beyond the CMC, the disorganized clustering of surfactant micelle gradually hinders the friction reduction ability of the lubricant.

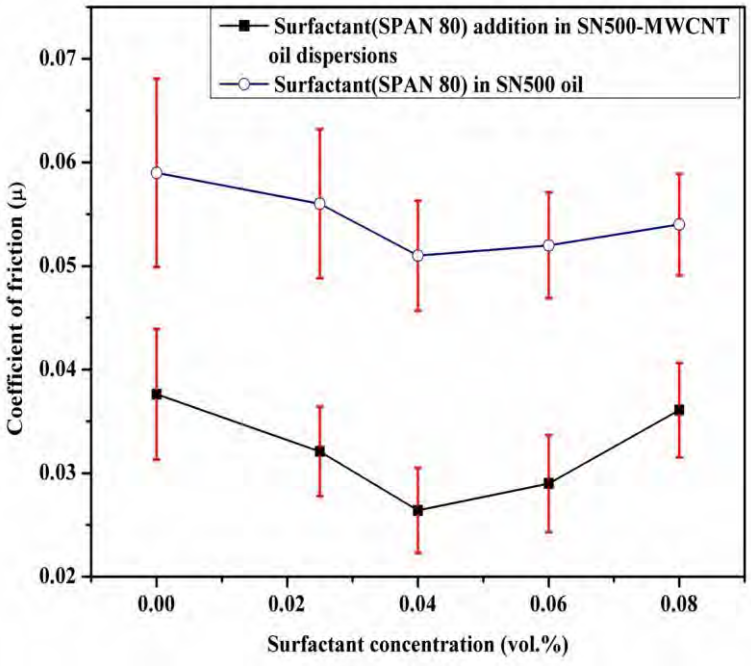

Figure 6.5: Effect of surfactant concentration on frictional coefficient in mineral oil and MWCNT-oil dispersions

6.3 COMPARATIVE FRICTION AND WEAR CHARACTERISTICS USING SN500 AND SAE20W50 OILS

A comprehensive investigation is carried out to explore the comparative tribological behaviour, once the selection process of various ingredients of the base formulation is completed, viz, a suitable oil, oil additive, and surfactant. Before the detailed comparative investigation, a Stribeck curve (Fig. 6.6) were generated for each type of lubricant to evaluate the operating lubrication regime, corresponding to sliding velocities ranging from 0.1 m/s to1.25 m/s under a normal load of 9.81 N. From Fig. 6.6 it is evident that with the addition of surfactant functionalized MWCNT, fully formulated oil exhibited the superior frictional performance. This is followed by the surfactant-functionalized MWCNT-SN500 lubricant. Moreover, it is observed that there is an inverse relationship between sliding velocity and coefficient of friction.

The wear rate for hybrid composite under various lubricated conditions (at a sliding speed of 0.5 m/s) is presented in Fig. 6.7. Here also, it is observed that the addition of MWCNT and functionalized-MWCNT in the lubricant brings along the significant improvement in the antiwear performance for both the oils.

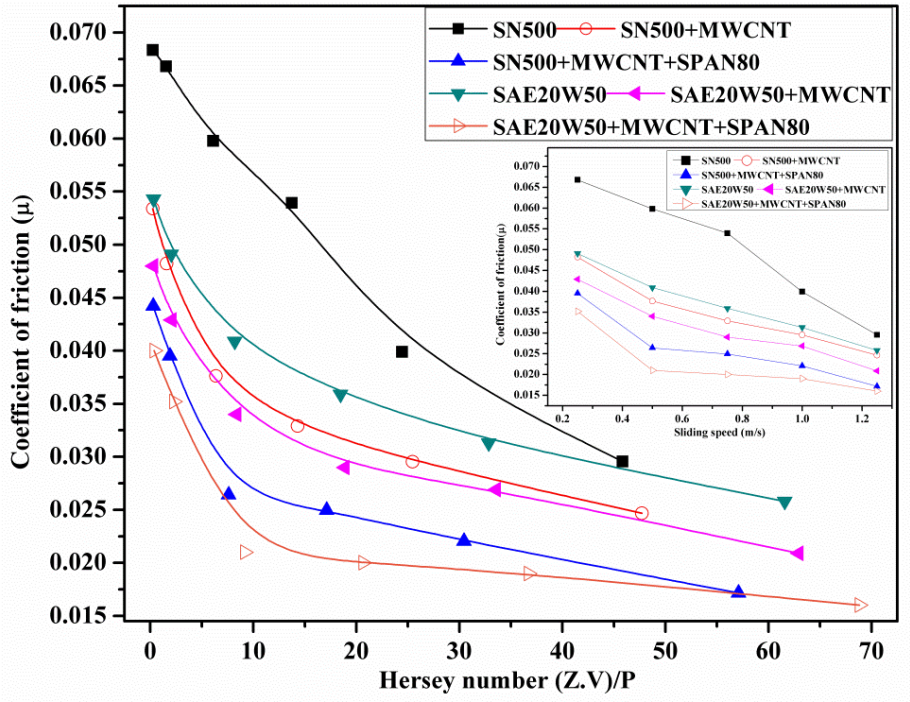

Figure 6.6: Stribeck behavior of SN500 and SAE20W50 oils. (Inset: The effect sliding speed on the coefficient of friction for various lubricated sliding contacts)

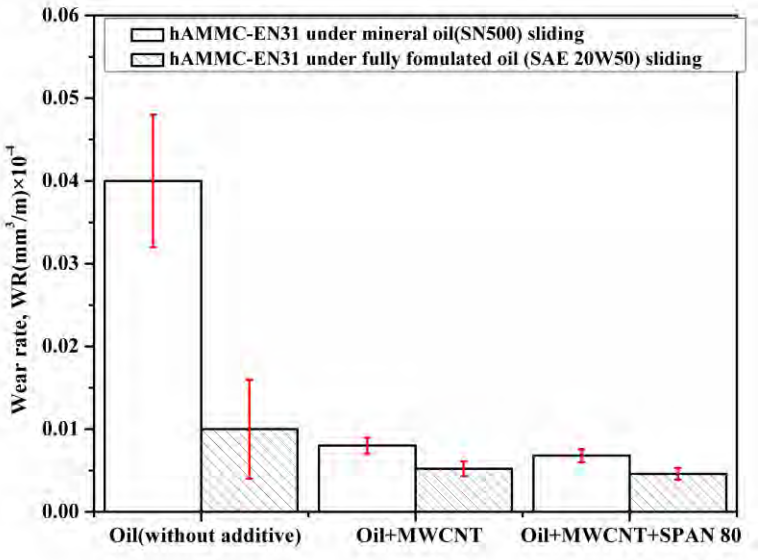

Figure 6.7: Wear rates of composite pins sliding under SN500 and SAE20W50 lubrication.

Thus, it can be realized the potential tribological gain that can be achieved by using MWCNT for the composite sliding contacts. This might be a benchmark study for the usage of MWCNTs in a commercially formulated oil package; of course, the other stringent parameters like oxidation

stability etc. are to be ensured. This motivates the authors to explore the underlying lubrication and friction-wear mechanisms involving this particle additive under the selected contact.

For better realization of the beneficial effect of surfactant a comparison of antiwear performance of lubricant with MoS_2 and MWCNT particles in the presence or absence of surfactant (SPAN 80) under the selected pair is further validated. It is noticed from the figure 6.8 that MWCNT additive are more effective in controlling friction those MoS_2 additive. Besides, surfactant-assisted MWCNT dispersions showed excellent performance, among other wet sliding conditions.

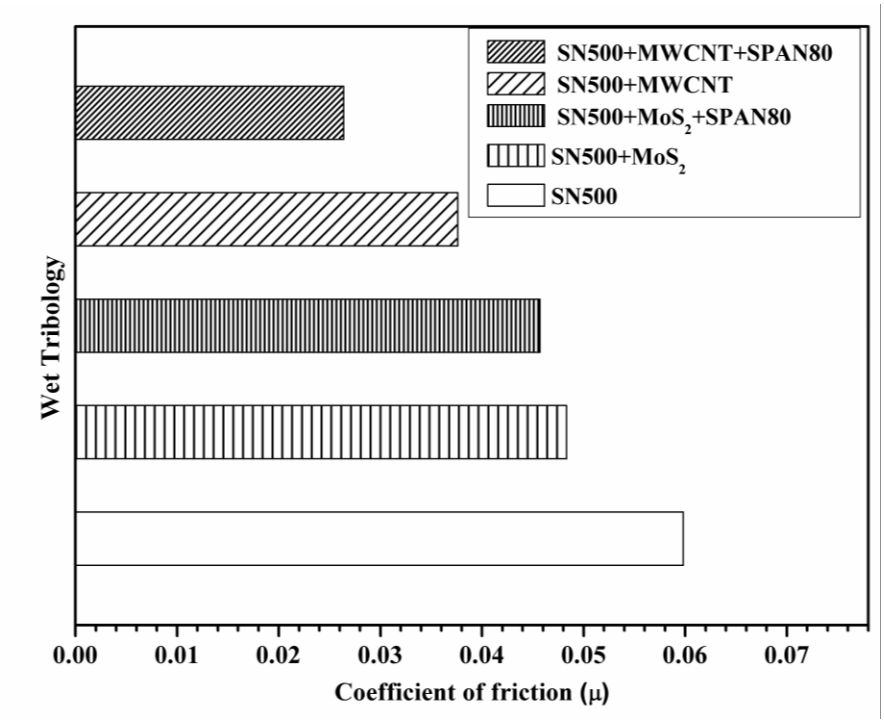

Figure 6.8: Coefficient of friction for various wet sliding conditions using MoS_2 and MWCNT

6.4. FRICTION-WEAR-LUBRICATION MECHANISM OF SURFACTANT FUNCTIONALIZED MWCNT-OIL DISPERSION UNDER AMMC/STEEL CONTACTS

6.4.1 Lubrication Mechanism

To find the root cause of the improved and differential friction-wear behaviour, it is essential to explore the underlying lubrication mechanism. A close examination at an operating speed of 0.5 m/s reveals a unified boundary-mixed regime of lubrication that exists under the contact. This can be validated through a detailed roughness parameter analysis of the worn-out surfaces, along with the estimated film parameters. The film parameter identifies the characteristic lubrication

regime, which is influenced by the fluid rheology and operating conditions such as the normal force and sliding speed. The process of estimation of minimum film thickness (h) and film parameter (λ) of lubrication is explained earlier [207,208].

Lubrication characteristics are greatly influenced by rheological properties of using fluids and contact operating conditions such as the applied force and sliding velocity. Film thickness for given sliding contact operated under mineral oil conditions can be approximated by the following equation [208,209].

$$h_{cen} = 1.55\alpha^{0.53}(\eta U_m)^{0.67}(E)^{0.061}R^{0.33}(p_o)^{-0.201} \quad (6.2)$$

Where, $h_{cen}, \alpha, \eta, U_m, E, R$ and p_o denotes central film thickness, pressure viscosity coefficient, viscosity, mean velocity, reduced Young's modulus, radius, and Hertzian pressure, respectively.

Pressure calculation (p_o)is essential to estimate load (W) supported by lubricating film, and it is calculated using equation (6.3).

$$p_o = \frac{3W}{2\Pi a^2} \quad (6.3)$$

$$a = \sqrt[3]{\frac{3WR}{2E}} \quad (6.4)$$

Now, the film thickness ratio (λ) based on central film thickness can be estimated using the eq. (6.5) below, which is the ratio of film thickness and root mean square roughness of two contacting surfaces say σ_1 and σ_2, respectively.

$$\lambda = \frac{h_c}{\sqrt{(\sigma_1)^2 + (\sigma_2)^2}} \quad (6.5)$$

To estimate the lubrication regime, the value of λ plays an important role. Of course, the friction mechanism is further related to this information.

The values of viscosity-pressure coefficients and viscosities for the selected oils, which are used for the estimation of film thickness and film parameters following Hamrock and Dowson's equation [208] , are given in Table 6.3.

Table 6.3: Information about pressure-viscosity coefficient, viscosity, film thickness, and film parameter

Oil	**Pressure-viscosity coefficient ,α(Pa^{-1})**	**Viscosity, η (Pa.s)**	**Film thickness, h (μm)**	**Film parameter, λ**
SN500	2.1×10^{-8} [210]	0.133	0.154	0.178
SAE 20W50	3.4×10^{-8} [28]	0.179	0.242	0.318

From figure 6.9, it is noticed that there is a significant reduction of roughness parameter with the use of MWCNT-in-oil. This is further enhanced in the case of surfactant-functionalized MWCNT-in-oil. The reason for this friction reduction can be attributed to the entrapment of solid additive under such contacts and hence encouraging the polishing mechanism under the sliding action.

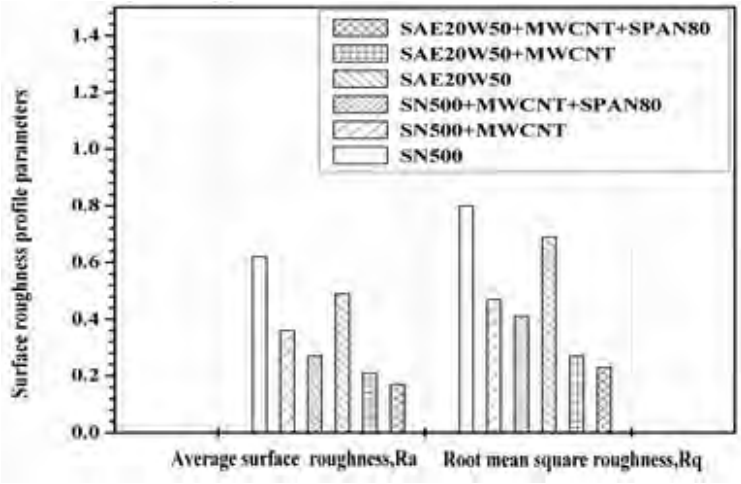

Figure 6.9: Root means square roughness (R_q) and average surface roughness (R_a) of composite pins for various wet sliding conditions.

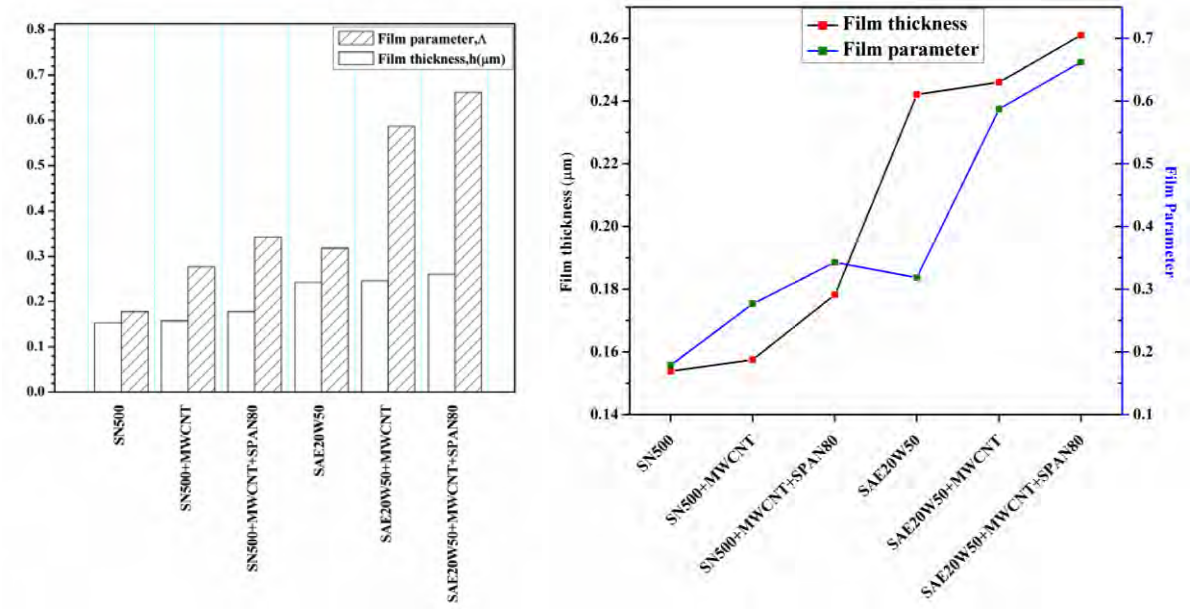

Figure 6.10: Film thickness (μm) and film parameter for various wet sliding conditions

Film thickness and film parameters for various wet sliding conditions are depicted in Figure 6.10. A close comparison of these Figs. imply that fully formulated oil exhibits better frictional performance than base oils with the addition of MWCNT and surfactant functionalized MWCNT, which in turn results in the reduced roughness parameter and higher film thickness. The estimated film parameter ranges confirmed the prevailing mixed lubrication regime [211]. The analysis shows that the lubrication regime is found to be shifting from the boundary to unified boundary-mixed regime for both the oils in the presence of surfactant functionalized MWCNT. Hence, there is a reduction in friction as well as cumulative wear. The various influencing factors which might be playing critical role in defining the underlying lubrication mechanism is discussed below.

6.4.1.1 Stability of the nanodispersions

Span80 and MWCNT was mixed using a ball mill to disentangle the CNTs, prior to it is dispersed in the base oil. In this way, the MWCNTs were physically coated with SPAN80. This was then followed by dispersion in the base oil using ultrasonication method. It modifies the surface of MWCNTs to create steric repulsions between individual nanotubes. Previous research suggested that surfactant adsorption on the surface of MWCNTs helps in reducing their surface energy, thereby preventing agglomeration [152]. Initially, the stability study was carried out using sedimentation test to ensure that any aggregates are not appeared in the prepared samples.

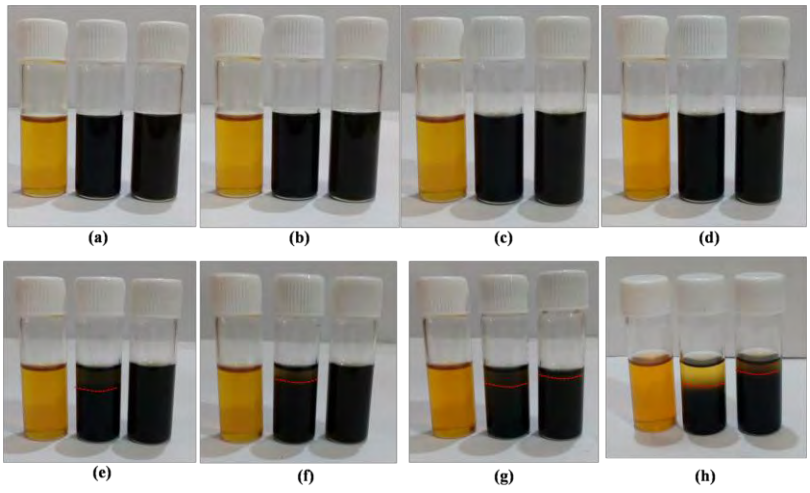

Figure 6.11: Visual inspection of stability of CNTs and surfactant assisted CNTs in oil solutions (starting from left: fresh oil, CNT-in-oil & surfactant functionalized CNT-in-oil). (a) after 1 day, (b) after 7 days, (c) after 14 days, (d) after 21 days, (e) after 28 days, and (f-h) with the passage of time in subsequent weeks.

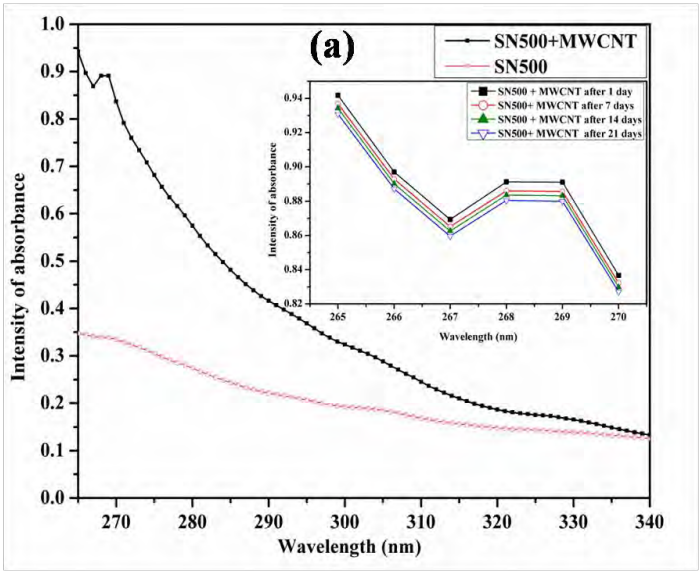

Figure 6.12: UV-spectrum of fresh oil, MWCNT-in-oil dispersions and surfactant-modified MWCNT-in-oil dispersions (Inset: stability of surfactant-modified MWCNT-base oil suspension over a span of 21days)

Figure 6.11 shows the dispersion of MWCNTs and surfactant assisted MWCNTs in oil after the passage of time. MWCNTs in the suspension aggregated and settled to the bottom after 28 days in the absence of surfactant. However, it is apparent that the addition of surfactant improved the dispersion stability even lasting for more than one month.

To get the better insight into the stability of the lubricant, UV-vis spectrometry was carried out to analyze the MWCNT dispersed suspensions. Figure 6.12 shows the observations of a typical study carried out for MWCNT-in-Oil suspension. It is evident from the Fig. 6.12 that MWCNT based lubricants have good stability even after twenty-one days, as there was an insignificant change in absorbency over the span of 21 days and maximum absorbance was observed at a wavelength close to 268 nm. The bands appearing at ~320 nm of UV absorption spectrum, as shown in Fig. 4(b) indicates the presence of Span 80 in the solution [212].

6.4.1.2 Thermophysical properties of nanodispersions

It is noticed from the Figure 6.13 and 6.14 that fully formulated oil SAE 20W50 shows better thermophysical properties than the mineral base oil (SN500). The addition of a surfactant shows a positive effect in enhancing the viscosity of fluid dispersion, while it has an adverse effect on the thermal conductivity for both oils. MWCNT addition restricts the motion of fluid layers, owing to the high exposure of surface area and the filament-like morphological features and their aggregation to form large asymmetric geometric distributions in the fluid. This, in turn, affects the rheological properties of dispersions. The improvement of viscosity in the presence of the surfactant is because of stable and homogenous dispersions of particle additive, which improves and redesigns the shearing forces among the fluid layers.

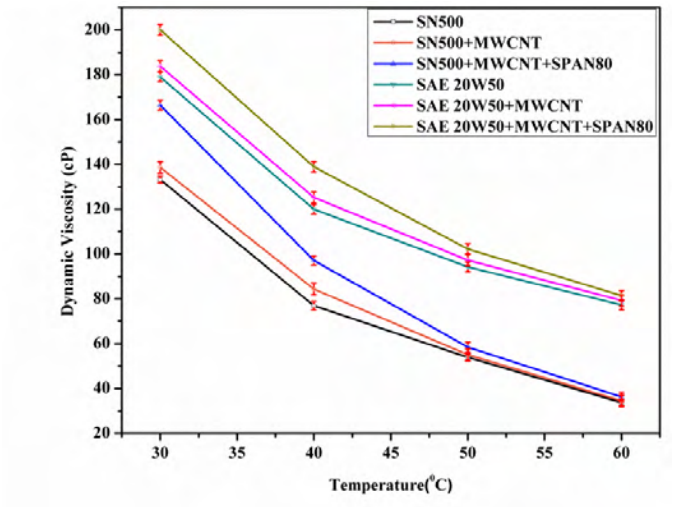

Figure 6.13: Dynamic viscosities of base oils and commercial oils in the presence and absence of additives

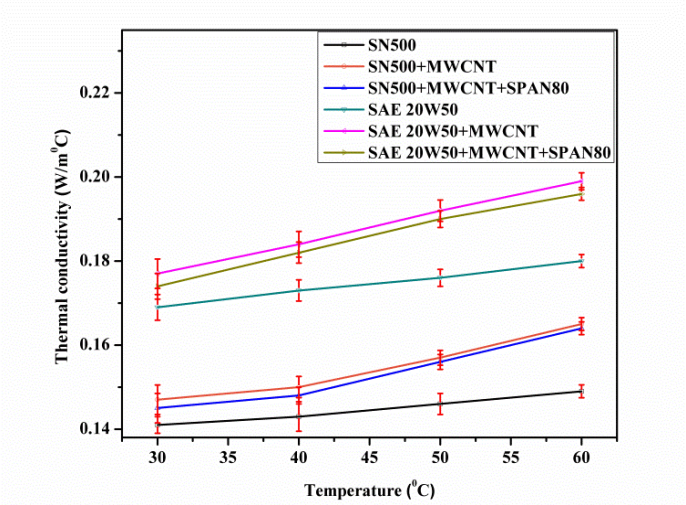

Figure 6.14: Thermal transport properties of various lubricating suspensions.

Excellent high thermal conductivity of MWCNT additive (~ 3000 W/m^{0}C) and ability to form solid-like structure at the liquid-solid interface with the introduction of MWCNT into lubricating oil [213–215], might be the possible cause of an increase in thermal conductivity. Another possible reason of superior thermal property can be illustrated in terms of its thermal stability. The thermal stability of MWCNT was also assessed using on TGA and DTG (Figure 6.15). Thermal stability of the MWCNT sample was investigated in the nitrogen environment (50 ml. min^{-1}) with the heating rate of 10°C min^{-1}. It is noticed from Fig. 6.15 that thermal conductivity is not dependent on the temperature of MWCNT up to 5000C. The decomposition of the MWCNT is initiated at around 500°C, and the maximum weight loss (ca. 20%) was observed between 500°C to 900°C. This indicates that MWCNT has superior thermal stability at room temperature and up to temperature of 500°C.

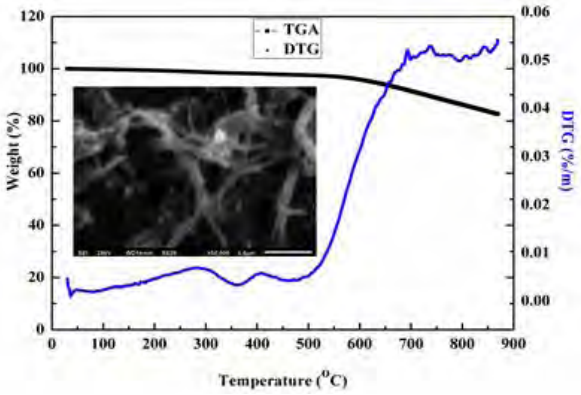

Figure 6.15: Thermo-gravimetric analysis (TGA) and differential thermo gravimetric (DTG) plot for MWCNT additive.

However, with the addition of non-ionic surfactant, a slight decrease in thermal conductivity has been observed, owing to the low thermal conductivity of surfactant molecules that wraps the MWCNT solids and act as a thermal-barrier [216]. However, there is an adequate difference in the value of thermal conductivity of base and commercial oils without any additive and surfactant, so the use of SPAN80 cannot be limited for further formulation.

6.4.1.3 Improved oil-MWCNT-surfactant interaction of surfactant modified MWCNT-oil nanodispersions (leads to enhanced oxidation stability and shear sliding property)

In this section, a mechanistic approach for the CMC formation and surfactant-particle-oil interaction is presented. The micelle formation involves the self-assemblies of the surfactant molecules to form a variety of structures such as spheres, bilayers, and vesicles, etc. From the pilot study, it was observed that the surfactant concentration of 0.04 vol.% exhibits the optimal lubricious characteristics, interestingly which lies close to the critical micelle concentration (CMC) value of this surfactant. It is a known fact that the micelle shape is linked to a critical packing parameter (CPP) [217].

$$\text{CPP}= \frac{V}{a_h . I_C} \tag{6.6}$$

Where V is the hydrocarbon chain volume, I_C is the maximum chain length (effective) and a_h is the area of the head group. However, an approximation for the area requires sophisticated special experimental procedures [217]. Still, there are empirical methods [218] that give the area for non-ionic surfactant molecules, based on that the selected given surfactant SPAN80, the area of the head group yields to a value 0.479 nm^2 and CPP value nears about~ 0.44, which is a close approximation with the literature results [219].

The CPP value of the range of 0.33- 0.5 lies for cylindrical micelles and the range from 0.5 to 1 for flexible bilayers. A little consideration shows that the presence of oil as a matrix medium enhances the value of CPP due to the micelle core swelling [220]. Some of the authors revealed that low HLB amphiphilic tends to form layered structures than spherical structures [217,221].

MWCNT interacts surfactant by non-covalent bonding methods, in which hydrophobic part of the adsorbed molecules interact with nanotubes through van der Waals, Π-Π and CH-Π, etc. and solubility is imparted by the hydrophilic part of the molecules [221]. Some authors believe that Π-Π interactions of CNT and surfactant molecules offer for sustainable adequate adherence. In a nutshell, the hydrophobic interaction is the driving force to adsorption on the surface of nanotubes. The adsorption of molecules on MWCNT in this manner does not alter the graphene

sheet system [222]. SN500-mineral oil, which consists of aliphatic chains and non-polar nature, interacts with the hydrophilic part of the surfactant by induced dipole-dipole forces [223].

When the concentration of surfactant goes beyond CMC, alkyl chains of the adsorbed parts tend to aggregate by forming hemi-micelle. These hemi-micelles play a vital role in the lubrication sliding. It is essential to mention that the selected mineral oil is assumed to be non-polar solvent as it has a very low zeta potential value, i.e., $\zeta = \sim < 0.3$ millivolts. The surfactant in nonpolar media assembles to form reverse micelles, exposing the hydrophobic tails to the solvent media and concealing the hydrophilic polar heads in the micelle core. It is also important to mention that due to the nonionic nature of the surfactant, the steric repulsion between the cylindrical micelles is responsible for the stable suspension of the additive in the oil phase.

Besides the structural interaction and stability, which favors the tribology of contact pair as discussed above, it is also essential to explore the oxidation stability of the formulated dispersions under the sliding contacts. The oxidation stability of these dispersions was investigated using FTIR Spectra, as depicted in Figure 6.16.

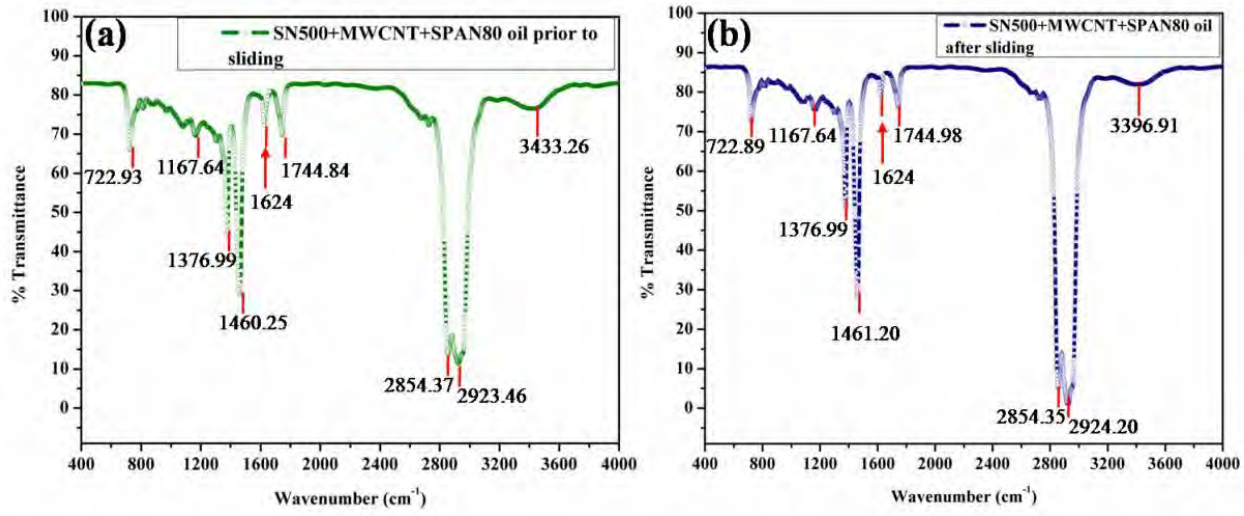

Figure 6.16: FTIR Spectra of functionalized MWCNT-oil dispersions before and after the sliding test.

The main objective of FTIR studies is to ensure that there is a minimization of oil degradation due to oxidation. From the FTIR spectrum it is observed that the peaks around the wavenumbers 2924 cm^{-1}, 2854 cm^{-1}, 1461 cm^{-1}, 1377 cm^{-1} and 722.9 cm^{-1}, comes from the hyrdocarbons of oil. The stretching vibrations of CH_2 groups are encountered at 2924 cm^{-1} and 2854 cm^{-1} and the bending of vibrations of CH_2 groups are occurred at 1377 cm^{-1}. The absorption peaks around at

1461 cm^{-1} and 722.9 cm^{-1} corresponds to aliphatic chain of C-C bond and the rocking vibration of long chain alkanes, respectively. It is important to mention that an absorption peak was also observed at 960-965 cm^{-1} for the commercial oil which corresponds to the presence of zinc based antiwear additive. This is in agreement with the earlier reported literature[183,224].

However, the absorption peaks near to 1624 cm^{-1} represents the characteristic C=C aromatic stretching, corresponding to the absorption peaks of MWCNTs. This is intact in both the spectrum. This outcome confirms the existence of hexagonal structured MWCNTs [225,226], before and after the sliding test. Besides, FTIR peaks near 1744.84 cm^{-1}, 1167.6 cm^{-1} and 3397-3433 cm^{-1} are quoted for the presence of interaction of SPAN 80 with CNTs. With the addition of a low HLB surfactant, a distinct absorption peak at 3433/3397 cm^{-1} is observed which is attributed to the O-H stretching vibration coming from a surfactant molecule. Besides, the characteristic absorption peaks at 1744.84 $cm^{-1}$and 1167.6 cm^{-1} suggested for the presence of esterification compounds [227]. As one can see from the FTIR spectrum that there is no significant difference in the characteristic peaks of functionalized oils before and after the sliding; even the oxidation peaks (1715-1719 cm^{-1}) [228] are not distinctly visible. Thus, it is clear that no signs of chemical reaction or forming of unwanted products from the reaction of MWCNT and surfactant with oil. Hence, from these observations, we can conclude that oil degradation due to frictional heating and sliding is constrained by the use of surfactant grafted MWCNT oil dispersions. SPAN80, with a concentration close to the CMC form aggregates and packed them to micelle structures that shears under the traction forces and releases oil under the contact to ease in the lubrication process. They are generally adsorbed onto the surface [229] rather than the process of electrostatic or chemisorptions [230]. Thus, it seems that the specific particle-surfactant-oil interaction forming the bilayered structures led to the improved lubrication under the selected tribopair. Thus, a hypothesis on shear sliding mechanism can be proposed based on the building of a tribochemical film, which is driven by the favourable surfactant-particle-oil interaction (Figure 6.17). This is explained as follows.

Figure 6.17 shows a schematic of various interactions that prevailed between molecules of oil, additives, and surfactant, *viz.* oil-surfactant, MWCNT-oil, MWCNT-surfactant, and micelle-micelle interactions. As discussed earlier, low HLB amphiphilic tends to form a bilayer structure in which the inter-layer plane exhibits hydrophobic methyl terminals on both sides [231].

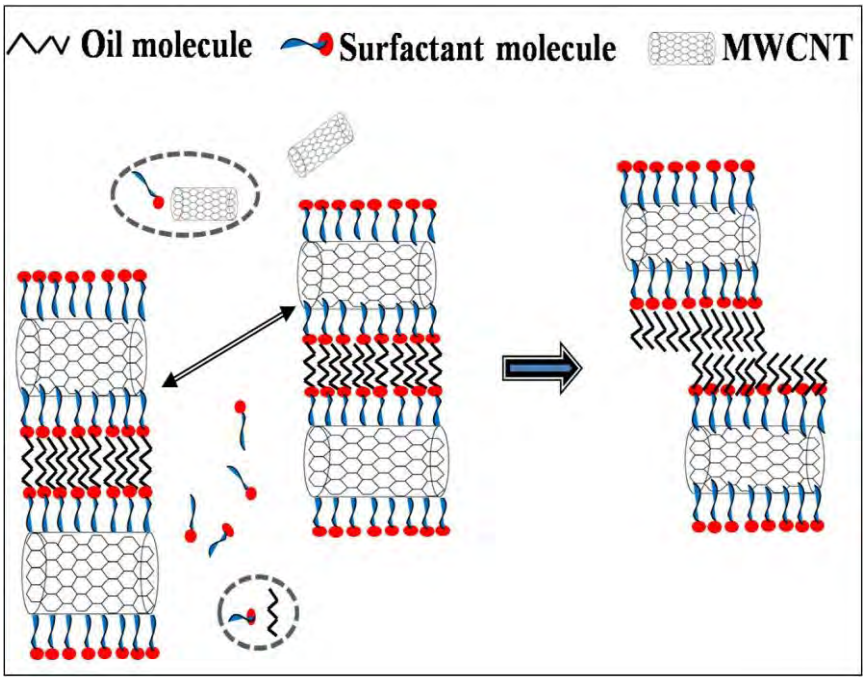

Figure 6.17: (a) Formation of micellar structures, (b) Shear sliding of micellar structures.

It is worth to mention here that the bilayer structured micelles involve less amount of energy required during breaking and shearing the micelle than other spherical types of the micelle. It is worthwhile to mention that thick and adherent films are formed in-between the contact due to these bilayer structures. The adherence of the formed film remains intact by Van der Waals type forces acting between the nonionic surfactant and the tribopairs under lubricated sliding [232].

6.4.2 Friction-wear mechanism (Fractography analysis)

The SEM micrographs of wear tracks of h-AMMC pins sliding under various lubricated conditions are shown in Fig. 6.18 and various zones are marked, followed by a detailed EDS analysis on each marked zone. Table 6.4 shows the elemental composition on the pin wear tracks (in the absence of any additive). As shown in Fig. 6.18(a), few lean wear patterns and pits are visible on the wear track when the pin is sliding under SN500 (without any additive). The presence of iron Fe and C (Spectra 2, Table 6.4) in a considerable amount supports the fact of the formation of a mechanically mixed layer in the case of Fig 6.18(a). There are some areas in the SEM micrograph (Fig 6.18(a)) where a notable amount of cracks are observed owing to the oxidation of materials (Spectra 1, Table 6.4) and fatigue fractures. Zone 3 of Fig 6.18(a) is relatively smooth, which causes significant plastic deformation of the Al matrix in the presence

of a lubricant layer, preventing the direct metallic contact but with no significant oxidation as confirmed by spectra 3 (Table 6.4).

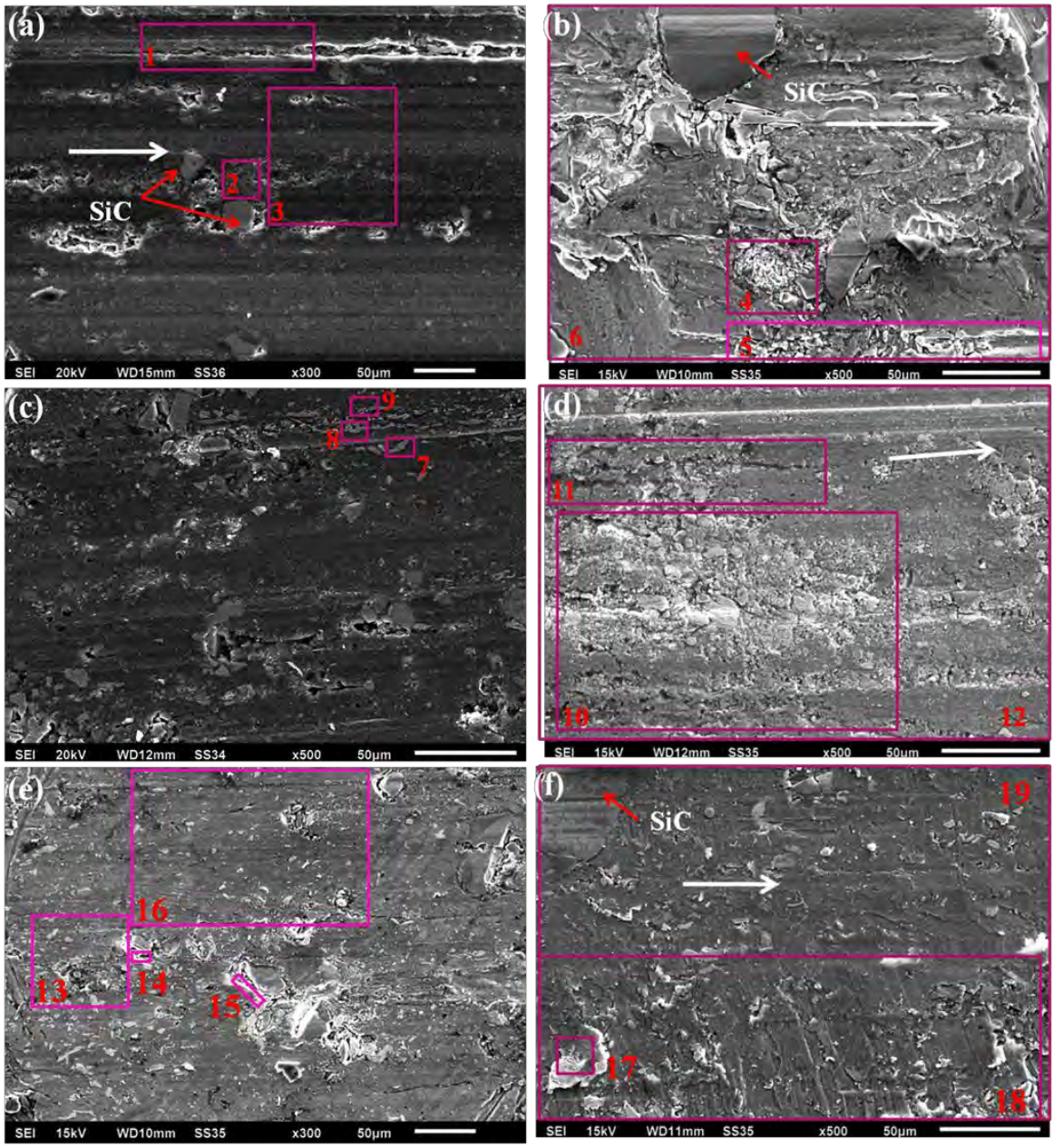

Figure 6.18: SEM micrographs of wear tracks of h-AMMC pins under various lubricated conditions (a) SN500, (b) SAE 20W50, (c) SN500+MWCNT, (d) SAE20W50+MWCNT, (e) SN500+MWCNT +SPAN 80 & (f) SAE20W50+MWCNT+SPAN 80. Inset rectangles drawn in the figures indicated the selected EDS zones.

On the other hand, fully formulated oil with no additive shows different characteristics (Fig 6.18b) as compared to the mineral base oil. Significant amounts of Fe, Si, and C are detected from EDS investigations, as shown in the spectra 4-6 (Table 6.4). This shows the possibility of material transfer, rupturing of SiC, and oxidation; besides the adhesive wear. Additionally, the presence of Zn and P, as seen in Table 6.4, might be due to the formation of zinc phosphate and iron sulfide compounds under tribological action. This is confirmed from the XRD investigation (Fig. 6.19a). The presence of these compounds indicates the formation of antiwear layers, which is in agreement with reported literature.

Table 6.4: Elemental analysis (wt.%) on the worn-out AMMC pins sliding against steel surfaces under fresh and commercial oil lubrication without any additive.

Oil	Spectra	C K	O K	Mg K	Al K	Si K	Mn K	Cr K	Fe K	P K	S K	Zn L
SN500	1	18.10	31.80	0.24	44.26	0.64	-	-	4.97			
SN500	2	11.98	20.87	0.36	35.48	7.51	-	-	23.79			
SN500	3	12.38	9.04	-	72.76	2.44	-	-	3.39			
SAE20W50	4	35.33	7.62	0.61	23.35	10.96			21.61			
SAE20W50	5	33.13	8.35	0.42	35.26	9.09	0.09	0.16	12.70	0.09	0.06	
SAE20W50	6	25.70	7.30	0.47	45.85	11.55	0.20	0.20	7.93			0.11

Table 6.5: Elemental analysis (wt.%) on the worn-out AMMC pins sliding against steel surfaces under MWCNT-oil lubrication

Oil	EDS spectra	C K	O K	Mg K	Al K	Si K	Mn K	Cr K	Fe K	P K	S K	Zn L
SN500	7	11.80	9.49		39.02	3.01	-	-	36.69			
SN500	8	14.37	6.85	0.48	41.26	0.14	-	-	36.90			
SN500	9	17.89	6.40	0.49	60.43	1.30	-	-	13.49			
SAE20W50	10	19.22	21.50	0.17	34	1.77			23.04	0.03	0.07	0.15
SAE20W50	11	30.33	16.54	0.27	37.51	3.68			11.20	0.10		0.14
SAE20W50	12	20.16	19.85	0.31	41.87	2.56			14.78	0.06		0.02

Table 6.6: Elemental analysis (wt.%) on the worn-out AMMC pins sliding against steel surfaces under surfactant functionalized MWCNT-oil lubrication.

Oil	EDS spectra	C K	O K	Mg K	Al K	Si K	Mn K	Cr K	Fe K	P K	S K	Zn L
SN500	13	20.91	8.22	0.42	55.07	6.10	0.22	0.25	8.80			
SN500	14	22.37	2.55	0.11	2.34	0.86	0.79	0.40	70.58			
SN500	15	28.42	12.03	0.87	33.03	5.71	-	0.13	19.93			
SN500	16	19.59	8.46	0.44	60.71	5.79	0.31	0.39	4.31			
SAE20W50	17	18.51	7.61	0.42	50.62	1.94	0.32	0.16	19.32	0.06	0.05	0.15
SAE20W50	18	19.39	8.44	0.64	62.43	3.42	0.18	0.18				
SAE20W50	19	17.01	7.04	0.61	62.18	7.73	0.21	0.05	5.0			

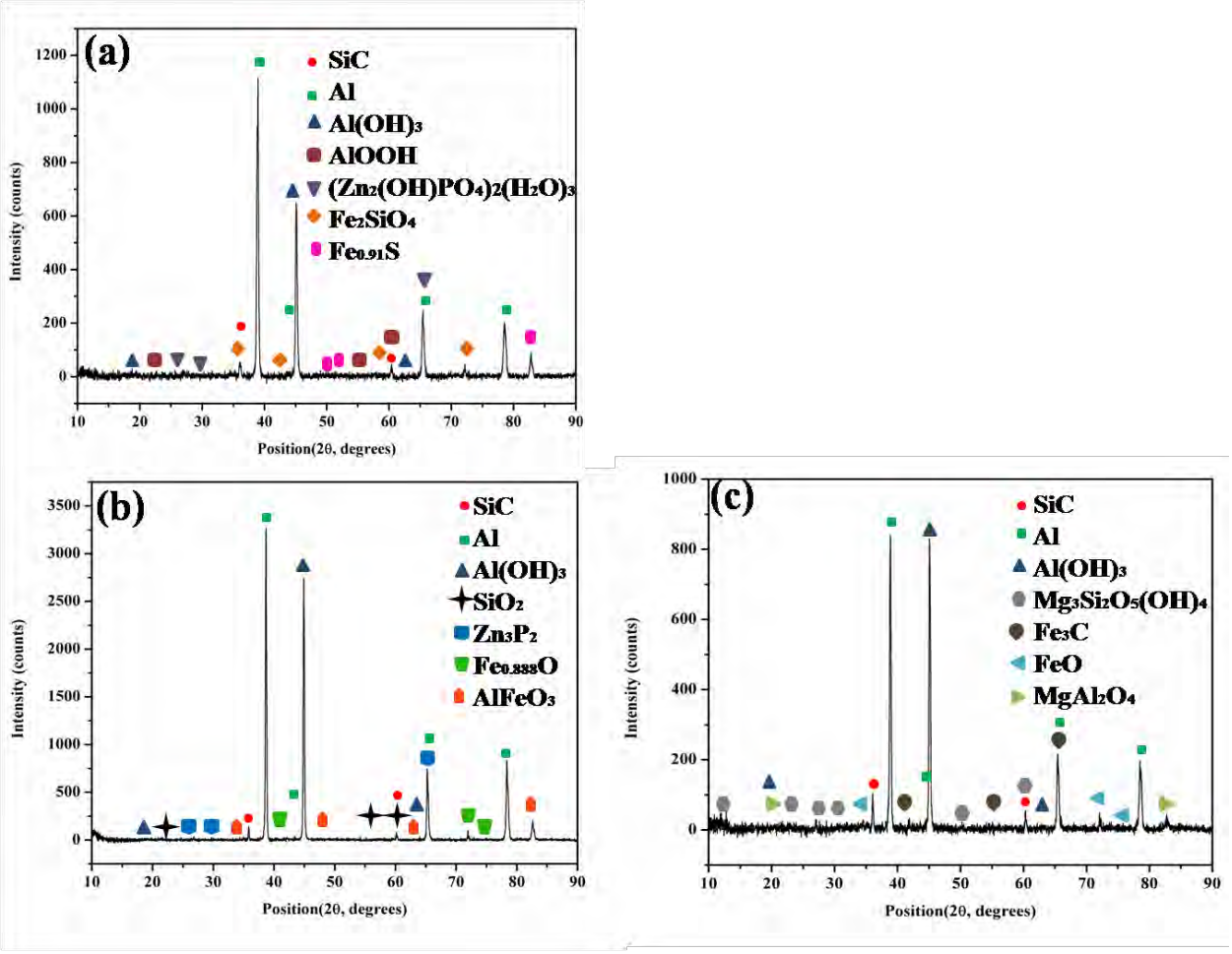

Figure 6.19: XRD spectrum of worn-out hybrid composite pins sliding under (a) fully formulated oil, (b) fully formulated oil with MWCNT, (c) fully formulated oil with MWCNT and surfactant.

In the case of MWCNT-laden base oil sliding, there is a formation of a distinctive Fe based material transfer layer on the pin surface as suggested by spectra 7 and 8 (Fig 6.18c and Table 6.5). However, in the case of MWCNT-laden fully formulated oil, smoother pattern due to mixed layers, primarily rich in Fe is visible (Fig 6.18d and spectra 10-12 of Table 6.5). The significant presence of C in the EDS composition naturally shows the presence of MWCNT in abundance in the wear track. Along with this, there is a high possibility of intermixing of carbon compounds coming from the synergic effect of doped graphite from the composite and carbon content from hydrocarbon oil.

Moreover, the significant presence of oxygen in XRD implies that there is also the formation of oxide layers. Amorphous aluminium hydroxide, iron oxide, and zinc phosphide compounds are also detected in XRD (Fig 6.19b), which are undoubtedly responsible for improved friction-wear properties of such contacts. Zinc phosphide can be formed by the reaction of elemental zinc with phosphorus [233] as follows.

$$3Zn + 2P \rightarrow Zn_3P_2 \quad (6.7)$$

In the case of surfactant functionalized MWCNT-in-oil-lubricated sliding conditions, relatively smooth surfaces in contrast to previously discussed SEM micrographs are observed for both types of oils (Fig 6.18e,f). The oil-additive-surfactant interaction is finely modulated in this scenario as compared to the previous case. Besides, EDS spectra from Table 6.6 the significant presence indicates the formation of continuous carbonaceous layer for surfactant-functionalized-MWCNT-in-base oil and surfactant-functionalized-MWCNT-commercial oil. The presence of MWCNT in the wear track of fully formulated oil is confirmed by the XRD patterns (Fig. 6.20a), detected at a 2Θ value 25.9-26.7°. The presence of MWCNT-based layer on the wear track generated in surfactant-functionalized-MWCNT-in-oil lubrication is also identified through Raman spectroscopy (Fig. 6.20).

However, a significant presence of magnesium silicates and iron carbide in the wear track is observed in case of surfactant-functionalized-MWCNT-in-commercial oil (Fig. 6.19c).

Formation of magnesium silicate from magnesium oxide and silicon dioxide, as seen in Fig 6.19(c), can be described by the following reaction [195]:

$$MgO+SiO_2 \longrightarrow MgO.SiO_2 \quad (6.8)$$

Polymorphism of magnesium silicate compounds was also discussed by some authors [195,196]. Various tribologists have already reported on the self-repairing and friction-reducing capabilities

of hydroxyl magnesium silicate compounds [234,235]. Thus, in the case of surfactant functionalized MWCNT-laden oils, better rheological properties, the formation of continuous carbonaceous and non-carbonaceous layer, and shear gliding of micelles under sliding action favors the excellent tribological behaviour.

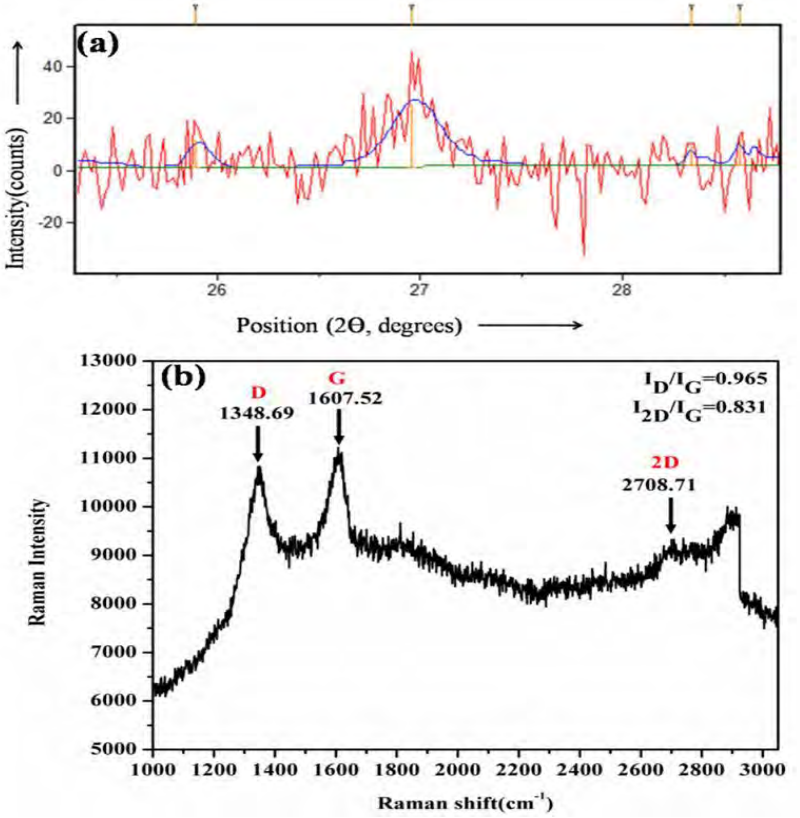

Figure 6.20: (a) XRD, (b) Raman spectrum on worn-out surface sliding under oil-MWCNT-Span80 (30min, 0.5m/s and 9.81N), depicting the presence of MWCNT in wear tracks.

6.4.3 Schematic friction-wear-lubrication model for surfactant-functionalized-MWCNT-in-oil

Based on the above discussion on lubrication and friction-wear characteristics a qualitative model can be proposed for the surfactant functionalized MWCNT-based particle lubricant under hAMMC/EN31 contact. The schematic of this is shown in Figure 6.21.

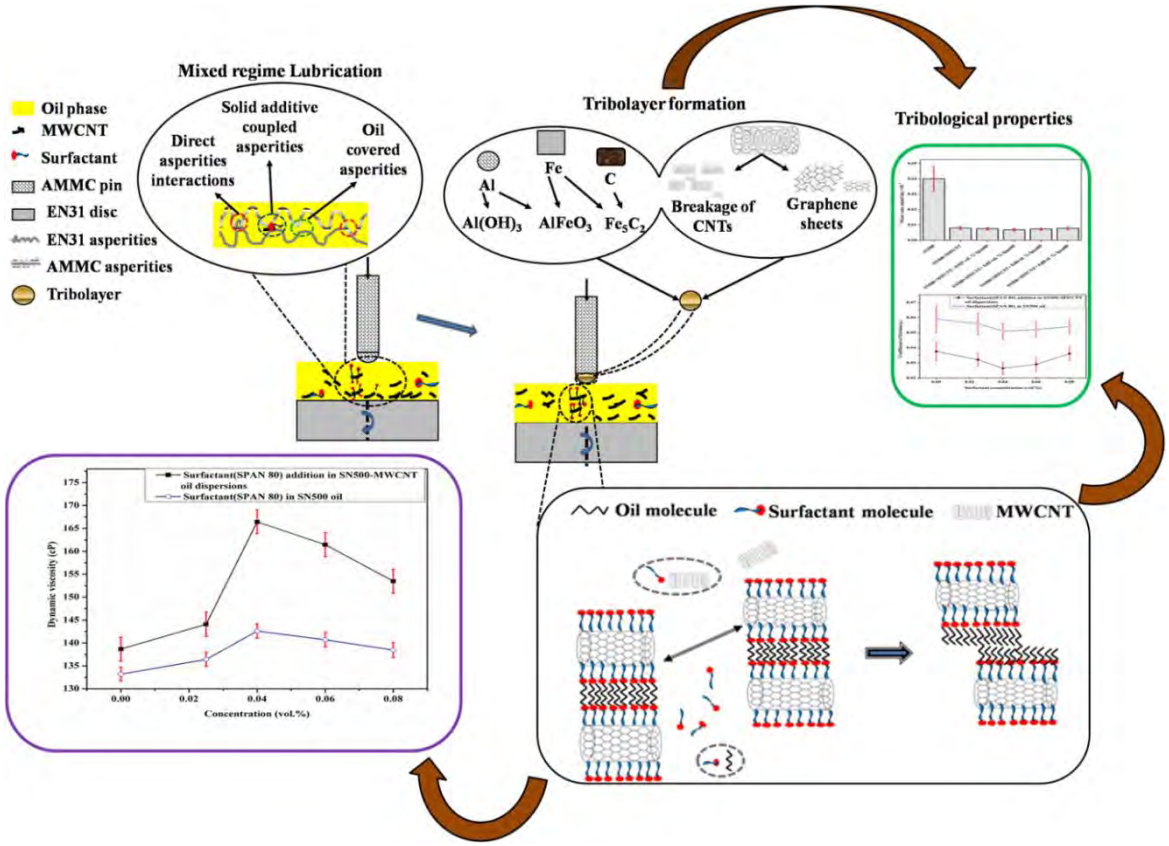

Figure 6.21: Schematic of lubrication mechanism for surfactant-functionalized-MWCNT-in-oil (under hAMMC/EN31)

6.5 INFLUENCE OF APPLIED LOADING ON THE WEAR BEHAVIOR

6.5.1 Wear transition plot

On realizing the beneficial effect of MWCNT-in-oil and surfactant functionalized MWCNT-in-oil on the tribology of hAMMC, an extended study was carried out to explore the tribological performance of the surfactant functionalized MWCNT-laden base oil under varying speeds and loading conditions. This is followed by a comparison of the tribological performance of this prepared lubricant with that of fully formulated oils (SAE20W50). Accordingly, to explore the role of load on the underlying friction and wear mechanism, wear tests and fractography analysis is carried out for surfactant functionalized MWCNT-in-oil lubricant under varying loads.

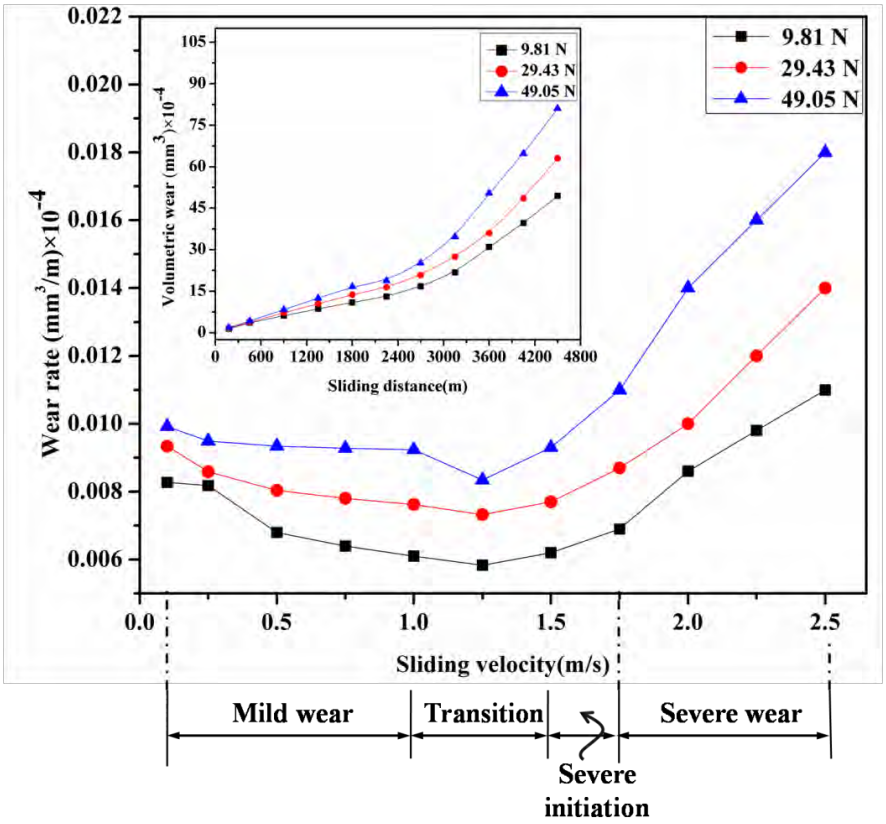

Figure 6.22: Wear transition plot showing different wear regimes for AMMC-EN31 contacts under surfactant functionalized MWCNT- oil sliding (Inset: wear rate versus sliding distance plot under different loading conditions).

From the wear transition plot (Fig. 6.22) it is clear that mild wear emerges at low to moderate sliding speed (0.1 m/s to 1.0 m/s) under various applied loading conditions (9.81 N to 49.05 N). Typically, this wear region is regarded as a safe wear regime [236]. Severe wear comes into existence after the transition regime (induced by the compounding of two or multiple wear mechanisms) at a moderate speed to high speed operating conditions (1.5m/s to 2.5m/s). Once the applied load is increased, mild to severe wear transition comes earlier into sight. In the mild wear region, volumetric wear loss and sliding distance (up to 1800 m) shows a linear relationship (Fig.6.22), indicating that wear evolves under steady-states. Once this transition starts, the wear losses have non- linear dependence on the sliding distance (1800-2700 m).

6.5.2 Fractography of worn-out tracks

The morphology of the wear tracks and corresponding roughness profile generated due to variable applied loadings are shown in Figure 6.23. The EDS analysis on these tracks is shown in Table 6.7. From the SEM micrographs it is seen that at low load (Fig 6.23a) the presence of

surfactant-assisted MWCNT-oil suspensions significantly reduces the cumulative wear, as compared to the higher loads (Fig 6.23(d,g)). It is sensible to mention here that an excessive amount of carbon in the entire EDS spectra of worn-out track (namely spectra 1, 2, 3, and 4 in Fig. 6.23(a)) is detected due to the formation of the stable carbonaceous layer, as already investigated earlier. Besides this formed layer, tribolayer formation may occur by the tribo-chemical action as well as by mechanical mixing of components. Figure 6.23a and spectra 1-4 of Table 6.7 and the detailed investigation made in the previous sections validated this fact. These formed layers influence the friction-wear properties of contact pairs. Abrasive mode of wear is significantly decreased by using surfactant-assisted MWCNT-oil owing to the simultaneous effect of the tribo-chemical and deformed carbonaceous layers, and their synergic effect enhances the tribological performance of the contact pairs.

When the load is increased to 29.43N, more irregularities, plowing action, and material transfer is observed as shown in Fig. 6.23(b). EDS spectra 5 from the marked zone in the figure represents the signs of material transfer (Fe, element detected around 75 % by wt.). Due to plowing action, SiC particles may flush out from the surface exposing the matrix material (the presence of Al on the wear track as indicated by Spectra 6 & 7). Material oxidation and carbide formation might also be there, as confirmed by the presence of a significant amount of oxygen (Spectra 6, 7 & 8). However, there is still a reduced amount of abrasive and adhesive wear, which was the principal wear mechanism of the pin, thus making the morphologies of wear scars smoother. In addition to all these wear modes, presence of a noticeable amount of carbon in all the spectra on wear track, indicates the possible presence of MWCNTs and carbonaceous tribolayer.

In case of severe load it is observed that the delamination, abrasive action, and oxidation are the predominant modes of wear. In this case, significant surface damage is observed due to the increased contact pressure. Black areas marked in the image indicate the possible accumulation of carbon content (spectra 10 and spectra 12).

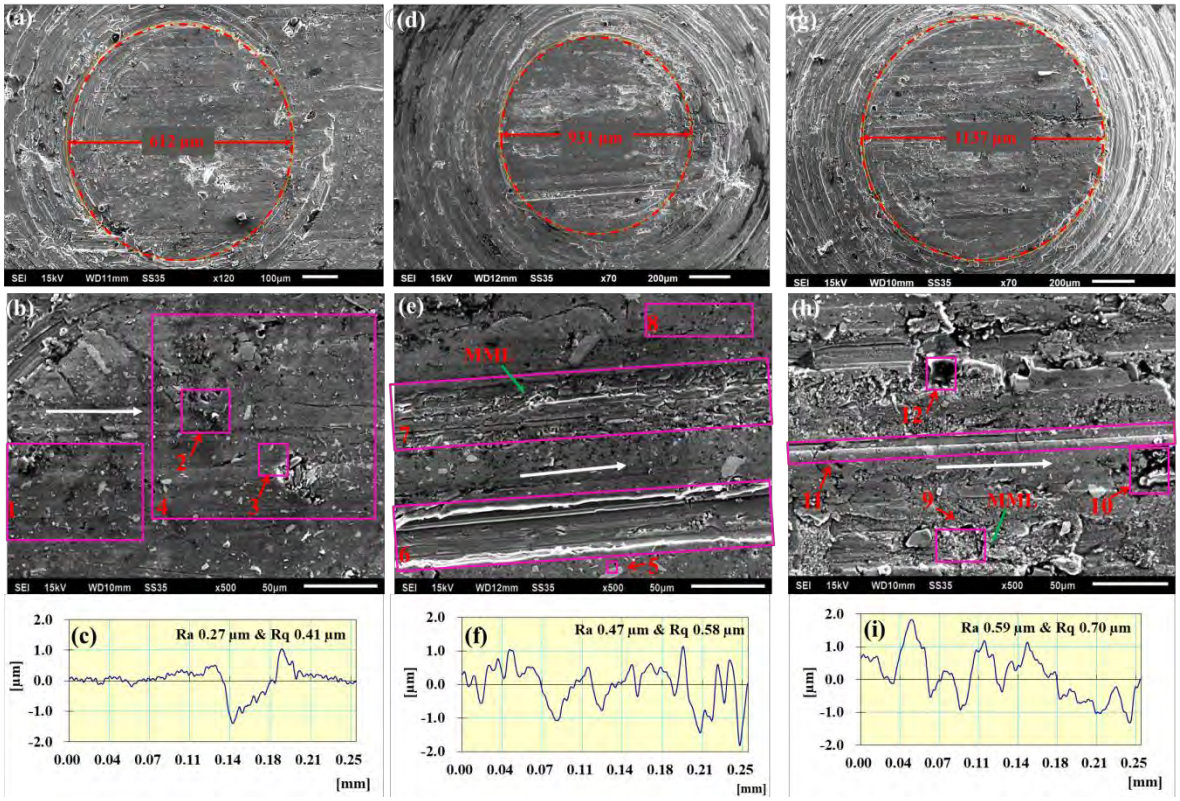

Figure 6.23: SEM micrographs and roughness profiles of Al6061-SiC-Gr composite worn-out pins, sliding at 0.5 m/s, under surfactant-assisted MWCNT-oil lubrication for varying load conditions (a, b, c) 9.81 N, (d, e, f) 29.43 N, and (g, h, i) 49.05 N. Inset rectangles represent the selected EDS areas. White arrows represent the sliding direction.

However, all other regions of this micrograph also reflect the presence of significant amount carbonaceous materials. This might be due to the accumulations of graphite and exfoliated sheets of MWCNT, but not able to act as a continuous protective layer, reason of which needs further investigation. This can be further assessed by Raman spectroscopy. The average amount of material oxidation is also high in this case. There are some areas in the figure where mechanical mixing might have occurred as identified by the significant amount of Fe, Al & C.

Table 6.7: Elemental analysis (wt. %) on worn-out Al6061-SiC-Gr composite pins sliding under various loads in the presence of surfactant-assisted MWCNT-in-oil dispersions

Applied load (N)	EDS spectrum	C K	O K	Mg K	Al K	Si K	Mn K	Cr K	Fe K
9.81 N	1	20.91	8.22	0.42	55.07	6.10	0.22	0.25	8.80
9.81 N	2	22.37	2.55	0.11	2.34	0.86	0.79	0.40	70.58
9.81 N	3	28.42	12.03	0.87	33.03	5.71	-	0.13	19.93
9.81 N	4	19.59	8.46	0.44	60.71	5.79	0.31	0.39	4.31
29.43 N	5	13.36	1.03	0.08	7.53	0.41	0.23	0.91	75.66
29.43 N	6	16.93	6.41	0.34	71.98	2.83	0.02	-	1.49
29.43 N	7	19.56	10.45	0.54	64.05	4.02	-	0.02	1.37
29.43 N	8	9.28	14.57	1.20	64.28	9.22	-	-	1.44
49.05 N	9	31.02	15.78	0.49	29.81	2.75	-	0.36	19.79
49.05 N	10	52.64	12.32	0.34	21.05	9.97	-	-	3.68
49.05 N	11	21.67	11.80	0.68	54.73	2.53	0.41	-	8.19
49.05 N	12	62.31	27.82	0.06	6.60	0.20	-	-	1.02

6.5.3 Raman spectroscopy of worn-out tracks

In the Raman spectrum, distinct peaks are noticed at around 1348 cm^{-1}, 1600 cm^{-1}, and 2700 cm^{-1} that relate to D, G, and 2D graphitic structures, respectively [142,237–239] for all the three loading conditions (Figure 6.24). Further investigation is made to get insight on the structural and phase transition of this carbonaceous phases present in the wear tracks.

In Fig. 6.25 (a), the G-band positioning gives information on the stress experienced by CNTs. It is proposed that highly strained graphene structures have a shift in the wavenumber. Changes in interatomic distances of graphene may lead to generate residual stresses in the specimens [240]. The reduction in Full Width at Half Maximum (FWHM) value of the D band represents the reduction in structural disorder and the increase in FWHM of G band indicates the higher rates of graphitization. However, for nanocarbons there is a higher degree of graphitization if D and G bands are more constrict. It was shown that MWCNT has superior thermal stability up to500°C. However, a gradual decomposition of MWCNT additive may initiate at around 500°C. Under the tribocontact, there is the possibility of a localized heating effect due to which flash temperature at the asperity contact can reach well above the melting temperature of 6061 aluminium alloy.

Due to the constant exposure to this elevated temperature, there is a distinct possibility of growing domain of graphitization.

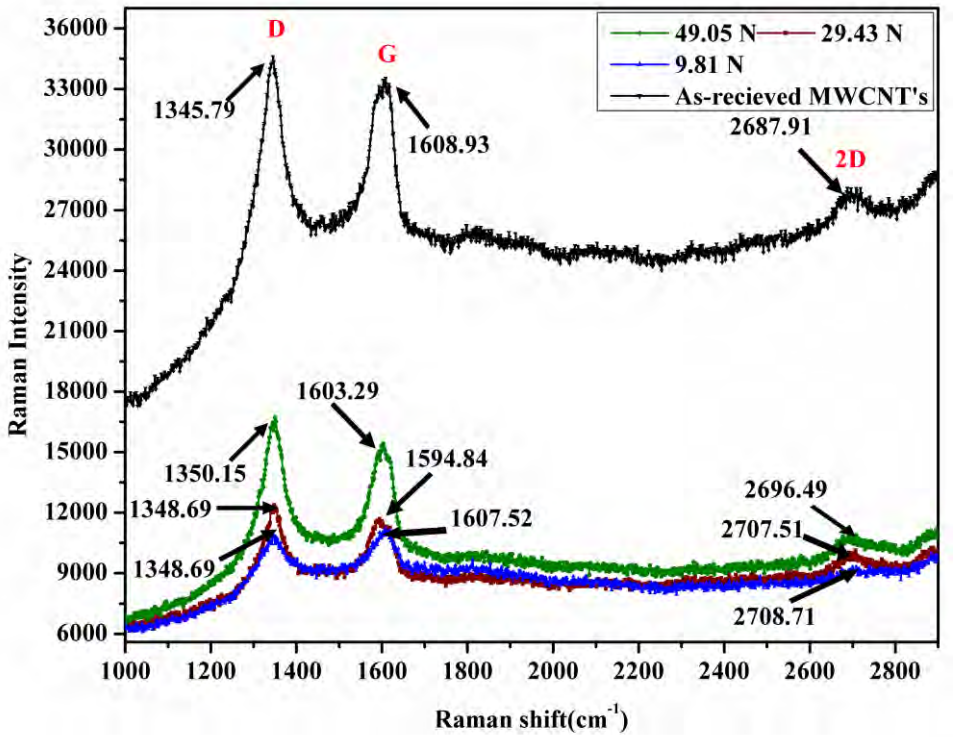

Figure 6.24: Raman spectrum of worn-out pin surface sliding under surfactant-assisted MWCNT oil dispersion, at variable loading conditions.

It is clear from Fig. 6.25(a) that G-band positioning is shifting from lower to higher wavenumbers as the applied load is increased from 29.43 N to 49.05 N. This Raman shifting refers to a transient state of the nanotubes, i.e., accumulation of the affected graphitic natured particles [241].

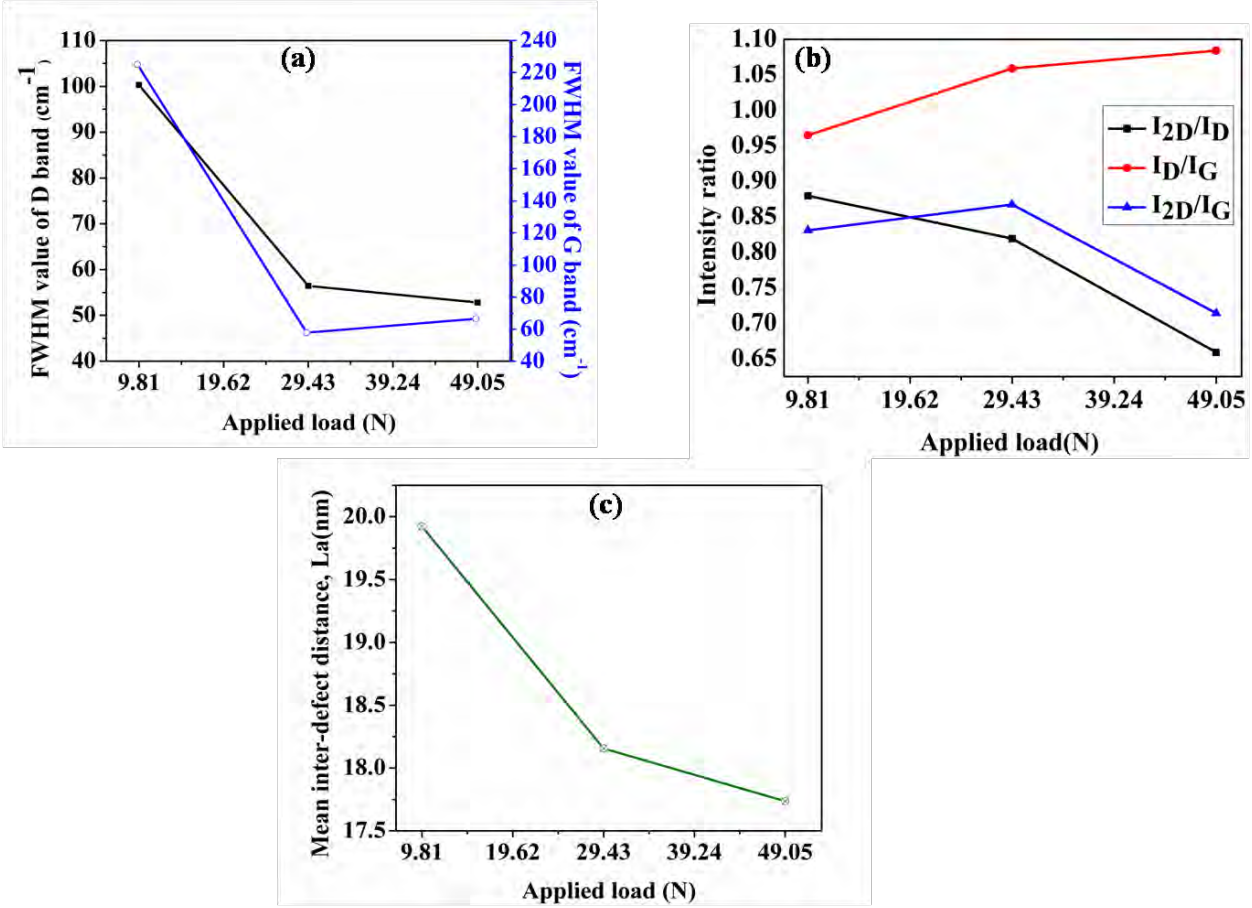

Figure 6.25: (a) Change in the value of FWHM of D band and G band, (b) I_D/I_G ,I_{2D}/I_G ratios, and (c) Mean inter defect distance with respect to applied loading conditions.

In Fig. 6.25(b) it is observed that the intensity ratio of I_D/ I_G is enhanced from 0.96 to 1.08 as the magnitude of applied load increases. This indicates that there is an increase in the disorder or defect density in graphitic structures. However, the rate of this increase is reduced on further loading. The shape and position of the 2D peak gives an adequate background on the stacking sequence of nanographite. The intensity ratio I_{2D}/I_G is increased when load is increased from 9.81 N to 0.86 at 29.43N. This increase in ratio relates to the disintegration of graphite and exfoliation of graphitic layers under sliding action [242]. However, the ratio is dropped at 49.05N since the number of graphene layers is reduced owing to the physical action or very large stress originated from the applied force, which subsequently facilitate the separation of graphene sheets from each other. Additionally, the purity index of a graphitic substance can be assessed with the help of

intensity ratio I_{2D}/I_D [241,243–247], which is found to decrease as the applied load is increased in the present investigation.

Moreover, there is an inverse relationship between the intensity of the D band (I_D) and carbon grain size, L_g [244]. An empirical relationship was developed between the excitation wavelength and intensity ratio of the D and G band [241,244] to calculate the inter-defect distance. In another study, the double resonance nature of the D band was related to the mean inter defect distance L_a (Eq. 6.9) [241,244]. It was derived to describe the mean in-plane crystallite size in graphite [245], which has been found equally effective for graphitic materials in general, including nano-carbons and CNTs [246–248]. This length depicts the distance that separates two consecutive structural defects on the structure [249]. Reduction in inter defect distance gives vivid degradation of the CNTs structural quality under higher applied loads.

$$\text{Mean inter defect distance, La} = (2.4 \times 10^{-10}).\ {}^{4}.\left(\frac{I_D}{I_G}\right)^{-1} \quad (6.9)$$

6.5.4 Development of wear map

Wear is a complicated evolution, and typically one or more mechanistic studies are encountered in a failure of the structure under a specified speed/loading combination. Wear mechanisms map is created using Minitab 17 software by contour plotting of speed (S) and load (L) as predictor variables and wear rate (WR) as response variable, using distance power interpolation method. In wear rate map (Fig. 6.26), contour lines represent the wear rate under different loading conditions. These contour plots facilitate the safe utilization of a mechanical system for a particular loading condition [250]. In these maps, contour lines of constant wear rate were plotted, and wear rate under different operating conditions is represented by a different contour line. The boundaries for wear transition are identified using wear rates at different loading conditions and the worn-out surface analysis based on SEM micrographs at different loading conditions, along with the wear rate states for particular load-speed conditions [251].

It is worth to mention here that there is an inverse relationship between the sliding speed and wear rate is observed prior to attaining the severe wear regime. This might be attributed to the oxidation of aluminum composite surfaces that generated an oxide layer at high interfacial temperature conditions through tribo-chemical action at higher interfacial temperature, and hence shielding the surface and hampers the rate of wearing out [252]. Moreover, it is sensible to mention that during friction action, Fe element may be oxidized to form a tribo-favorable

product which acts as a solid lubricant that helps to minimize wear [253,254]. The presence of $Al(OH)_3$ and $AlFeO_3$ in the XRD spectra supports this fact.

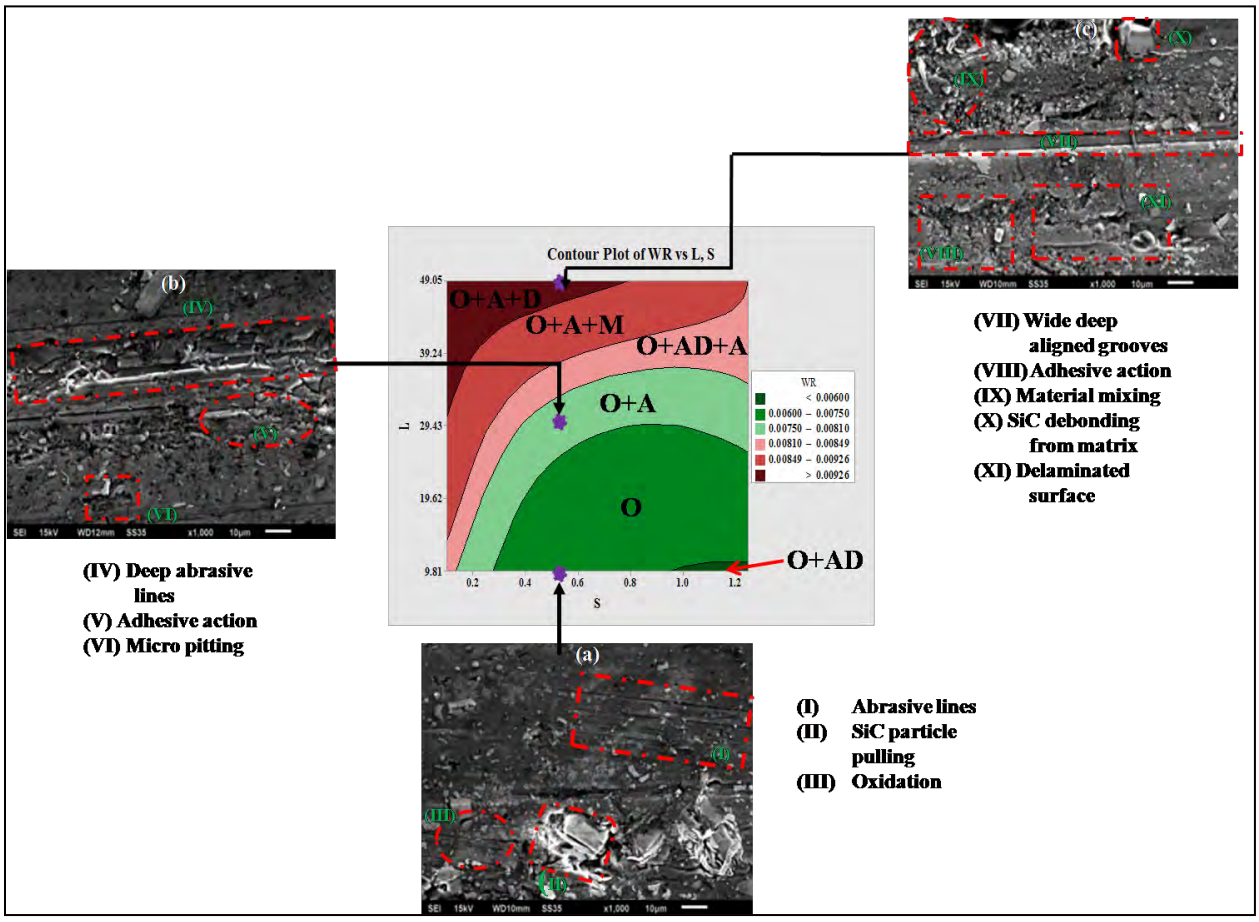

Figure 6.26: Wear mechanism plot for hAMMC sliding under surfactant functionalized MWCNT-oil. (In the contour plot, O, A, D, M, AD denotes for oxidation, abrasion, delamination, material transfer and adhesion.)

Hence, these stable oxide tribofilms can reduce friction between the surfaces efficiently. During the sliding of composite-steel surfaces, a mechanically mixed layer (MML) that exhibits a hardness value roughly six times that of the bulk composite was also generated. Hence, the generated work-hardened layer also minimizes the wear rate as the sliding speed enhances [255]. In the present case, the existence of MML and the worn-out particles in the form of debris (generally high in Fe and Cr) governed the wear rate.

The direct influence of applied load with wear rate is observed owing to an increase in the interface temperature between the tribocouples [256,257]. At mild loading conditions, the

supplementary ceramic SiC particles remain unbroken during sliding action and act as load-bearing members. These embedded particles were also shown in SEM images that support the above fact. With the increase in load, the stress-induced in the system exceeds the rupture strength of the materials. This fractured SiC materials may elevate the transfer of materials from the counter surface during friction action [258,259]. Symptoms of material transfer (even at low loads) can be seen easily in the SEM micrographs. Thus, the fact that the wear rate is increased with applied load and decreased with an increase in the sliding velocity is justified by the above discussion and experimental evidences, thereof. It is worth to mention here that an inverse relationship between the wear rate and sliding distance was also observed. This can be attributed to the fact that there might be a synergistic effect caused by the smearing out of the solid lubricant from the AMMC matrix [260], abrasion resistance provided by SiC and sustainability of MWCNT-induced graphitic layer and MMLs between the contacting surfaces.

6.6 USE OF PREDICTIVE FRICTION MODEL TO ESTIMATE THE PERFORMANCE PARAMETERS

Integrated experimental-analytical approach is to be utilized to develop a frictional mapping of the contacts for specified lubrication regimes. In present times, the tribology research for minimizing the friction effects has been observed to bifurcate into two distinct segments. One segment studies fundamental tribological investigations of various materials such as alloy steels, composites, coatings, and functionally graded material claddings. These studies involve the enhancement in lubrication properties induced by dry or lubricated form under the different regimes of lubrication. The other segment develops modeling solutions committed to applied tribological problems. Key contributions in either of these concepts are highlighted in the following paragraphs of this section.

Mixed friction; quasi-hydrodynamic lubrication belongs to a regime of lubrication where the applied forces on the tribo-contact were sustained by both the lubricating film and the contacting stresses aroused in tribo pair materials involved [261]. However, contemporary knowledge about mechanisms and modeling approaches remains undeveloped at best. Both the vital benchmarks are attained by a popular rationale on the unified boundary-mixed lubrication regimes and behaviour of rough surface morphology as well as topography.

In recent times, integrated approaches of micro-EHD (elasto-hydrodynamics) and load sharing concepts are gaining a keen interest of tribologists. Hertzian Sliding contact (point/line) theories had been applied to develop a semi-empirical model based on the load-sharing concept that distinguishes both the components such as dry asperity and liquid lubrication; highlighting the importance of simplified tribosystems in friction monitoring.

A very few researchers carried out experimental lubricated studies considering the influence of microgeometry in the context of pin-on-disc surfaces for high-performance transmissions. Frictional performance for bearing steel/gear steel contacts under fully formulated commercial lubricant (80W90) is examined by Humphrey et al. [262]. The results indicated that the formed tribolayer characteristics are in a relationship of microscale regime of lubrication and wear. Another analytical and experimental representative sliding contact study of piston ring against a cylinder liner insert under fully formulated commercial lubricants (SAE10W40) for boundary or mixed regime of lubrication [263]. The authors conducted the analysis study of the developed correlation between theoretical and experimental results of specific film thickness and frictional coefficient.

6.6.1 Load carried by asperities

In the pin-on-disc setup, an analytical continuum contact mechanics approach is used for modeling of pin/disc contacts. This approach explores the experimental results in a better way by touching various arenas like contact profile, surface topographic characteristics, and much more frictional forces by linking the scale-dependent measured parameters of the lubricant-surface system. As per the classical Hertzian theory [264,265], the contact pressure and worn spot dimensions are estimated using the following equation.

$$A = \pi.\left(\frac{3wR}{4E}\right)^{2/3} \tag{6.10}$$

$$p = \frac{3}{2}\bar{p} = \left(\frac{6wE'^2}{\pi^3 R^2}\right)^{1/3} \tag{6.11}$$

However, the apparent area, A, can also be measured form the dimensions of the worn spot using a profile projector or SEM. Where, p and $\bar{p}$ are the Hertzian and mean pressures of the contact.

$$A_a = \pi^2.(\xi\beta\sigma)^2.A.F_2(\lambda) \tag{6.12}$$

$$W_a = \frac{16\sqrt{2}}{15}.\pi.(\xi\beta\sigma)^2.\sqrt{\frac{\sigma}{\beta}}.E'.A.F_{5/2}(\lambda) \quad (6.13)$$

It is essential to mention that the Hertzian approach is based on the assumption of nominally smooth frictionless elastic bodies of revolution. Nevertheless, in the course of real engineering surfaces, comparatively rough and their relative motion originates about friction. The level of interaction can be approximated based on the asperity contact area (A_a) and the load shared by the asperity tip contacts (W_a) [266].

In the above equations, ($\xi\beta\sigma$) is called the roughness parameter, is used to describe surface topographic relationship with asperity interactions. ξ, β, and σ are used to represent the asperity peak density, mean asperity peak radius, and composite RMS roughness parameter of the tribo-contacts, respectively. As these equations are based on Gaussian distribution, this assumption does not yield the results for all engineering surfaces. Multiple Gaussian curves are fit to model the experimental results. Results indicate that Gaussian fitted curves and experimental curves are justifying (as, R^2=0.99) the use of the above asperity interaction approach.

In the present study, ξ, β, and σ are evaluated from surface topography to the specific surface. For the estimation of mean asperity peak radius (β), a parameter asperity peak radius, r_c, is measured for all Gaussian fitted peak curves [267].

$$r_c = \frac{I_Y}{2} + \frac{{I_X}^2}{8.I_Y} \quad (6.14)$$

In the above asperity interaction equations, $F_2(\ )$ and $F_{5/2}(\ )$ are functions of the film parameter ( ) which are often estimated by a fifth-order polynomial function of [268].

Based on the outcome of the present work, a relationship between the film parameter and roughness parameters (σ and $\xi\beta\sigma$) are described in the Figure 6.27. From the results it is evident that higher film thickness parameter values lead to lower surface roughness topographic characteristics.

For the present work, asperity level interaction parameters such as W_a , roughness parameter and film parameters are plotted for two different loading under the lubricated sliding contacts (Figure 6.27).

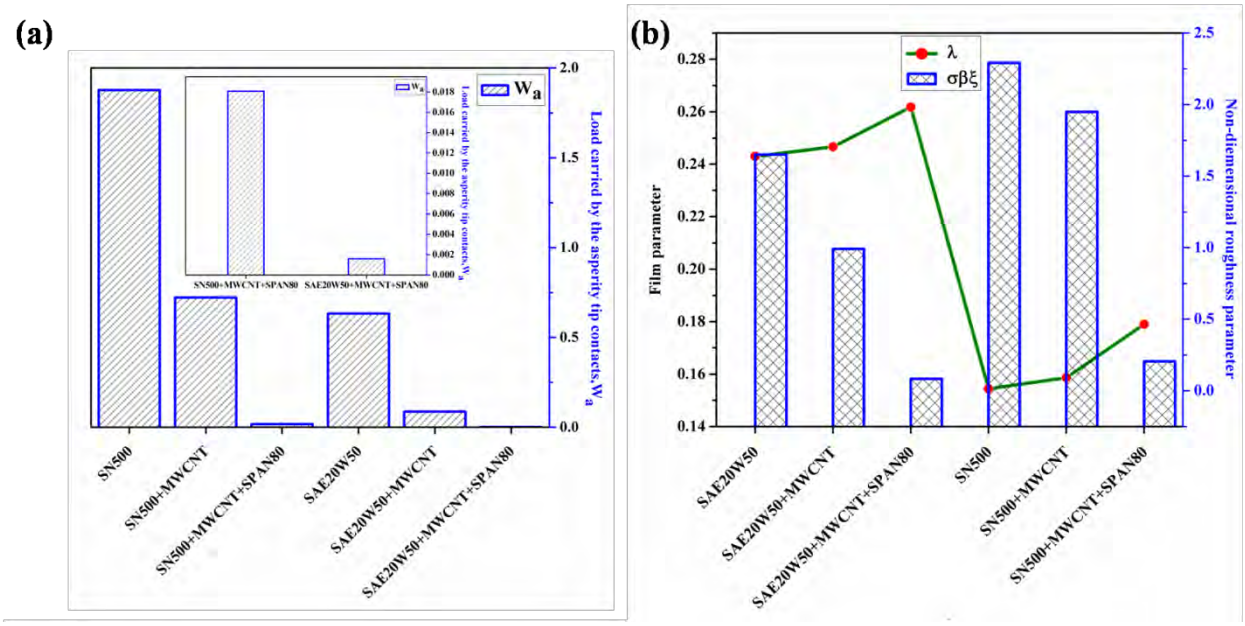

Figure 6.27: For the various lubricated conditions the (a) load shared by asperity tip contacts, (b) the film paramter and roughness parameters at applied loads of 9.81 N

It is noticed from the figure that fully formulated oils yield for lessening the parameters in contrast to mineral oil. This motivates the usage of fully formulated oils over mineral oils, and surfactant functionalized oils optimize the results for both the selected oils. This decrease in load parameter must be balanced by the hydrodynamic capacity of lubricants, involved.

6.6.2 Hydrodynamic load shared by the lubricant film

In order to find out the hydrodynamic load shared by a lubricant film, a non-dimensional parameter (ζ) is initially approximated using the following equation [269].

$$\zeta = \frac{4}{\pi} \cdot \frac{k_{lub}}{\left({}^{h_0}/_{R}\right)} \left(\frac{\bar{p}}{E'.R.k_s.\rho_s.c_{ps}.U_m} \right)^{1/2} \tag{6.15}$$

$$f_a = \tau_a A_a \tag{6.16}$$

$$\tau_a = \tau_0 + \varsigma . p_{mean} \tag{6.17}$$

$$p_{mean} = \frac{W_a}{A_a} \tag{6.18}$$

where k_s, ρ_s, c_{ps} are the thermal conductivity, density, and specific heat capacity of the bulk solid surface material. Also, τ_0 is the characteristic Eyring shear stress, $\bar{p}$ is the average (Pascal)

contact pressure; k_{lub} , the lubricant's thermal conductivity; α_0 is the lubricant pressure-viscosity index, ς is the pressure coefficient of boundary shear strength.

Some of the authors also approximated the forces of traction within the Newtonian boundary by approximating the non-dimensional thermal parameter [269].

$$\chi^{-1} = \left(\frac{h_0}{R}\right).R.\left(\frac{{\tau_0}^2\beta}{2k_{lub}\eta}\right)^{1/2} = 1.23(1+9.6\zeta)^{-1/2} \tag{6.19}$$

$$\chi = \left(\frac{1}{\tau_0.h_0}\right)\left(\frac{2k_{lub}\eta}{\beta}\right)^{1/2} \tag{6.20}$$

χ, ζ are the non-dimensional parameters.

Then viscous frictional coefficient based on traction for thin films under Newtonian and non-Newtonian shear is evaluated using the equations below.

$$\mu_V = \frac{1.33}{\bar{p}.h_0}.\left(\frac{2.k_{lub}.\eta}{\beta}\right)^{1/2} \tag{6.21}$$

or

$$\mu_v = 0.87\alpha_0\tau_0 + 1.74\frac{\tau_0}{\bar{p}}.\ln\left[\frac{1.2}{\tau_0.h_0}\left(\frac{2.k_{lub}.\eta_0}{1+9.6\zeta}\right)^{0.5}\right] \tag{6.22}$$

The hydrodynamic load shared is calculated using this equation.

$$w_V = \frac{F_V}{\mu_V} = \frac{\tau_V.A}{\mu_V} = \frac{(\frac{\eta.U}{h_0}).A}{\mu_V} \tag{6.23}$$

Here, viscous friction is estimated from the shear stress caused by the lubricant drawn into the tribo-contact by the relative motion of the hemispherical pin with respect to the flat disc specimen. In the present study, the component of a pressure gradient that induces shear is ignored owing to marginal values for thin films and low-pressure contacts, particularly under unified boundary-mixed regimes of lubrication. The calculation procedure for film thickness is described in the previous chapter. Higher traction friction coefficient holds higher values for fully formulated oils in contrast to mineral oils, leads to a lesser amount of hydrodynamic shearing of the lubricating film.

Figure 6.28 shows the variation of hydrodynamic load shared by lubricating film for the different lubricated conditions; at the applied load of 9.81 N. The hydrodynamic load sheared by the lubricating film w_v, as shown in Figure 6.28 is calculated using eq. (6.23). For this purpose, F_v

was calculated from the viscous stress caused by the lubricant drawn into the tribo-contact by the relative motion of the hemispherical pin with respect to the flat disc specimen, and μ_v was estimated using eq. (6.22).

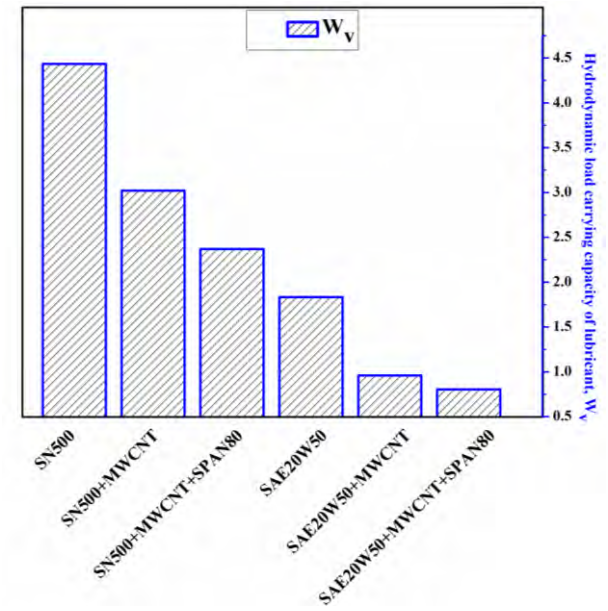

Figure 6.28: Hydrodynamic load shared by lubricating film at 9.81 N

Based on the predictive model developed here to estimate the hydrodynamic load shared by the lubricant film it is observed from the Figure 6.28 that the hydrodynamic load shared by the lubricant is decreased when the lubricants are blended with MWCNT particles. As the dispersion of the nanoparticles is further enhanced with the addition of surfactant, the load shared by the base lubricant is further reduced. On the other hand, from Figure 6.27 it is evident that the loads shared by the asperities are also getting reduced with the addition of MWCNT and surfactant. However, the total applied load is assumed to be shared by the asperities and the lubricant film. This implies that a major fraction of the applied load is being shared by the nanoparticles themselves, which is evident from the figure 6.27 and 6.28. This shifting of load sharing to the nanoparticles becomes significant when they are well dispersed to their primary size levels. Thus it elucidates the effect of the addition of non-treated and surfactant-treated MWCNT in both types of oils. Since the fully formulated oils are having greater numbers of additives in addition to MWCNT, so there is a pronounced effect of this phenomenon in the case of fully formulated oil.

CHAPTER 7
CONCLUSIONS AND RECOMMENDATION FOR THE FUTURE WORKS

In this chapter, the major conclusions from the present research work are presented, followed by recommendations for future work in this area. The primary objective of the present study was to characterize the wet tribology of aluminum metal matrix composites. The influence of particle additives and addition of surfactant makes the results more exciting and novel. The major conclusions drawn from the present study are summarized below.

7.1 CONCLUSIONS

Work presented in this thesis includes fabrication and characterization of stir cast hybrid AMMC with silicon carbide (10% by wt.) and graphite (3% by wt.) as reinforcements. This is followed by a systematic investigation on the influence of MWCNT particle additives on the tribological behavior of prepared composites under dry (ambient air, 35-40% RH) as well as liquid lubricated conditions. Then the particle-laden lubricants were tested for two potential tribopairs, viz. Hybrid AMMC-CI and hybrid AMMC-EN31. The study revealed the following attractive facts:

- The study shows that the particle-based lubrication package for AMMCs can be developed by suitably selecting the solid lubricants, such as Nanoclay, Boric acid, MoS_2 and MWCNT as oil additives.
- It is noticed that MWCNT is more effective in controlling friction and wear in particle based lubrication of Composite contacts. The MWCNT additive is found to be a significant antiwear additive for the selected tribo-contact as it reduces the wear rate at least by one order of magnitude. This is attributed to the better mechanical and thermal properties, inherent layered structures of additive and the effortless dislodgement to individual graphene sheets, as well as shear gliding properties of the lubricant.
- The reduction of COF & wear rate under MWCNT-Oil lubrication is recorded as high as 36.9% and 80% as compared to the base oil lubrication of AMMC-Steel contacts.

- Non-ionic surfactant with low HLB value with an optimized concentration can be used for the suitable formulation of lubricant for the AMMC-steel sliding tribo-contact (in the present case it is Span80 with concentration nearly 0.04 %).
- It was observed that the h-AMMC/Steel sliding under MWCNT-in-oil and surfactant functionalized MWCNT-in-oil reduces the coefficient of friction by more than 1.5 and 2 times respectively, as compared to the base oil. The wear rate of AMMC pin was reduced by as much as 5 and 6 times, for the respective conditions.
- Tribological characteristics are greatly influenced by the lubrication regime, such as rheological properties of using fluids and contact operating conditions such as the applied force and sliding velocity. In order to predict the lubrication regime, stribeck curves were also developed.
- It was observed that the addition of surfactant in MWCNT-in-oil, the lubrication condition shifts towards the mixed regime and film thickness ratio for surfactant-MWCNT-oil is increased by 47%.
- From the FTIR observations it was concluded that the oil degradation due to frictional heating and sliding is constrained by the use of surfactant grafted MWCNT oil dispersions.
- It is noticed that SN500 and SAE 20W50 oils showed better performance in contrast to mineral oils and fully formulated oils respectively.
- As expected, fully formulated commercial oils exhibit better rheological, thermal transport and tribological characteristics as compared to the base oil formulations. However, with the addition of surfactant functionalized MWCNT the performance of base formulations is found to be competitive enough to be used it for fully formulated lubricant package for the tribocontacts involving h-AMMC.
- In-depth investigation on the underlying lubrication mechanism reveals that four primary sub mechanisms are responsible for the improved tribological characteristics of surfactant functionalized MWCNT-in-oil lubrication- improved rheological behavior, favorable oil-surfactant-particle interaction, formation of bilayered structures under the contact, reduced oil degradation; formation of a tribolayer composed of aluminium hydroxide, iron carbide and aluminium iron oxide; formation of MML and smearing of doped graphite into the contact; and adhesion of MWCNT to the worn out surface via effortless

exfoliation of individual graphene sheets of carbon nanotubes under shear stress and the breaking of the nanotubes.

- It was observed that abrasion, oxidation and material transfer were the predominant wear modes prevailed under different loading conditions.
- A comprehensive wear mapping has been performed for the developed lubricant sliding under specified tribopair which can be used in future to predict the operating wear regime.
- Finally, the excellent tribological properties exhibited by the surfactant functionalized MWCNT nano suspensions signified that the fundamental insight obtained from the present investigation will be in great aid for the complex lubrication formulation needed for the advanced industrial application in the future.

7.2 RECOMMENDATION FOR FUTURE WORK

In the present research, a systematic approach for the development and application of particle-based lubrication under the AMMC/steel contact has been presented. Through this study, some of the critical issues, such as selection of particle additive and surfactant, and the underlying friction-wear-lubrication mechanism is explored and highlighted. This will undoubtedly be a benchmark while developing the fully formulated commercial lubricant package for any novel composite materials. However, to realize the actual benefit of particle-based lubricant in the tribological behavior of composite materials in real-world applications, extended work should be carried out, which are not within the domain of the present research work. Some of the recommendations for the future scope of work are listed below.

- Mixed/hybrid Nanolubricants with surfactants and EP/corrosion inhibitors can be explored while developing the new industrial oil package for such tribological applications involving composite materials.
- The mathematical and multiphysics modeling of tribological behaviour of the lubricated AMMC sliding contact can be carried out.
- The compositions and development of AMMC can be further improved to achieve better mechanical and tribological properties.
- Tribological performance of fully formulated particle-based oil can be investigated in high temperature environment.

References

[1] Holmberg K, Erdemir A. Influence of tribology on global energy consumption, costs and emissions. Friction 2017;5:263–84. doi:10.1007/s40544-017-0183-5.

[2] Menezes PL, Ingole SP, Nosonovsky M, Kailas S V., Lovell MR. Tribology for Scientists and Engineers. vol. 9781461419. New York, NY: Springer New York; 2013. doi:10.1007/978-1-4614-1945-7.

[3] Nakasa M. Engine Friction Overview. Int. Tribol. Conf., Yokohama, Japan: 1995.

[4] Liu G, Li X, Qin B, Xing D, Guo Y, Fan R. Investigation of the mending effect and mechanism of copper nano-particles on a tribologically stressed surface. Tribol Lett 2004;17:961–6. doi:10.1007/s11249-004-8109-6.

[5] Erdemir A. Solid lubricants and self-lubricating films. 2000. doi:10.1201/9780849377877.ch22.

[6] Berman D, Erdemir A, Sumant A V. Graphene: A new emerging lubricant. Mater Today 2014;17:31–42. doi:10.1016/j.mattod.2013.12.003.

[7] American Petroleum Institute. Annex E- API Base Oil Interchangeaility guidelines for passenger car motor oils and diesel engine oils. API Handbooks 2015:1–13.

[8] Don M. Pirro; Martin Webster; Ekkehard Daschner. Lubrication Fundamentals. Third Edit. CRC Press.; 2016.

[9] Dai W, Kheireddin B, Gao H, Liang H. Roles of nanoparticles in oil lubrication. Tribol Int 2016;102:88–98. doi:10.1016/j.triboint.2016.05.020.

[10] Hwang Y, Lee C, Choi Y, Cheong S, Kim D, Lee K, et al. Effect of the size and morphology of particles dispersed in nano-oil on friction performance between rotating discs. J Mech Sci Technol 2011;25:2853–7. doi:10.1007/s12206-011-0724-1.

[11] Chaudhury MK. Complex fluids: Spread the word about nanofluids. Nature 2003;423:131–2. doi:10.1038/423131a.

[12] Elechiguerra JL, Reyes-Gasga J, Yacaman MJ. The role of twinning in shape evolution of anisotropic noble metal nanostructures. J Mater Chem 2006;16:3906–19. doi:10.1039/b607128g.

[13] Kleinstreuer C, Li J, Koo J. Microfluidics of nano-drug delivery. Int J Heat Mass Transf 2008;51:5590–7. doi:10.1016/j.ijheatmasstransfer.2008.04.043.

[14] Ohmae N, Martin JM, Mori S. Micro and Nanotribology. Micro and Nanotribology 2010. doi:10.1115/1.802310.

[15] Sutor P. Solid Lubricants: Overview and recent developments. MRS Bull 1991;16:24–30. doi:10.1557/S0883769400056864.

[16] Summers-Smith D. Handbook of lubrication: Theory and practice of tribology. Tribol Int 1984;17:174–5. doi:10.1016/0301-679x(84)90012-4.

[17] LANDSDOWN AR. Molybdenum disulphide lubrication. Tribol Ser 1974;35:1–380.

[18] Wang HD, Xu BS, Liu JJ, Zhuang DM. Microstructures and tribological properties on the composite MoS2 films prepared by a novel two-step method. Mater Chem Phys 2005;91:494–9. doi:10.1016/j.matchemphys.2004.12.039.

[19] Si PZ, Choi CJ, Lee JW, Geng DY, Zhang ZD. Synthesis, structure and tribological performance of tungsten disulphide nanocomposites. Mater Sci Eng A 2007;443:167–71. doi:10.1016/j.msea.2006.08.026.

[20] Bhowmick H, Biswas SK. Tribology of ethyleneair diffusion flame soot under dry and lubricated contact conditions. J Phys D Appl Phys 2011;44. doi:10.1088/0022-3727/44/48/485401.

[21] Lee J, Cho S, Hwang Y, Lee C, Kim SH. Enhancement of lubrication properties of nano-oil by controlling the amount of fullerene nanoparticle additives. Tribol Lett 2007;28:203–8. doi:10.1007/s11249-007-9265-2.

[22] Xu Tao, Zhao JZ, Xu K. The ball-bearing effect of diamond nanoparticles as an oil additive. J Phys D-Applied Phys 1996;29:2932–7.

[23] Chinas-Castillo F, Spikes HA. Mechanism of action of colloidal solid dispersions. J Tribol 2003;125:552–7. doi:10.1115/1.1537752.

[24] Rico EF, Minondo I, Cuervo DG. The effectiveness of PTFE nanoparticle powder as an EP additive to mineral base oils. Wear 2007;262:1399–406. doi:10.1016/j.wear.2007.01.022.

[25] Liu G, Li X, Lu N, Fan R. Enhancing AW/EP property of lubricant oil by adding nano Al/Sn particles. Proc ASME/STLE Int Jt Tribol Conf IJTC 2004 2004;18:325–33.

[26] Demas NG, Timofeeva E V., Routbort JL, Fenske GR. Tribological effects of BN and MoS2 nanoparticles added to Polyalphaolefin oil in piston skirt/cylinder liner tests. ASME/STLE 2012 Int. Jt. Tribol. Conf., American Society of Mechanical Engineers;

2012, p. 5–7. doi:10.1115/IJTC2012-61062.

[27] Bhowmick H, Majumdar SK, Biswas SK. Tribology of soot suspension in hexadecane as distinguished by the physical structure and chemistry of soot particles. J Phys D Appl Phys 2012;45:175302. doi:10.1088/0022-3727/45/17/175302.

[28] Charoo MS, Wani MF. Tribological properties of h-BN nanoparticles as lubricant additive on cylinder liner and piston ring. Lubr Sci 2017;29:241–54. doi:10.1002/ls.1366.

[29] Paul G, Hirani H, Kuila T, Murmu NC. Nanolubricants dispersed with graphene and its derivatives: An assessment and review of the tribological performance. Nanoscale 2019;11:3458–83. doi:10.1039/c8nr08240e.

[30] Sunqing Q, Junxiu D, Guoxu C. Tribological properties of CeF3 nanoparticles as additives in lubricating oils. Wear 1999;230:35–8. doi:10.1016/S0043-1648(99)00084-8.

[31] Dong J, Chen G. Preparation of Ni nanoparticles and evaluation of their tribological performance as potential additives in oils. J Tribol 2001;123:441–3. doi:10.1115/1.1286152.

[32] Joshi UA, Joshi P, Harsha SP, Sharma SC. Evaluation of the mechanical properties of CNT based composites using hexagonal RVE. J Nanotechnol Eng Med 2010;1. doi:10.1115/1.4002044.

[33] Joshi UA, Sharma SC, Harsha SP. Influence of dispersion and alignment of nanotubes on the strength and elasticity of carbon nanotubes reinforced composites. J Nanotechnol Eng Med 2011;2. doi:10.1115/1.4005664.

[34] Zhang C, Song Y, Zhang H, Lv B, Qiao J, Yu N, et al. Mechanical properties of carbon nanotube fibers at extreme temperatures. Nanoscale 2019;11:4585–90. doi:10.1039/c8nr09637f.

[35] Mu M, Teblum E, Figiel Ł, Nessim GD, McNally T. Correlation between MWCNT aspect ratio and the mechanical properties of composites of PMMA and MWCNTs. Mater Res Express 2018;5:045305. doi:10.1088/2053-1591/aab82d.

[36] Singer IL. Solid lubrication processes. Fundam Frict Macrosc Microsc Process 1992;220:237–61. doi:10.1007/978-94-011-2811-7_13.

[37] Bryant PJ, Gutshall PL, Taylor LH. A study of mechanisms of graphite friction and wear. Wear 1964;7:118–26. doi:10.1016/0043-1648(64)90083-3.

[38] Savage RH, Schaefer DL. Vapor lubrication of graphite sliding contacts. J Appl Phys

1956;27:136–8. doi:10.1063/1.1722322.

[39] Dieter GE. The friction and lubrication of solids. J Franklin Inst 1965;279:479–80. doi:10.1016/0016-0032(65)90286-3.

[40] Greenberg R, Halperin G, Etsion I, Tenne R. The effect of WS2 nanoparticles on friction reduction in various lubrication regimes. Tribol Lett 2004;17:179–86. doi:10.1023/B:TRIL.0000032443.95697.1d.

[41] Srolovitz DJ, Safran SA, Homyonfer M, Tenne R. Morphology of nested fullerenes. Phys Rev Lett 1995;74:1779–82. doi:10.1103/PhysRevLett.74.1779.

[42] Tenne R, Homyonfer M, Feldman Y. Nanoparticles of layered compounds with hollow cage structures (Inorganic Fullerene-like structures). Chem Mater 1998;10:3225–38. doi:10.1021/cm9802189.

[43] Düzcükoğlu H, Acaroğlu M. Lubrication properties of vegetable oils combined with boric acid and determination of their effects on wear. Energy Sources, Part A Recover Util Environ Eff 2010;32:275–85. doi:10.1080/15567030802606053.

[44] Lovell MR, Kabir MA, Menezes PL, Higgs CF. Influence of boric acid additive size on green lubricant performance. Philos Trans R Soc A Math Phys Eng Sci 2010;368:4851–68. doi:10.1098/rsta.2010.0183.

[45] Sumlo Iijima. Helical microtubules of graphitic carbon. Nature 1991;354:56–8.

[46] Loiseau A. Understanding carbon nanotubes: from basics to applications. Springer 2006:552. doi:10.1007/b10971390.

[47] Scarselli M, Castrucci P, De Crescenzi M. Electronic and optoelectronic nano-devices based on carbon nanotubes. J Phys Condens Matter 2012;24:1–36. doi:10.1088/0953-8984/24/31/313202.

[48] Zhang W, Ma GJ, Wu CW. Anti-friction, wear-proof and self-lubrication application of carbon nanotubes. Rev Adv Mater Sci 2014;36:74–87.

[49] Lee SM, Tiwari D. Organo and inorgano-organo-modified clays in the remediation of aqueous solutions: An overview. Appl Clay Sci 2012;59–60:84–102. doi:10.1016/j.clay.2012.02.006.

[50] Uddin MK. A review on the adsorption of heavy metals by clay minerals, with special focus on the past decade. Chem Eng J 2017;308:438–62. doi:10.1016/j.cej.2016.09.029.

[51] Uddin F. Clays, nanoclays, and montmorillonite minerals. Metall Mater Trans A Phys

Metall Mater Sci 2008;39:2804–14. doi:10.1007/s11661-008-9603-5.

[52] Liu W, Chen S. An investigation of the tribological behaviour of surface-modified ZnS nanoparticles in liquid paraffin. Wear 2000;238:120–4. doi:10.1016/S0043-1648(99)00344-0.

[53] Ye P, Jiang X, Li S, Li S. Preparation of NiMoO2S2 nanoparticle and investigation of its tribological behavior as additive in lubricating oils. Wear 2002;253:572–5. doi:10.1016/S0043-1648(02)00042-X.

[54] Skibinski J, Frydrych J, Rebis J, Rozniatowski K. Cheap nano-clay additive as a lubricating enhancer. J Power Technol 2017;97:103–9.

[55] Jlassi K, Krupa I, Chehimi MM. Overview: Clay preparation, properties, modification. Clay-Polymer Nanocomposites 2017:1–28. doi:10.1016/B978-0-323-46153-5.00001-X.

[56] Chen Y, Renner P, Liang H. Dispersion of nanoparticles in lubricating oil: A critical review. Lubricants 2019;7:7. doi:10.3390/lubricants7010007.

[57] Neville A, Morina A, Haque T, Voong M. Compatibility between tribological surfaces and lubricant additives-How friction and wear reduction can be controlled by surface/lube synergies. Tribol Int 2007;40:1680–95. doi:10.1016/j.triboint.2007.01.019.

[58] Vencl A, Rac A BI. Tribology of the Al-Si alloy based MMCs and their application in automotive industry. Eng. Met. Matrix Compos. Form. Methods, Mater. Prop. Ind. Appl., New York: Nova Science Publishers; 2013, p. 127–66.

[59] Donomoto T, Funatani K, Miura N, Miyake N. Ceramic fiber reinforced piston for high performance diesel engines. SAE Tech. Pap., 1983, p. DOI: 10.4271/830252. doi:10.4271/830252.

[60] Dolata-Grosz A, Dyzia M, Śleziona J, Wieczorek J, Sleziona J, Wieczorek J. Composites applied for pistons. Arch Foundry Eng 2007;7:37–40.

[61] Kumar GBV, Rao CSP, Selvaraj N, Bhagyashekar MS. Studies on Al6061-SiC and Al7075-Al2O3 metal matrix composites. J Miner Mater Charact Eng 2010;9:43–55. doi:10.4236/jmmce.2010.91004.

[62] Padmavathi KR, Ramakrishnan R. Tribological behaviour of Aluminium Hybrid Metal Matrix Composite. Procedia Eng 2014;97:660–7. doi:10.1016/j.proeng.2014.12.295.

[63] Swamy NRP, Ramesh CS, Chandrashekar T. Effect of heat treatment on strength and abrasive wear behaviour of Al6061-SiCp composites. Bull Mater Sci 2010;33:49–54.

doi:10.1007/s12034-010-0007-y.

[64] Chennakesava Reddy A, Zitoun E. Matrix al-alloys for silicon carbide particle reinforced metal matrix composites. Indian J Sci Technol 2010;3:1184–7. doi:10.17485/ijst/2010/v3i12/29857.

[65] Krishna MV, Xavior AM. An investigation on the mechanical properties of hybrid metal matrix composites. Procedia Eng 2014;97:918–24. doi:10.1016/j.proeng.2014.12.367.

[66] Pai A, Sharma SS, D'Silva RE, Nikhil RG. Effect of graphite and granite dust particulates as micro-fillers on tribological performance of Al 6061-T6 hybrid composites. Tribol Int 2015;92:462–71. doi:10.1016/j.triboint.2015.07.035.

[67] Guo MLT, Tsao CYA. Tribological behavior of self-lubricating aluminium/SiC/graphite hybrid composites synthesized by the semi-solid powder-densification method. Compos Sci Technol 2000;60:65–74. doi:10.1016/S0266-3538(99)00106-2.

[68] Bisane VP, Sable YS, Dhobe MM, Sonawane MM. Recent development and challenges in processing of ceramic reinforced Al matrix composite through stir casting: A Review. Int J Eng Res Appl Sci 2015;2:11–6.

[69] Nturanabo F, Masu LM, Govender G. Automotive light-weighting using aluminium metal matrix composites. Mater Sci Forum 2015;828–829:485–91. doi:10.4028/www.scientific.net/MSF.828-829.485.

[70] M. M, M. R, A. E-H, Y. M. Automotive Applications of Aluminum Metal Matrix Composites. Int Conf Aerosp Sci Aviat Technol 2001;9:1–12. doi:10.21608/asat.2001.24850.

[71] Macke A, Schultz BF, Rohatgi P. Metal matrix: Composites offer the automotive industry an opportunity to reduce vehicle weight, improve performance. Adv Mater Process 2012;170:19–23.

[72] Azman NF, Samion S. Dispersion stability and lubrication mechanism of nanolubricants: A review. Int J Precis Eng Manuf - Green Technol 2019;6:393–414. doi:10.1007/s40684-019-00080-x.

[73] Lu X, Khonsari MM, Gelinck ERM. The Stribeck curve: Experimental results and theoretical prediction. J Tribol 2006;128:789–94. doi:10.1115/1.2345406.

[74] Ruddy BL, Dowson D, Economou PN. A review of studies of piston ring lubrication. 1983. doi:10.1016/b978-0-408-22161-0.50019-6.

[75] Rycroft JE, Taylor RI, Scales LE. Elastohydrodynamic effects in piston ring lubrication in modern gasoline and diesel engines. Tribol Ser 1997;32:49–54. doi:10.1016/s0167-8922(08)70435-8.

[76] Rapoport L, Bilik Y, Feldman Y, Homyonfer M, Cohen SR, Tenne R. Hollow nanoparticles of WS2 as potential solid-state lubricants. Nature 1997;387:791–3. doi:10.1038/42910.

[77] Rapoport L, Feldman Y, Homyonfer M, Cohen H, Sloan J, Hutchison JL, et al. Inorganic fullerene-like material as additives to lubricants: Structure-function relationship. Wear 1999;225–229:975–82. doi:10.1016/S0043-1648(99)00040-X.

[78] Holinski R, Gänsheimer J. A study of the lubricating mechanism of molybdenum disulfide. Wear 1972;19:329–42. doi:10.1016/0043-1648(72)90124-X.

[79] Moser J, Lèvy F. MoS2-x lubricating films: structure and wear mechanisms investigated by cross-sectional transmission electron microscopy. Thin Solid Films 1993;228:257–60. doi:10.1016/0040-6090(93)90611-R.

[80] Chinas-Castillo F, Spikes HA. The behavior of colloidal solid particles in elastohydrodynamic contacts. Tribol Trans 2000;43:387–94. doi:10.1080/10402000008982354.

[81] Rapoport L, Leshchinsky V, Lapsker I, Volovik Y, Nepomnyashchy O, Lvovsky M, et al. Tribological properties of WS2 nanoparticles under mixed lubrication. Wear 2003;255:785–93. doi:10.1016/S0043-1648(03)00044-9.

[82] Bhushan B, Gupta BK, Van Cleef GW, Capp C, Coe J V. Fullerene (C60) films for solid lubrication. Tribol Trans 1993;36:573–80. doi:10.1080/10402009308983197.

[83] Schwarz UD, Zwörner O, Köster P, Wiesendanger R. Quantitative analysis of the frictional properties of solid materials at low loads. I. Carbon compounds. Phys Rev B - Condens Matter Mater Phys 1997;56:6987–96. doi:10.1103/PhysRevB.56.6987.

[84] Golan Y, Drummond C, Israelachvili J, Tenne R. In situ imaging of shearing contacts in the surface forces apparatus. Wear 2000;245:190–5. doi:10.1016/S0043-1648(00)00478-6.

[85] Lahouij I, Dassenoy F, De Knoop L, Martin JM, Vacher B. In situ TEM observation of the behavior of an individual fullerene-like MoS2 nanoparticle in a dynamic contact. Tribol Lett 2011;42:133–40. doi:10.1007/s11249-011-9755-0.

[86] Lee CG, Hwang YJ, Choi YM, Lee JK, Choi C, Oh JM. A study on the tribological

characteristics of graphite nano lubricants. Int J Precis Eng Manuf 2009;10:85–90. doi:10.1007/s12541-009-0013-4.

[87] Wahl KJ, Singer IL. Quantification of a lubricant transfer process that enhances the sliding life of a MoS2 coating. Tribol Lett 1995;1:59–66. doi:10.1007/BF00157976.

[88] Tannous J, Dassenoy F, Lahouij I, Le Mogne T, Vacher B, Bruhács A, et al. Understanding the tribochemical mechanisms of IF-MoS2 nanoparticles under boundary lubrication. Tribol Lett 2011;41:55–64. doi:10.1007/s11249-010-9678-1.

[89] Cizaire L, Vacher B, Le Mogne T, Martin JM, Rapoport L, Margolin A, et al. Mechanisms of ultra-low friction by hollow inorganic fullerene-like MoS2 nanoparticles. Surf Coatings Technol 2002;160:282–7. doi:10.1016/S0257-8972(02)00420-6.

[90] Joly-Pottuz L, Martin JM, Dassenoy F, Belin M, Montagnac G, Reynard B, et al. Pressure-induced exfoliation of inorganic fullerene-like WS2 particles in a Hertzian contact. J Appl Phys 2006;99:023524. doi:10.1063/1.2165404.

[91] Lahouij I, Dassenoy F, Vacher B, Martin JM. Real time TEM imaging of compression and shear of single fullerene-like MoS2 nanoparticle. Tribol Lett 2012;45:131–41. doi:10.1007/s11249-011-9873-8.

[92] Tevet O, Goldbart O, Cohen SR, Rosentsveig R, Popovitz-Biro R, Wagner HD, et al. Nanocompression of individual multilayered polyhedral nanoparticles. Nanotechnology 2010;21:365705. doi:10.1088/0957-4484/21/36/365705.

[93] Peng Y, Hu Y, Wang H. Tribological behaviors of surfactant-functionalized carbon nanotubes as lubricant additive in water. Tribol Lett 2007;25:247–53. doi:10.1007/s11249-006-9176-7.

[94] Lu HF, Fei B, Xin JH, Wang RH, Li L, Guan WC. Synthesis and lubricating performance of a carbon nanotube seeded miniemulsion. Carbon N Y 2007;45:936–42. doi:10.1016/j.carbon.2007.01.001.

[95] Chen CS, Chen XH, Xu LS, Yang Z, Li WH. Modification of multi-walled carbon nanotubes with fatty acid and their tribological properties as lubricant additive. Carbon N Y 2005;43:1660–6. doi:10.1016/j.carbon.2005.01.044.

[96] Kristiansen K, Zeng H, Wang P, Israelachvili JN. Microtribology of aqueous carbon nanotube dispersions. Adv Funct Mater 2011;21:4555–64. doi:10.1002/adfm.201101478.

[97] Erdemir A, Fenske GR, Erck RA, Nichols FA, Busch DE. Tribological properties of boric

acid and boric-acid-forming surfaces. Part II. Mechanisms of formation and self-lubrication of boric acid films on boron- and boric oxide-containing surfaces. Lubr Eng 1991;47:179–84.

[98] Sawyer WG, Ziegert JC, Schmitz TL, Barton T. In situ lubrication with boric acid: Powder delivery of an environmentally benign solid lubricant. Tribol Trans 2006;49:284–90. doi:10.1080/05698190600639939.

[99] Erdemir A, Halter M, Fenske GR. Preparation of ultralow-friction surface films on vanadium diboride. Wear 1997;205:236–9. doi:10.1016/S0043-1648(96)07508-4.

[100] Erdemir A, Eryilmaz OL, Fenske GR. Self-replenishing solid lubricant films on boron carbide. Surf Eng 1999;15:291–5. doi:10.1179/026708499101516605.

[101] Wei J, Erdemir A, Fenske GR. Dry lubricant films for aluminum forming. Tribol Trans 2000;43:535–41. doi:10.1080/10402000008982374.

[102] Brannen W, Burt G, McDonald R. Phosphite amine lubricant additives. 4,965,002, 1990.

[103] Liang H, Jahanmir S. Boric acid as an additive for core-drilling of alumina. J Tribol 1995;117:65–73. doi:10.1115/1.2830608.

[104] Rao KP, Wei JJ. Performance of a new dry lubricant in the forming of aluminum alloy sheets. Wear 2001;249:86–93. doi:10.1016/s0043-1648(01)00526-9.

[105] Rao KP, Xie CL. A comparative study on the performance of boric acid with several conventional lubricants in metal forming processes. Tribol Int 2006;39:663–8. doi:10.1016/j.triboint.2005.05.004.

[106] Barton T, Steffens J, Sawyer W, Schmitz T, Ziegert J, Lovell M. In situ solid lubricant deposition for environmentally benign forming. Proc. STLE Annu. Meet. Toronto, Canada, 2004, p. 17–20.

[107] Deshmukh P, Lovell M, Sawyer WG, Mobley A. On the friction and wear performance of boric acid lubricant combinations in extended duration operations. Wear 2006;260:1295–304. doi:10.1016/j.wear.2005.08.012.

[108] Charoo MS, Hanief M. Improving the tribological characteristics of a lubricating oil by nano sized additives. Mater Today Proc 2020. doi:10.1016/j.matpr.2020.01.219.

[109] Calabi Floody M, Theng BKG, Reyes P, Mora ML. Natural nanoclays: applications and future trends – a Chilean perspective. Clay Miner 2009;44:161–76. doi:10.1180/claymin.2009.044.2.161.

[110] Raji M, Mekhzoum MEM, Qaiss A el K, Bouhfid R. Nanoclay modification and functionalization for nanocomposites development: Effect on the structural, morphological, mechanical and rheological properties. In: Jawaid M, Qaiss A BR, editor. Eng. Mater., Singapore: Springer Singapore; 2016, p. 1–34. doi:10.1007/978-981-10-1953-1_1.

[111] Nazir MS, Mohamad Kassim MH, Mohapatra L, Gilani MA, Raza MR, Majeed K. Characteristic properties of nanoclays and characterization of nanoparticulates and nanocomposites. In: Essabir H, Raji M BR, editor. Nanoclay Reinf. Polym. Compos., Springer; 2016, p. 35–55. doi:10.1007/978-981-10-1953-1_2.

[112] Ambre AH, Katti KS, Katti DR. Nanoclay based composite scaffolds for bone tissue engineering applications. J Nanotechnol Eng Med 2010;1. doi:10.1115/1.4002149.

[113] Peña-Parás L, Maldonado-Cortés D, Taha-Tijerina J. Eco-friendly nanoparticle additives for lubricants and their tribological characterization. In: Martínez L KO and KB, editor. Handb. Ecomater., vol. 5, Springer; 2019, p. 3247–67. doi:10.1007/978-3-319-68255-6_72.

[114] Zhao J, He Y, Wang Y, Wang W, Yan L, Luo J. An investigation on the tribological properties of multilayer graphene and MoS2 nanosheets as additives used in hydraulic applications. Tribol Int 2016;97:14–20. doi:10.1016/j.triboint.2015.12.006.

[115] Rajini N, Jappes JW, Suresha B, Rajakarunakaran S, Siva I, Azhagesan N. Effect of organically modified montmorillonite clay on wear behavior of naturally woven coconut sheath/polyester composite. Proc Inst Mech Eng Part J J Eng Tribol 2014;228:483–97. doi:10.1177/1350650113515199.

[116] Srinath G, Gnanamoorthy R. Effect of nanoclay reinforcement on tensile and tribo behaviour of Nylon 6. J Mater Sci 2005;40:2897–901. doi:10.1007/s10853-005-2439-0.

[117] Sieczkarek P, Wernicke S, Gies S, Tekkaya AE, Krebs E, Wiederkehr P, et al. Wear behavior of tribologically optimized tool surfaces for incremental forming processes. Tribol Int 2016;104:64–72. doi:10.1016/j.triboint.2016.08.028.

[118] Pena-Paras L, Maldonado-Cortes D, Castillo F, Leal J, Garza S. Application of nanoclay lubricants for lowering wear of tools for steel meshing - A case study. IOP Conf. Ser. Mater. Sci. Eng., vol. 400, 2018. doi:10.1088/1757-899X/400/7/072004.

[119] Sánchez-Fernández A, Peña-Parás L, Vidaltamayo R, Cué-Sampedro R, Mendoza-

Martínez A, Zomosa-Signoret V, et al. Synthesization, characterization, and in vitro evaluation of cytotoxicity of biomaterials based on Halloysite nanotubes. Materials (Basel) 2014;7:7770–80. doi:10.3390/ma7127770.

[120] Peña-Parás L, Maldonado-Cortés D, García P, Irigoyen M, Taha-Tijerina J, Guerra J. Tribological performance of halloysite clay nanotubes as green lubricant additives. Wear 2017;376–377:885–92. doi:10.1016/j.wear.2017.01.044.

[121] Hu KH, Hu XG, Xu YF, Huang F, Liu JS. The effect of morphology on the tribological properties of MoS2 in liquid paraffin. Tribol Lett 2010;40:155–65. doi:10.1007/s11249-010-9651-z.

[122] An V, Irtegov Y, De Izarra C. Study of tribological properties of nanolamellar WS2 and MoS2 as additives to lubricants. J Nanomater 2014;2014:865839. doi:10.1155/2014/865839.

[123] Ilie F, Constantin T. Tribological behaviour of molybdenum disulphide nanoparticles. Int. Conf. Diagnosis Predict. Mech. Eng. Syst., 2009, p. 38–40.

[124] Charoo MS WM. Tribological properties of IF-MoS2 nanoparticles as lubricant additive on cylinder liner and piston ring tribo-pair. Tribol Ind 2016;38:156–62.

[125] Gansheimer J, Holinski R. Molybdenum disulfide in oils and greases under boundary conditions. J Tribol 1973;95:242–6. doi:10.1115/1.3451783.

[126] Wo HZ, Hu KH, Hu XG. Tribological properties of MoS2 nanoparticles as additive in a machine oil. Mocaxue Xuebao/Tribology 2004;24:33–7.

[127] Bartz W, Oppelt J. Lubricating effectiveness of oil-soluble additives and Molybdenum disufide dispersed mineral oil. Lubr Eng 1980;36:579–85.

[128] Sliney HE. Dynamics of solid dispersions in oil during the lubrication of point contacts, part iimolybdenum disulfide. ASLE Trans 1982;25:190–7. doi:10.1080/05698198208983080.

[129] Rosentsveig R, Gorodnev A, Feuerstein N, Friedman H, Zak A, Fleischer N, Tannous J, Dassenoy F TR. Fullerene-like MoS2 nanoparticles and their tribological behavior. Tribol Lett 2009;36:175–82.

[130] Praveena M, Jayaram V, Biswas SK. Friction between a steel ball and a steel flat lubricated by MoS2 particles suspended in hexadecane at 150 °c. Ind Eng Chem Res 2012;51:12321–8. doi:10.1021/ie3011337.

[131] Rabaso P, Ville F, Dassenoy F, Diaby M, Afanasiev P, Cavoret J, et al. Boundary lubrication: Influence of the size and structure of inorganic fullerene-like MoS2 nanoparticles on friction and wear reduction. Wear 2014;320:161–78. doi:10.1016/j.wear.2014.09.001.

[132] Kalin M, Kogovšek J, Remškar M. Mechanisms and improvements in the friction and wear behavior using MoS2 nanotubes as potential oil additives. Wear 2012;280–281:36–45. doi:10.1016/j.wear.2012.01.011.

[133] Zhang Z, Liu J, Wu T, Xie Y. Effect of carbon nanotubes on friction and wear of a piston ring and cylinder liner system under dry and lubricated conditions. Friction 2017;5:147–54. doi:10.1007/s40544-016-0126-6.

[134] Zhang B, Xue Y, Qiang L, Gao K, Liu Q, Yang B, et al. Assembling of carbon nanotubes film responding to significant reduction wear and friction on steel surface. Appl Nanosci 2017;7:835–42. doi:10.1007/s13204-017-0622-7.

[135] Kiu SSK, Yusup S, Chok VS, Taufiq A, Kamil RNM, Syahrullail S, et al. Comparison on tribological properties of vegetable oil upon addition of carbon based nanoparticles. IOP Conf. Ser. Mater. Sci. Eng., vol. 206, 2017, p. 012043. doi:10.1088/1757-899X/206/1/012043.

[136] Su Y, Tang Z, Wang G, Wan R. Influence of carbon nanotube on the tribological properties of vegetable-based oil. Adv Mech Eng 2018;10:1–11. doi:10.1177/1687814018778188.

[137] Cornelio JAC, Cuervo PA, Hoyos-Palacio LM, Lara-Romero J, Toro A. Tribological properties of carbon nanotubes as lubricant additive in oil and water for a wheel-rail system. J Mater Res Technol 2016;5:68–76. doi:10.1016/j.jmrt.2015.10.006.

[138] Vyavhare K, Aswath PB. Tribological properties of novel multi-walled carbon nanotubes and phosphorus containing ionic liquid hybrids in grease. Front Mech Eng 2019;5:15. doi:10.3389/fmech.2019.00015.

[139] Kałużny J, Merkisz-Guranowska A, Giersig M, Kempa K. Lubricating performance of carbon nanotubes in internal combustion engines – engine test results for CNT enriched oil. Int J Automot Technol 2017;18:1047–59. doi:10.1007/s12239-017-0102-9.

[140] Singh K, Suresh R. Behavior of composite nanofluids under extreme pressure condition. Int J Eng Res Technol 2012;1:1–7.

[141] Salah N, Alshahrie A, Alharbi ND, Khan ZH. Nano and micro structures produced from carbon rich fly ash as effective lubricant additives for 150SN base oil. J Mater Res Technol 2019;8:250–8.

[142] Salah N, Abdel-Wahab MS, Alshahrie A, Alharbi ND, Khan ZH. Carbon nanotubes of oil fly ash as lubricant additives for different base oils and their tribology performance. RSC Adv 2017;7:40295–302. doi:10.1039/c7ra07155h.

[143] Nunn N, Mahbooba Z, Ivanov MG, Ivanov DM, Brenner DW, Shenderova O. Tribological properties of polyalphaolefin oil modified with nanocarbon additives. Diam Relat Mater 2015;54:97–102. doi:10.1016/j.diamond.2014.09.003.

[144] Negm NA, Kailas S V., Pottirayil A, Abd-Elaal AA. Use of surfactants in metal cutting fluids formation. Surfactants Tribol 2014;4:259–79. doi:10.1201/b17691.

[145] Bhowmick H, Majumdar SK, Biswas SK. Tribology of soot suspension in hexadecane as distinguished by the physical structure and chemistry of soot particles. J Phys D Appl Phys 2012;45. doi:10.1088/0022-3727/45/17/175302.

[146] Srinivas V, Kodanda Rama Rao C, Abyudaya M, Jyothi ES. Extreme pressure properties of 600 N base oil dispersed with molybdenum disulphide nano particles. Univers J Mech Eng 2014;2:220–5. doi:10.13189/ujme.2014.020702.

[147] Aralihalli S, Biswas SK. Grafting of dispersants on MoS2 nanoparticles in base oil lubrication of steel. Tribol Lett 2013;49:61–76. doi:10.1007/s11249-012-0042-5.

[148] Sonali J, Sandhyarani N, Sajith V. Tribological properties and stabilization study of surfactant modified MoS2 nanoparticle in 15W40 engine oil. Int J Fluid Mech Mach 2014;1:1–5.

[149] Muzakkir SM, Lijesh KP, Hirani H. Effect of base oil on the anti-wear performance of multi-walled carbon nano-tubes (MWCNT). Int J Curr Eng Technol 2015;5:681–4.

[150] Muzakkir SM, Lijesh KP, Hirani H. Influence of surfactants on tribological behaviors of MWCNTs (multi-walled carbon nano-tubes). Tribol - Mater Surfaces Interfaces 2016;10:74–81. doi:10.1080/17515831.2016.1138636.

[151] Rabaso P, Dassenoy F, Ville F, Diaby M, Vacher B, Le Mogne T, et al. An investigation on the reduced ability of IF-MoS2 nanoparticles to reduce friction and wear in the presence of dispersants. Tribol Lett 2014;55:503–16. doi:10.1007/s11249-014-0381-5.

[152] Chebattina KRR, Srinivas V, Mohan Rao N. Effect of size of multiwalled carbon

nanotubes dispersed in gear oils for improvement of tribological properties. Advances in Tribology 2018;2018:1–13. doi:10.1155/2018/2328108.

[153] Lijesh KP, Muzakkir SM, Hirani H. Experimental tribological performance evaluation of nano lubricant using multi-walled carbon nano-tubes (MWCNT). Int J Appl Eng Res 2015;10:14543–50.

[154] Kumar SJJ, G.Santhosh, D.Nirmalkumar, A.Saravanakumar, Dr.P.Sasikumar, Dr.S.Sivasankaran, et al. Mechanical and dry sliding wear behavior of Al 6063/Al2O3/Graphite hybrid composites. Int J Innov Res Sci Eng Technol Vol 2014;3:1222–8. doi:10.1016/j.matpr.2017.11.497.

[155] Singh J. Fabrication characteristics and tribological behavior of Al/SiC/Gr hybrid aluminum matrix composites: A review. Friction 2016;4:191–207. doi:10.1007/s40544-016-0116-8.

[156] Miloradović N, Vujanac R, Mitrović S, Miloradović D. Dry sliding wear performance of ZA27/SiC/Graphite composites. Metals (Basel) 2019;9:717. doi:10.3390/met9070717.

[157] Mosleh-Shirazi S, Akhlaghi F. Tribological behavior of Al/SiC and Al/SiC/2 vol%Gr nanocomposites containing different amounts of nano SiC particles. Mater Res Express 2019;6:065039. doi:10.1088/2053-1591/ab0929.

[158] Lokesh T, Mallik US. Dry sliding wear behavior of Al/Gr/SiC hybrid metal matrix composites by Taguchi techniques. Mater Today Proc 2017;4:11175–80. doi:10.1016/j.matpr.2017.08.084.

[159] Babić M, Stojanović B, Mitrović S, Bobić I, Miloradović N, Pantić M, et al. Wear properties of A 356/10SiC/1Gr hybrid composites in lubricated sliding conditions. Tribology in Industry 2013;35:148–54.

[160] Walker JC, Rainforth WM, Jones H. Lubricated sliding wear behaviour of aluminium alloy composites. Wear 2005;259:577–89. doi:10.1016/j.wear.2005.01.001.

[161] Akhlaghi F, Zare-Bidaki A. Influence of graphite content on the dry sliding and oil impregnated sliding wear behavior of Al 2024-graphite composites produced by in situ powder metallurgy method. Wear 2009;266:37–45. doi:10.1016/j.wear.2008.05.013.

[162] Panwar N, Poonia RP, Singh G, Dabral R, Chauhan A. Effect of lubrication on sliding wear of red mud particulate reinforced aluminium alloy 6061. Tribology in Industry 2017;39:307–18. doi:10.24874/ti.2017.39.03.05.

[163] Pradhan S, Ghosh S, Barman TK, Sahoo P. Tribological behavior of Al-SiC metal matrix composite under dry, aqueous and alkaline medium. Silicon 2017;9:923–31. doi:10.1007/s12633-016-9504-y.

[164] Shrivastava AK, Singh KK, Dixit AR. Tribological properties of Al 7075 alloy and Al 7075 metal matrix composite reinforced with SiC, sliding under dry, oil lubricated, and inert gas environments. Proc Inst Mech Eng Part J J Eng Tribol 2018;232:693–8. doi:10.1177/1350650117726631.

[165] Poria S, Sutradhar G, Sahoo P. Corrosion and lubricated sliding tribological behavior of Al-TiB2-nano Gr hybrid composites. Mater Res Express 2018;5:076519. doi:10.1088/2053-1591/aad07b.

[166] Dev Srivyas P, Charoo MS. Tribological characterization of hybrid aluminum composite under boundary lubricating sliding conditions. Mater Today Proc 2020. doi:10.1016/j.matpr.2019.12.114.

[167] Dixit G, Khan MM. Sliding wear response of an aluminium metal matrix composite: Effect of solid lubricant particle size. Jordan J Mech Ind Eng 2014;8:351–8.

[168] Charoo MS, Wani MF. Friction and wear properties of nano-Si3N4/nano-SiC composite under nanolubricated conditions. J Adv Ceram 2016;5:145–52. doi:10.1007/s40145-016-0183-3.

[169] Mahajan A, Kingon A, Kukovecz Á, Konya Z, Vilarinho PM. Studies on the thermal decomposition of multiwall carbon nanotubes under different atmospheres. Mater Lett 2013;90:165–8. doi:10.1016/j.matlet.2012.08.120.

[170] Wang W, Xie G, Luo J. Black phosphorus as a new lubricant. Friction 2018;6:116–42. doi:10.1007/s40544-018-0204-z.

[171] Sevim F, Demir F, Bilen M, Okur H. Kinetic analysis of thermal decomposition of boric acid from thermogravimetric data. Korean J Chem Eng 2006;23:736–40. doi:10.1007/BF02705920.

[172] Golebiewski J, Galeski A. Thermal stability of nanoclay polypropylene composites by simultaneous DSC and TGA. Compos Sci Technol 2007;67:3442–7. doi:10.1016/j.compscitech.2007.03.007.

[173] Scott R. The practical handbook of machinery lubrication. Fourth Edition 2012.

[174] Sharma SK, Forster NH, Gschwender LJ. Effect of viscosity index improvers on the

elastohydrodynamic lubrication characteristics of a chlorotrifluoroethylene and a polyalphaolefin fluid. Tribol Trans 1993;36:555–64. doi:10.1080/10402009308983195.

[175] Dresselhaus MS, Jorio A, Hofmann M, Dresselhaus G, Saito R. Perspectives on carbon nanotubes and graphene Raman spectroscopy. Nano Lett 2010;10:751–8. doi:10.1021/nl904286r.

[176] Jorio A, Pimenta MA, Souza Filho AG, Saito R, Dresselhaus G, Dresselhaus MS. Characterizing carbon nanotube samples with resonance Raman scattering. New J Phys 2003;5. doi:10.1088/1367-2630/5/1/139.

[177] Cuesta, A., Dhamelincourt, P., Laureyns, J., Martínez-Alonso, A., & Tascón JMD. Raman microprobe studies on carbon materials. Carbon N Y 1994;32:1523–32.

[178] Rao AM, Chen J, Richter E, Schlecht U, Eklund PC, Haddon RC, et al. Effect of van der Waals interactions on the Raman modes in single walled carbon nanotubes. Phys Rev Lett 2001;86:3895–8. doi:10.1103/PhysRevLett.86.3895.

[179] Zeiger M, Jäckel N, Aslan M, Weingarth D, Presser V. Understanding structure and porosity of nanodiamond-derived carbon onions. Carbon N Y 2015;84:584–98. doi:10.1016/j.carbon.2014.12.050.

[180] Sinha A, Farhat Z. A Study of porosity effect on tribological behavior of cast Al A380M and sintered Al 6061 alloys. J Surf Eng Mater Adv Technol 2015;05:1–16. doi:10.4236/jsemat.2015.51001.

[181] Ghosh P, Hoque M, Karmakar G DM. Dodecyl methacrylate and vinyl acetate copolymers as viscosity modifier and pour point depressant for lubricating oil. Int J Ind Chem 2017;8:197–205.

[182] Tse JS, Song Y, Liu Z. Effects of temperature and pressure on ZDDP. Tribol Lett 2007;28:45–9. doi:10.1007/s11249-007-9246-5.

[183] Motamen Salehi F, Morina A, Neville A. Zinc Dialkyldithiophosphate additive adsorption on Carbon Black particles. Tribol Lett 2018;66:118. doi:10.1007/s11249-018-1070-6.

[184] Mazahery A, Shabani MO. Study on microstructure and abrasive wear behavior of sintered Al matrix composites. Ceram Int 2012;38:4263–9. doi:10.1016/j.ceramint.2012.02.008.

[185] Zhang ZF, Zhang LC, Mai YW. Particle effects on friction and wear of aluminium matrix composites. J Mater Sci 1995;30:5999–6004. doi:10.1007/BF01151519.

[186] Wilson S, Alpas AT. Wear mechanism maps for metal matrix composites. Wear 1997;212:41–9. doi:10.1016/S0043-1648(97)00142-7.

[187] Truhan JJ, Qu J, Blau PJ. A rig test to measure friction and wear of heavy duty diesel engine piston rings and cylinder liners using realistic lubricants. Tribol Int 2005;38:211–8. doi:10.1016/j.triboint.2004.08.003.

[188] Kapsiz M, Durat M, Ficici F. Friction and wear studies between cylinder liner and piston ring pair using Taguchi design method. Adv Eng Softw 2011;42:595–603. doi:10.1016/j.advengsoft.2011.04.008.

[189] Singh H, Singh P, Bhowmick H. Influence of MoS2 , H3BO3 , and MWCNT Additives on the Dry and Lubricated Sliding Tribology of AMMC–Steel Contacts. J Tribol 2018;140:041801. doi:10.1115/1.4038957.

[190] Ahlatci H, Koçer T, Candan E, Çimenoğlu H. Wear behaviour of Al/(Al2O3p+SiCp) hybrid composites. Tribol Int 2006;39:213–20. doi:10.1016/j.triboint.2005.01.029.

[191] Gurcan AB, Baker TN. Wear behaviour of AA6061 aluminium alloy and its composites. Wear 1995;188:185–91. doi:10.1016/0043-1648(95)06639-X.

[192] Bognár G, Vencl A. Experimental investigation of viscosity of glycerol based nanofluids containing carbon nanotubes. Tribol Ind 2019;41:267–73. doi:10.24874/ti.2019.41.02.12.

[193] Cornelio JAC, Lara-Romero J, Cuervo-Velásquez PA, Jaramillo-Zuluaga LF, Toro A, Ardila MI, et al. Rheological properties of carbon nanotubes as additive in a lubricating fluid. DYNA 2016;83:229–36. doi:10.15446/dyna.v83n199.54900.

[194] Spalvins T. A review of recent advances in solid film lubrication. J Vac Sci Technol A Vacuum, Surfaces, Film 1987;5:212–9. doi:10.1116/1.574106.

[195] Zirczy GN. Kinetics of Cordierite formation. Georgia Institute of Technology, 1972.

[196] Haggerty SE, Baker I. The alteration of olivine in basaltic and associated lavas - Part I: High temperature alteration. Contrib to Mineral Petrol 1967;16:233–57. doi:10.1007/BF00371094.

[197] Holmberg K, Matthews A. Coatings tribology: Properties, mechanisms, techniques and applications in surface engineering. Elsevier Ltd.; 2009.

[198] Gee MG, Jennett NM. High resolution characterisation of tribochemical films on alumina. Wear 1996;193:133–45. doi:10.1016/0043-1648(95)06612-8.

[199] Chaiwan S, Hoffman M, Munroe P. Investigation of sliding wear surfaces in alumina

using transmission electron microscopy. Sci Technol Adv Mater 2006;7:826–33. doi:10.1016/j.stam.2006.11.007.

[200] Nygren K, Samuelsson M, Flink A, Ljungcrantz H, Kassman Rudolphi Å, Jansson U. Growth and characterization of chromium carbide films deposited by high rate reactive magnetron sputtering for electrical contact applications. Surf Coatings Technol 2014;260:326–34. doi:10.1016/j.surfcoat.2014.06.069.

[201] Kopeliovich D. Effect of alloying elements on steel properties. Internet Http//Www Substech Com/Dokuwiki/Doku Php n.d.

[202] Blau PJ. Friction science and technology: From concepts to applications, second edition. CRC press; 2008.

[203] Kumar D, Singh A, Mishra DK. Role of surfactant head group and chain length in aqueous lubrication: Steel-steel contact. Proc Inst Mech Eng Part J J Eng Tribol 2016;230:968–73. doi:10.1177/1350650115621017.

[204] Kumar D, Mishra DK. Surfactant controlled lubricity of paraffin oil-based nano-emulsion. Tribol - Mater Surfaces Interfaces 2018;12:130–6. doi:10.1080/17515831.2018.1479093.

[205] Cookey G A NFU. Conductivity studies of binary mixtures of ionic and non-ionic surfactants at different temperatures and concentrations. J Appl Sci Environ Manag 2014;Vol. 18:530–4.

[206] Zakin J, Lui H. Variables affecting drag reduction by nonionic surfactant additives. Chem Eng Commun 1983;23:77–88.

[207] Singh H, Bhowmick H. Tribological behaviour of hybrid AMMC sliding against steel and cast iron under MWCNT-Oil lubrication. Tribol Int 2018;127:509–19. doi:10.1016/j.triboint.2018.06.030.

[208] Hamrock B. Fundamentals of fluid film lubrication. vol. 31. New York: McGraw-Hill; 1994. doi:10.5860/choice.31-6068.

[209] Echávarri Otero J, De La Guerra Ochoa E, Chacón Tanarro E, Del Río López B. Friction coefficient in mixed lubrication: A simplified analytical approach for highly loaded non-conformal contacts. Adv Mech Eng 2017;9:1687814017706266. doi:10.1177/1687814017706266.

[210] Stadler KE, Ciulli E PB. Elastohydrodynamic lubricated contact under transient conditions. (Doctoral Diss PhD Thesis Mech Eng VI Cycle, Univ Pisa) 2008.

[211] Guangteng G, Spikes HA. An experimental study of film thickness in the mixed lubrication regime. Tribol Ser 1997;32:159–66. doi:10.1016/s0167-8922(08)70445-0.

[212] Chatterjee M, Patra A. Cadmium Sulfide Aggregates through Reverse Micelles. J Am Ceram Soc 2004;84:1439–44. doi:10.1111/j.1151-2916.2001.tb00857.x.

[213] Echandía L, Mejía S, Osorio D, Rojas N. Efecto reológico de la agregación de nanopartículas a fluidos lubricantes. Rev Colomb Mater 2014:100–6.

[214] Chen L, Xie H, Li Y, Yu W. Nanofluids containing carbon nanotubes treated by mechanochemical reaction. Thermochim Acta 2008;477:21–4. doi:10.1016/j.tca.2008.08.001.

[215] Ohara T, Suzuki D. Intermolecular energy transfer at a solid-liquid interface. Microscale Thermophys Eng 2000;4:189–96. doi:10.1080/10893950050148142.

[216] Ghadimi A, Metselaar IH. The influence of surfactant and ultrasonic processing on improvement of stability, thermal conductivity and viscosity of titania nanofluid. Exp Therm Fluid Sci 2013;51:1–9. doi:10.1016/j.expthermflusci.2013.06.001.

[217] Israelachvili J. Intermolecular and Surface Forces. Academic Press; 2011. doi:10.1016/C2009-0-21560-1.

[218] Sottmann T, Strey R, Chen S-H. A small-angle neutron scattering study of nonionic surfactant molecules at the water–oil interface: Area per molecule, microemulsion domain size, and rigidity. J Chem Phys 1997;106:6483–91. doi:10.1063/1.473638.

[219] Peltonen L, Hirvonen J, Yliruusi J. The behavior of sorbitan surfactants at the water-oil interface: Straight-chained hydrocarbons from pentane to dodecane as an oil phase. J Colloid Interface Sci 2001;240:272–6. doi:10.1006/jcis.2001.7612.

[220] Israelachvili J. The science and applications of emulsions - an overview. Colloids Surfaces A Physicochem Eng Asp 1994. doi:10.1016/0927-7757(94)02743-9.

[221] Kocharova N, Ääritalo T, Leiro J, Kankare J, Lukkari J. Aqueous dispersion, surface thiolation, and direct self-assembly of carbon nanotubes on gold. Langmuir 2007;23:3363–71. doi:10.1021/la0631522.

[222] Martínez-Rubí Y, Guan J, Lin S, Scriver C, Sturgeon RE, Simard B. Rapid and controllable covalent functionalization of single-walled carbon nanotubes at room temperature. Chem Commun 2007:5146. doi:10.1039/b712299c.

[223] Lessard RR, DeMarco G. The significance of oil spill dispersants. Spill Sci Technol Bull

2000;6:59–68. doi:10.1016/S1353-2561(99)00061-4.

[224] Burkinshaw M, Neville A, Morina A, Sutton M. Lubrication of aluminium-silicon surfaces with ZDDP and detergents. Tribol - Mater Surfaces Interfaces 2012;6:53–8. doi:10.1179/1751583112Z.00000000011.

[225] Le VT, Ngo CL, Le QT, Ngo TT, Nguyen DN, Vu MT. Surface modification and functionalization of carbon nanotube with some organic compounds. Adv Nat Sci Nanosci Nanotechnol 2013;4:035017. doi:10.1088/2043-6262/4/3/035017.

[226] TermehYousefi A, Bagheri S, Shinji K, Rouhi J, Rusop Mahmood M, Ikeda S. Fast synthesis of multilayer carbon nanotubes from camphor oil as an energy storage material. Biomed Res Int 2014;2014:1–6. doi:10.1155/2014/691537.

[227] Huang X, Jiang G, He Y, An Y, Zhang S. Improvement of rheological properties of invert drilling fluids by enhancing interactions of water droplets using hydrogen bonding linker. Colloids Surfaces A Physicochem Eng Asp 2016;506:467–75. doi:10.1016/j.colsurfa.2016.07.011.

[228] Atakul Savrık S. Enhancement of tribological properties of mineral oil by addition of sorbitan monostearate and borate. İzmir Institute of Technology, 2010.

[229] Levitz PE. Non-ionic surfactants adsorption: structure and thermodynamics. Comptes Rendus Geosci 2002;334:665–73. doi:10.1016/s1631-0713(02)01806-0.

[230] Paria S, Khilar KC. A review on experimental studies of surfactant adsorption at the hydrophilic solid-water interface. Adv Colloid Interface Sci 2004;110:75–95. doi:10.1016/j.cis.2004.03.001.

[231] Akhmatov AS. Molecular physics of boundary friction. 1966.

[232] Rosen MJ KJ. Surfactants and interfacial phenomena. vol. 42. Wiley; 2012. doi:10.5860/choice.42-2832.

[233] Wagenknecht, F. and Juza R. Handbook of preparative inorganic chemistry. 1963. doi:10.1126/science.144.3619.703-a.

[234] Singh D, Thakre GD, Konathala LNS, Prasad VVDN. Friction reduction capabilities of Silicate compounds used in an engine lubricant on worn surfaces. Adv Tribol 2016;2016:1–9. doi:10.1155/2016/1901493.

[235] Zhang B, Xu BS, Xu Y, Zhang B Sen. Tribological characteristics and self-repairing effect of hydroxy-magnesium silicate on various surface roughness friction pairs. J Cent

South Univ Technol (English Ed 2011;18:1326–33. doi:10.1007/s11771-011-0841-0.

[236] Anbu selvan S, Ramanathan S. Dry sliding wear behavior of as-cast ZE41A magnesium alloy. Mater Des 2010;31:1930–6. doi:10.1016/j.matdes.2009.10.054.

[237] Wang Y, Li J, Wang L, Chen J, Xue Q. Tribological performances of graphite-like carbon films coupled to different ceramics in ambient air and water. Tribol Trans 2013;56:333–41. doi:10.1080/10402004.2012.752551.

[238] Li L, An B, Lahiri A, Wang P, Fang Y. Doublet of D and 2D bands in graphene deposited with Ag nanoparticles by surface enhanced Raman spectroscopy. Carbon N Y 2013;65:359–64. doi:10.1016/j.carbon.2013.08.039.

[239] Salah N, Alshahrie A, Iqbal J, Hasan PMZ, Abdel-wahab MS. Tribological behavior of diamond-like carbon thin films deposited by the pulse laser technique at different substrate temperatures. Tribol Int 2016;103:274–80. doi:10.1016/j.triboint.2016.07.013.

[240] Mohiuddin TMG, Lombardo A, Nair RR, Bonetti A, Savini G, Jalil R, et al. Uniaxial strain in graphene by Raman spectroscopy: g peak splitting, Grüneisen parameters, and sample orientation. Phys Rev B 2009;79:205433. doi:10.1103/PhysRevB.79.205433.

[241] Ferrari AC, Robertson J. Resonant Raman spectroscopy of disordered, amorphous, and diamondlike carbon. Phys Rev B 2001;64:075414. doi:10.1103/PhysRevB.64.075414.

[242] Sharma A, Mani Sharma V, Sahoo B, Joseph J, Paul J. Study of nano-mechanical, electrochemical and Raman spectroscopic behavior of Al6061-SiC-Graphite hybrid surface composite fabricated through friction stir processing. J Compos Sci 2018;2:32. doi:10.3390/jcs2020032.

[243] DiLeo RA, Landi BJ, Raffaelle RP. Purity assessment of multiwalled carbon nanotubes by Raman spectroscopy. J Appl Phys 2007;101:064307. doi:10.1063/1.2712152.

[244] Tuinstra F, Koenig JL. Raman spectrum of Graphite. J Chem Phys 1970;53:1126–30. doi:10.1063/1.1674108.

[245] Cançado LG, Takai K, Enoki T, Endo M, Kim YA, Mizusaki H, et al. General equation for the determination of the crystallite size La of nanographite by Raman spectroscopy. Appl Phys Lett 2006;88:163106. doi:10.1063/1.2196057.

[246] Cançado LG, Jorio A, Ferreira EHM, Stavale F, Achete CA, Capaz RB, et al. Quantifying defects in graphene via Raman spectroscopy at different excitation energies. Nano Lett 2011;11:3190–6. doi:10.1021/nl201432g.

[247] Souza N, Zeiger M, Presser V, Mücklich F. In situ tracking of defect healing and purification of single-wall carbon nanotubes with laser radiation by time-resolved Raman spectroscopy. RSC Adv 2015;5:62149–59. doi:10.1039/c5ra09316c.

[248] Suarez S, Lasserre F, Prat O, Mücklich F. Processing and interfacial reaction evaluation in MWCNT/Ni composites. Phys Status Solidi Appl Mater Sci 2014;211:1555–61. doi:10.1002/pssa.201431018.

[249] Pimenta MA, Dresselhaus G, Dresselhaus MS, Cançado LG, Jorio A, Saito R. Studying disorder in graphite-based systems by Raman spectroscopy. Phys Chem Chem Phys 2007;9:1276–91. doi:10.1039/b613962k.

[250] Rasool G, Stack MM. Wear maps for TiC composite based coatings deposited on 303 stainless steel. Tribol Int 2014;74:93–102. doi:10.1016/j.triboint.2014.02.002.

[251] Srinivasan V, Maheshkumar K V., Karthikeyan R, Palanikumar K. Application of probablistic neural network for the development of wear mechanism map for glass fiber reinforced plastics. J Reinf Plast Compos 2007;26:1893–906. doi:10.1177/0731684407082632.

[252] Al-Qutub AM, Allam IM, Abdul Samad MA. Wear and friction of Al-Al2O3 composites at various sliding speeds. J Mater Sci 2008;43:5797–803. doi:10.1007/s10853-008-2867-8.

[253] Alpas AT, Zhang J. Effect of SiC particulate reinforcement on the dry sliding wear of aluminium-silicon alloys (A356). Wear 1992;155:83–104. doi:10.1016/0043-1648(92)90111-K.

[254] Basavarajappa S, Chandramohan G, Subramanian R, Chandrasekar A. Dry sliding wear behaviour of Al 2219/SiC metal matrix composites. Mater Sci Pol 2006;24:357–66.

[255] Deuis RL, Subramanian C, Yellup JM. Dry sliding wear of aluminium composites - A review. Compos Sci Technol 1997;57:415–35. doi:10.1016/S0266-3538(96)00167-4.

[256] Seah KHW, Sharma SC, Rao PR, Girish BM. Mechanical properties of as-cast and heat-treated ZA-27/silicon carbide particulate composites. Mater Des 1995;16:277–81. doi:10.1016/0261-3069(96)00008-8.

[257] Sudarshan, Surappa MK. Dry sliding wear of fly ash particle reinforced A356 Al composites. Wear 2008;265:349–60. doi:10.1016/j.wear.2007.11.009.

[258] Sahin Y. Wear behaviour of aluminium alloy and its composites reinforced by SiC

particles using statistical analysis. Mater Des 2003;24:95–103. doi:10.1016/S0261-3069(02)00143-7.

[259] Banerji A, Prasad S V., Surappa MK, Rohatgi PK. Abrasive wear of cast aluminium alloy-zircon particle composites. Wear 1982;82:141–51. doi:10.1016/0043-1648(82)90288-5.

[260] Mahmoud TS. Tribological behaviour of A390/Grp metal-matrix composites fabricated using a combination of rheocasting and squeeze casting techniques. Proc Inst Mech Eng Part C J Mech Eng Sci 2008;222:257–65. doi:10.1243/09544062JMES468.

[261] Cameron A. The principles of lubrication: by A. Cameron. London: Longmans; 1966.

[262] Humphrey E, Morris N, Leighton M, Rahmani R, Rahnejat H. Multiscale friction in lubricant-surface systems for high-performance transmissions under mild wear. Tribol Lett 2018;66:77. doi:10.1007/s11249-018-1032-z.

[263] Gore M, Morris N, Rahmani R, Rahnejat H, King PD, Howell-Smith S. A combined analytical-experimental investigation of friction in cylinder liner inserts under mixed and boundary regimes of lubrication. Lubr Sci 2017;29:293–316. doi:10.1002/ls.1369.

[264] Johnson KL. Contact Mechanics. Cambridge: Cambridge University Press; 1985.

[265] Gohar R, Rahnejat H. Fundamentals of tribology. London: Imperial Collage Press; 2008. doi:10.1142/P553.

[266] Greenwood JA, Tripp JH. The contact of two nominally flat rough surfaces. Proc Inst Mech Eng 1970;185:625–33. doi:10.1243/PIME_PROC_1970_185_069_02.

[267] Nowicki B. Multiparameter representation of surface roughness. Wear 1985;102:161–76. doi:10.1016/0043-1648(85)90216-9.

[268] Teodorescu M, Balakrishnan S, Rahnejat H. Integrated tribological analysis within a multi- physics approach to system dynamics. Tribol Interface Eng Ser 2005;48:725–37. doi:10.1016/s0167-8922(05)80074-4.

[269] Evans CR, Johnson KL. Regimes of traction in elastohydrodynamic lubrication. Proc Inst Mech Eng Part C J Mech Eng Sci 1986;200:313–24. doi:10.1243/PIME_PROC_1986_200_135_02.

LIST OF PUBLICATIONS

List of SCI/SCIE papers

- Singh H, Bhowmick H. Lubrication characteristics and wear mechanism mapping for hybrid aluminium metal matrix composite sliding under surfactant functionalized MWCNT-oil. Tribology International. 2020 May 1;145:106152.
- Singh H, Bhowmick H. Lubricated tribology of hybrid AMMC–steel sliding contact: A comparative investigation between fully formulated commercial engine oils and surfactant functionalized MWCNT–base oil formulation. Proceedings of the Institution of Mechanical Engineers, Part J: Journal of Engineering Tribology. 2020 Jan 14:1350650119901221.
- Singh H, Bhowmick H. Tribological behaviour of hybrid AMMC sliding against steel and cast iron under MWCNT-Oil lubrication. Tribology International. 2018 Nov 1;127:509-19.
- Singh H, Singh P, Bhowmick H. Influence of MoS_2, H_3BO_3, and MWCNT additives on the dry and lubricated sliding tribology of AMMC–Steel contacts. Journal of Tribology. 2018 Jul 1;140(4).

List of SCOPUS/Conference papers

- Singh H, Bhowmick H. Influence of Nanoclay on the Thermophysical Properties and Lubricity Characteristics of Mineral Oil. Materials Today: Proceedings. 2019 Jan 1;18:1058-66.

APPENDIX: Abstracts of published papers

Tribology International 127 (2018) 509–519

Contents lists available at ScienceDirect

Tribology International

journal homepage: www.elsevier.com/locate/triboint

Tribological behaviour of hybrid AMMC sliding against steel and cast iron under MWCNT-Oil lubrication

Harpreet Singh, Hiralal Bhowmick*

Department of Mechanical Engineering, Thapar Institute of Engineering & Technology, Patiala, 147004 Punjab, India

ARTICLE INFO

Keywords:
Metal-matrix composite
Lubrication
Lubricant additive
MWCNT
Friction
Wear

ABSTRACT

The work presented here focused the tribological behaviour of aluminium metal matrix hybrid composites (AMMC) sliding against steel (EN31) and cast iron (CI), under particle laden oil lubricated condition. Tribological characteristics are evaluated using a pin-on-disc tribometer with Al6061-SiC-C pins sliding against EN31 and grey CI discs. For the particulate lubrication, multiwalled carbon nanotube (MWCNT) is dispersed in a SN500 grade base oil and a stable nano-lubricant is formed. From the experimental observation it is found that the MWCNT additive significantly enhanced the anti-wear and antifriction capabilities for the both the tribo-pairs. Further, the fractography and morphological studies of composite pins reveal the formation of tribolayers and mechanically mixed layers and illustrates the underlying friction and wear mechanism.

Tribology International 145 (2020) 106152

Contents lists available at ScienceDirect

Tribology International

journal homepage: http://www.elsevier.com/locate/triboint

Lubrication characteristics and wear mechanism mapping for hybrid aluminium metal matrix composite sliding under surfactant functionalized MWCNT-oil

Harpreet Singh *, Hiralal Bhowmick **

Department of Mechanical Engineering, Thapar Institute of Engineering & Technology, Patiala, 147004, Punjab, India

ARTICLE INFO

Keywords:
Metal matrix composite
Friction
Lubricant additives
Wear map

ABSTRACT

The friction-wear response of surfactant functionalized MWCNT-in-oil suspension under hybrid aluminium metal matrix composite/EN31 contact is presented. Composites were fabricated, characterized and tribological tests were performed with a pin-on-disc tribometer. Prior to tribological testing, thermophysical and stability analysis of the prepared lubricants were carried out. The operating regimes of the lubricants were predicted based on the estimated film thickness and friction responses. It is observed that the film thickness ratio for surfactant-MWCNT-oil is increased by 47% which helped in the shifting of lubrication towards the mixed regime. The findings of the study reveals that there is a remarkable enhancement in tribological behavior when surfactant functionalized MWCNT-in-oil is used. Finally, a wear map of the underlying wear mechanisms is also presented.

Original Article

Institution of MECHANICAL ENGINEERS
Journal of ENGINEERING TRIBOLOGY

Proc IMechE Part J:
J Engineering Tribology
0(0) 1–14

DOI: 10.1177/1350650119901221
journals.sagepub.com/home/pij
SAGE

Lubricated tribology of hybrid AMMC–steel sliding contact: A comparative investigation between fully formulated commercial engine oils and surfactant functionalized MWCNT–base oil formulation

H Singh and H Bhowmick

Abstract

The aim of the present study is to investigate the feasibility of developing surfactant-assisted multiwalled carbon nanotube (MWCNT)-laden lubricant for hybrid aluminum metal matrix composite (h-AMMC)/steel (EN31) pair sliding contact. For the preliminary screening, three grade-I base oils, two SAE grade fully formulated commercial oils, and two types of particle additives are used for the tribological investigation. Based on the detailed pilot study, a suitable grade of base oil (SN500), a fully-formulated commercial oil (SAE 20W50) and a solid particle additive (MWCNT) are finalized for the comprehensive tribological investigation. An amphiphilic surfactant, Sorbitan mono-oleate (SPAN 80) is added to MWCNT-in-oil dispersion to functionalize the MWCNT particles. For better insight of the lubrication and friction-wear mechanism, thermophysical properties of prepared suspensions and characterization of the worn-out surfaces of h-AMMC is carried out using various techniques such as scanning electron microscopy, energy-dispersive X-ray spectroscopy, X-ray diffraction, and Raman spectroscopy. The study reveals some interesting insights on the performance of MWCNT-laden lubricants in the presence of surfactant, which might be connoted for the future development of the lubricants to be used in the industrial applications.

Keywords

Lubricant, h-AMMC, tribology, multiwalled carbon nanotube, surfactant

Date received: 24 September 2019; accepted: 25 December 2019

Influence of MoS_2, H_3BO_3, and MWCNT Additives on the Dry and Lubricated Sliding Tribology of AMMC–Steel Contacts

Harpreet Singh
Mechanical Engineering Department,
Thapar University,
Patiala 147004, Punjab, India
e-mail: harpreetsingh6n2016@gmail.com

ParamPreet Singh
Mechanical Engineering Department,
Thapar University,
Patiala 147004, Punjab, India
e-mail: psingh.param@gmail.com

Hiralal Bhowmick[1]
Mechanical Engineering Department,
Thapar University,
Patiala 147004, Punjab, India
e-mail: hiralal.bhowmick@thapar.edu

The present study is focused on the performance evaluation of MoS_2, H_3BO_3, and multiwall carbon nanotubes (MWCNT) used as the potential oil additives in base oil for aluminum metal matrix composites (AMMC)–steel (EN31) tribocontact. Al–B_4C composite is used for this purpose; based on a set of preliminary investigation under unlubricated and fresh oil lubrication, three different types of AMMCs (Al–SiC, Al–B_4C, and Al–SiC–B_4C) were used. A pin-on-disk tribometer is used for all the friction and wear tests under operating condition of load 9.8 N and sliding velocity of 0.5 m/s. From the particle-based wet tribology, it is clear that both the additives H_3BO_3 and MWCNT improve the friction as well as wear behavior for selected composite contacts. Multiwall carbon nanotubes emerged out as superior among all the additives, whereas MoS_2 additives show marginal enhancement in frictional performance under given operating conditions. Fractography and morphological study of pin specimens are carried out to identify the underlying friction and wear mechanisms. [DOI: 10.1115/1.4038957]

Keywords: aluminum, metal-matrix composite, sliding friction, sliding wear, solid lubricants, lubricant additives, electron microscopy

Available online at www.sciencedirect.com

ScienceDirect

Materials Today: Proceedings 18 (2019) 1058–1066

materialstoday: PROCEEDINGS

www.materialstoday.com/proceedings

ICN3I-2017

Influence of Nanoclay on the Thermophysical Properties and Lubricity Characteristics of Mineral Oil

Harpreet Singh[a], Hiralal Bhowmick[a]*

[a]*Thapar Institute of Engineering and Technology, Mechanical Engineering Department, Patiala 147004, India*

Abstract

Heat transfer and lubrication has prime importance for the advancement of turbines, engines as well as metal cutting fluids. In the present study, Nanoclay (NC) is added to mineral oil to prepare dispersions of varying concentration from 0.005-0.1 mass per volume fraction. The effect of NC concentration and variation of temperature on the thermo-physical properties of the fluid dispersions has been carried out to explore the performance of these additives in the base oil. All the rheological and thermal conductivity measurements were conducted from 30°C to 60°C. From the experimental studies it is found that clay additives significantly improve the viscosity and thermal conductivity of the base oil. The rheology and thermal transport phenomena of the blend base oil has been compared with the existing theoretical models. However, it is observed that the popular existing rheological and thermal transport models developed for micro/nanofluids are unable to predict adequately the rheology and thermal transport phenomena of the nanoparticles-oil dispersions. On the other hand, now-a-days particle additive based lubricants, having excellent thermo-physical properties, are widely being used to enhance the tribological characteristics of the sliding contacts. Accordingly, the NC-oil dispersions are tested under aluminium-steel sliding contact using a Pin-on-Disc tribometer to explore their lubricity characteristics. Friction and wear results are compared for unlubricated, dry lubricated and wet lubricated conditions. Results show that there is a significant influence of NC in enhancing the friction as well as antiwear characteristics of lubricant. This study will invoke the research on particle based lubricant formulations for cutting fluid in metal forming industries as well as the fundamental basis of lubrication formulation for the enhanced tribological behaviour of ever demanding yet challenging aluminium metal matrix composites, that are widely used in the automotive industry.

Keywords: Nanoclay, Lubrication, Rheology, Thermal Conductivity, Friction, Wear